MycoKeys 45: 1–24 (2019)
doi: 10.3897/mycokeys.45.29350
http://mycokeys.pensoft.net

RESEARCH ARTICLE

A peer-reviewed open-access journal
MycoKeys
Launched to accelerate biodiversity research

Two additional species of *Gymnopus* (Euagarics, Basidiomycotina)

Ronald H. Petersen[1], Karen W. Hughes[1]

1 *Ecology & Evolutionary Biology, University of Tennessee, Knoxville, TN 37996-1100*

Corresponding author: *Karen W. Hughes* (khughes@utk.edu)

Academic editor: *S. Redhead* | Received 27 August 2018 | Accepted 12 December 2018 | Published 14 January 2019

Citation: Petersen RH, Hughes KW (2019) Two additional species of *Gymnopus* (Euagarics, Basidiomycotina). MycoKeys 45: 1–24. https://doi.org/10.3897/mycokeys.45.29350

Abstract

For more than a decade, a combination of molecular phylogenetic analyses and morphological characterisation has led to a renovation of the Omphalotaceae, especially of *Gymnopus* sensu lato. Numerous new genera have been proposed, but *Gymnopus* sensu stricto has also seen an accretion of species and species complexes. In this manuscript, two species are added to *Gymnopus* sensu stricto within Section *Androsacei*.

Keywords

Fungal barcode, Marasmius, Omphalotaceae, phylogenetics, taxonomy

Introduction

Ongoing research on marasmioid and gymnopoid fungi (Antonín and Noordeloos 2010; Antonín et al. 2014; Mata et al. 2004; Petersen and Hughes 2016, 2017; Wilson and Desjardin 2005), has led to significant renovation of *Gymnopus* sensu lato. Several additional genera have been proposed and molecular phylogenetic analyses have revealed numerous small clades within *Gymnopus* sensu stricto. One such clade includes *Marasmius brevipes* Berk. & Ravenel. The result is the necessary transfer of *M. brevipes* to *Gymnopus* and proposal of a new species, *G. portoricensis*.

Nomenclaturally, recombination of *Marasmius brevipes* into *Gymnopus* produces a conflict between two potential homonyms, of which *Gymnopus brevipes* (Bull.) S.F. Gray has priority. A new name is required for *Marasmius* (*Gymnopus*) *brevipes* and this is introduced below as *Gymnopus neobrevipes*.

Materials and methods

The following abbreviations and acronyms are noted: RHP, KWH = initials of the authors; GSMNP, Great Smoky Mountains National Park; M = Marasmius; Ma = Marasmiellus; Mi = Micromphale; My = Mycetinis. Colour names enclosed in quotation marks ("") are from Ridgway (1912) and those cited alphanumerically are from Kornerup and Wanscher (1967). BF = bright field microscopy; PhC = phase contrast microscopy. Microscopic structures were observed in 3% aqueous potassium hydroxide (KOH) without staining. Spore metrics are expressed as Q = the range of spore length divided by spore width; Q^m = mean value of Q.

All photos of microscopic structures were taken using a Q_c Olympus camera mounted on an Olympus BX60 research microscope fitted with phase contrast microscopy.

Molecular methods were described in Petersen and Hughes (Petersen and Hughes 2016; see also Petersen and Hughes 2017). An LSU-based PhyML phylogeny illustrates general placement of section *Androsacei* within *Gymnopus* and related taxa (Fig. 1). An ITS-based PhyML phylogeny was constructed to show more detailed placement of the two species below within Section *Androsacei* (Fig. 2). ITS and LSU sequences used in this paper are available in GenBank. Aligned ITS and LSU sequences are available in the Dryad depository (ITS: https://doi.org/10.5061/dryad.rd1df0c; LSU : https://doi.org/10.5061/dryad.4081h).

Results

Phylogenetic placement

Clade A of Mata et al. (2007) containing section *Androsacei* falls within /gymnopus of Wilson and Desjardin (2005) based on nuclear LSU sequences with moderate bootstrap support (Fig. 1). The small clade containing *G. portoricensis* and *G. neobrevipes* also appears in /A. At the ITS level, *G. portoricensis* and *G. neobrevipes* appear as a sister clade to *Gymnopus androsaceus* (Fig. 2). Two environmental sequences from Okinawa and *Gymnopus cremeostipitatus* (South Korea), placed by Antonín et al. (2014) within Section *Androsacei*, are also related to *G. portoricensis* and *G. neobrevipes*.

Taxonomy

1. *Gymnopus neobrevipes* R.H. Petersen, nom. nov.
Figs 3–9
Index Fungorum no. 555346

≡ *Marasmius brevipes* Berk. & Ravenel in Berkeley & Curtis. 1853. Ann. Mag. nat. Hist., Ser. 2 12: 426.
≡ *Micromphale brevipes* (Berk. & Ravenel) Singer in Dennis. 1953. Kew Bull. 8(1): 42

[NOT *Agaricus brevipes* Bulliard. 1791. Herbier Fr. (Paris) 11: tab. 521 (with legend); ≡ *Gymnopus brevipes* (Bull.) Gray. 1821. Nat. Arr. Brit. Pl. (London) 1: 609, pre-occupied homonym] (See *Index Fungorum* for additional combinations of Bulliard's epithet)

≠ *Gymnopus westii* (Murrill) César et al. 2018 Mycokeys 42: 31. (Basionym: *Marasmius westii* Murrill. Proc. Florida Acad. Sci. 7:110. 1945.

Holotype. United States, South Carolina, Santee Canal, June, Ravenel no. 1527, on dead twigs of oak (K). Type studies: Dennis 1953; Desjardin 1989; Desjardin and Petersen 1989.

Epitype (IF no. 555711) Mississippi, George Co., Pascagoula Wildlife Management Area, vic. Boat Ramp off Rte. 26, 30°53.789'N, 88°44.848'W, 12.VII.2014, coll. KWH, TFB 14505 (TENN-F-069197). GenBank: MH673477-8.

Diagnosis. 1) Long, hair-like rhizomorphs usually common to dominant; 2) basidiomata small (pileus usually <10 mm broad), arising from woody substrates or as branches of rhizomorphs; 3) clamp connections ubiquitous; 4) stipe short (<5 mm long), often strongly curved; 5) stipe medullary hyphae coherent; 6) pileipellis elements usually semi-gelatinised; 7) south-eastern United States.

Description. Basidiomata (Fig. 3) small with very short stipe, sometimes appearing resupinate or pseudostipitate (but not so), arising directly from substrate twig usually in fissures in thin bark or as side branches of extensive, black, interwoven rhizomorphs which often occur without associated basidiomata. **Pileus** 2–6(–9) mm broad, at first convex to conchate, usually becoming plano-convex or applanate by maturity, often folding closed like a clam-shell upon drying, matt, often strongly sulcate-striate almost to centre, irregularly corrugate or tuberculate, very thin but pliable; disc "burnt umber" (7E7) to "wood brown" (7C4); limb near "pinkish-cinnamon"(7B5), "avellaneous" (7B3), "wood brown" (7C4), "fawn colour," sometimes brown (7E5-7) to dark brown (7F5) to light brown (6D-E5-6) or brownish-orange (6C4) overall or with pale striations; margin even when young, wavy in age, not striate, sometimes pale to "tilleul buff" (7B2) ; pileus flesh thin, tough, pliable. **Lamellae** adnate, distant to very distant, shallow, fold-like to sublamelloid, thickish, occasionally weakly anastomosing, "tilleul buff" (7B2), "pale pinkish cinnamon" (6A2), pale brown (7D4), "avellaneous" (7B3), "vinaceous cinnamon" (7B4), usually becoming brownish, "sayal brown" (6C5) upon drying and storage; short lamellulae common. **Stipe** 0.5–6 × 0.5–1.5 mm, more or less terete, usually equal, central, strongly ageotropic (more or less straight when occurring on upper surface of substrate, strongly curved when occurring on vertical surface, almost pseudostipitate when occurring on lower surface of substrate), glabrous to unpolished, "fawn colour" (7C5), "army brown" (8D5) "fuscous" (6E4), "burnt umber" (7E7) to dark reddish-brown (8F6-8), black at base; insertion broad with minute, brown basal tuft, usually associated with small fissures in thin bark, rarely as a side branch of aerial rhizomorph; adventitious "stipes" occasionally hypertrophic and then clavate to fusiform. **Rhizomorphs** (Figs 3, 4A, B) rarely absent, usually dominant, –80(–450) × 0.3–0.6 mm, hair-like, matt to glabrous but not polished, black, tough, occasionally

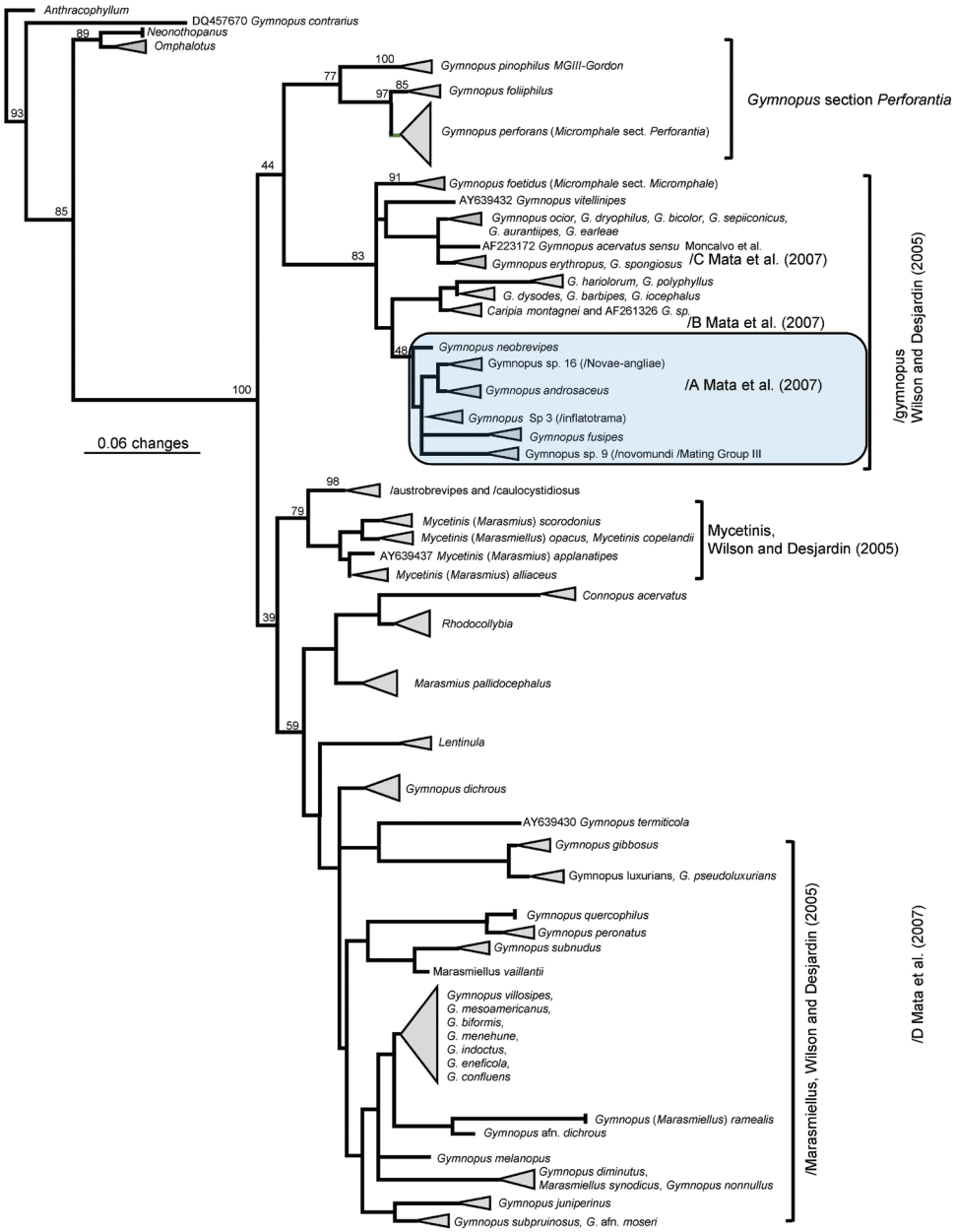

Figure 1. PhyML-based phylogeny of gymnopoid taxa based on nuclear LSU sequences showing the placement of *G. neobrevipes* within /gymnopus and allied with sect. *Androsacei*.

branched with spur branches, rarely anastomosed, but commonly braiding so as to appear thicker than individually, ranging from resupinate on woody substrate (black, adhering to substrate by minute fringe of brown hyphae) to producing ascending individuals (and then somewhat more slender than resupinate individuals), often

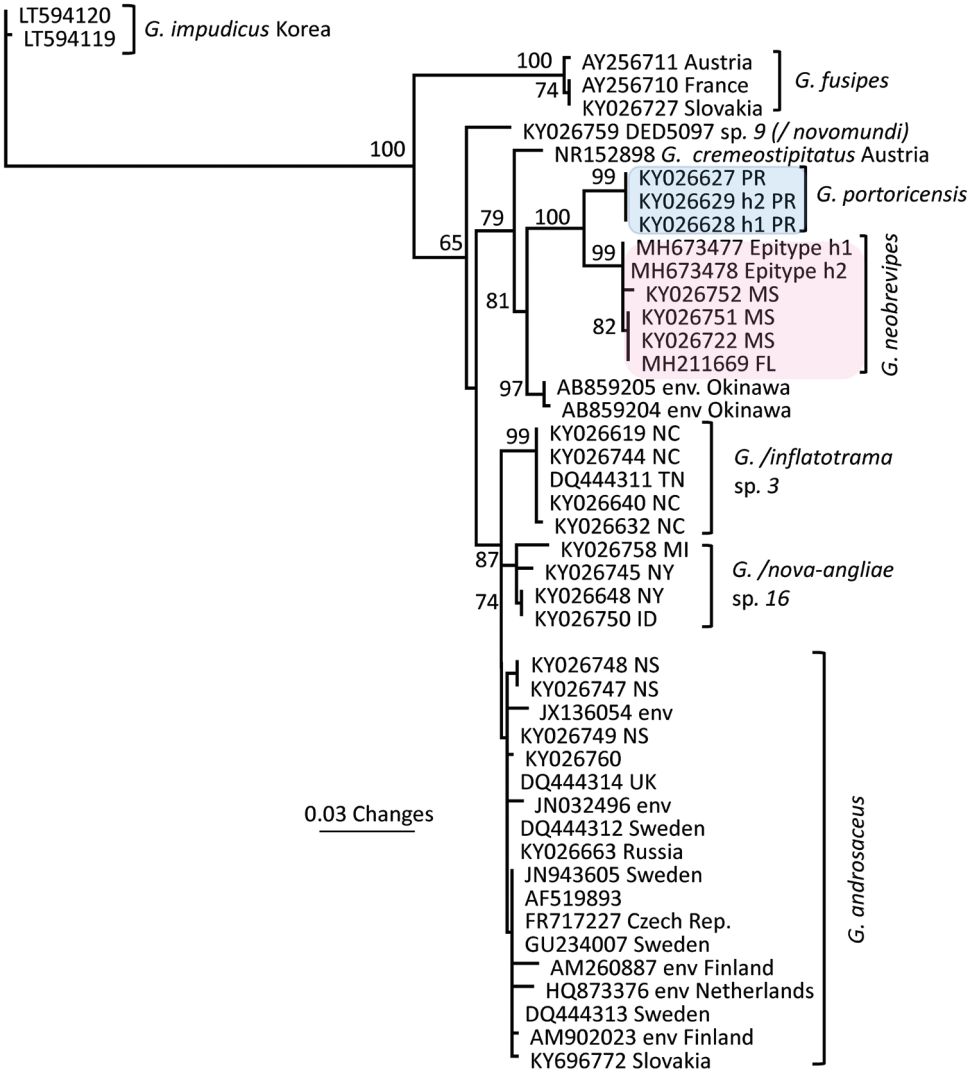

Figure 2. PhyML-based phylogeny based on ITS sequences, showing the relationship of *G. neobrevipes* and *G. portoricensis* to other androsaceoid taxa.

colonising suspended leaves and twigs to form a substrate net, occasionally producing basidiomata on side branches, often 3–4 in a file. **Taste** negligible or weakly alliaceous (reportedly weakly krauty); **odour** negligible.

Habitat and phenology. Basidiomata on dead small branches of broad-leafed trees, in temperate forests often on fallen branches of *Quercus* or *Rhododen*dron m*aximum* in mixed forest including *Tsuga*, usually at or near ground level; sterile rhizomorphs decumbent on dead, small (usually 18–24 mm diam.) boughs. In tropical climates, (see Pegler 1983, 1987, 1988, Dennis 1953, 1970) encountered year-round; in temperate forests mid-Summer to early Autumn. *Gymnopus neobrevipes* sometimes

Figure 3. *Gymnopus neobrevipes*. Habit view. TFB 14489 (TENN-F-069182). Scale bar: 10 mm.

shares the same habitat as *Anthracophyllum lateritium* (Berk. & Curtis) Singer – dead *Rhododendron maximum* boughs over streams.

Pileipellis composed of four elements: 1) slender "pileal hairs" occasional, 2.5–4.5 µm diam., hyaline, minutely decorated with "flakes," usually subcapitate; capitulum often decorated with minute needle-like crystals; 2) diverticulate hyphae (Figs 5A, 6B–D) inflated -10 µm diam., thin-walled, beset with vermiform setulae, with parent hypha often subgelatinised but with setulae remaining; 3) non-orientated, repent hyphae (Fig. 6A) 3–6 µm diam., firm-walled, involved in some slime matrix, encrusted to varying degrees (from conspicuous stripes or rings with plate-like profile calluses, to flat profile calluses with only "shadow" stripes or none at all); these hyphae (overnight in KOH) tend to gelatinise walls, apparently without clamp connections; and 4) more or less erect, modified broom structures, extremely rare and usually partially gelatinised, composed of a stalk (usually with flake-like scabs) and complex series of branchlets ending in the digitate diverticulate processes, often dichotomous, as in a Rameales-structure. Pileus trama (and lamellar trama) loosely interwoven; hyphae 3–18 µm diam., firm- to thick-walled (wall -1.0 µm thick, hyaline), occasionally but conspicuously clamped, encrusted with minute debris and embedded in thin slime matrix. **Pleurocystidia** (Figs 5B, 7) common, 18–24 × 5.6–7.5 µm, fusiform to fusiform-mammilate, conspicuously clamped. Basidioles (Figs 5B, 8A) clavate, occasionally subcapitulate; **basidia** (Figs 5B, 8B–D, 9B–C) 24–27 × 7–9 µm, clavate, 4-sterigmate, obscurely clamped; contents minutely multiguttulate when mature. **Basidiospores** (Figs 5C, 8E) (6.5–)8–9 × 3.5–4(–4.5) µm (Q = 1.86–2.29; Q^m = 2.08; L^m = 8.10 µm), ellipsoid to

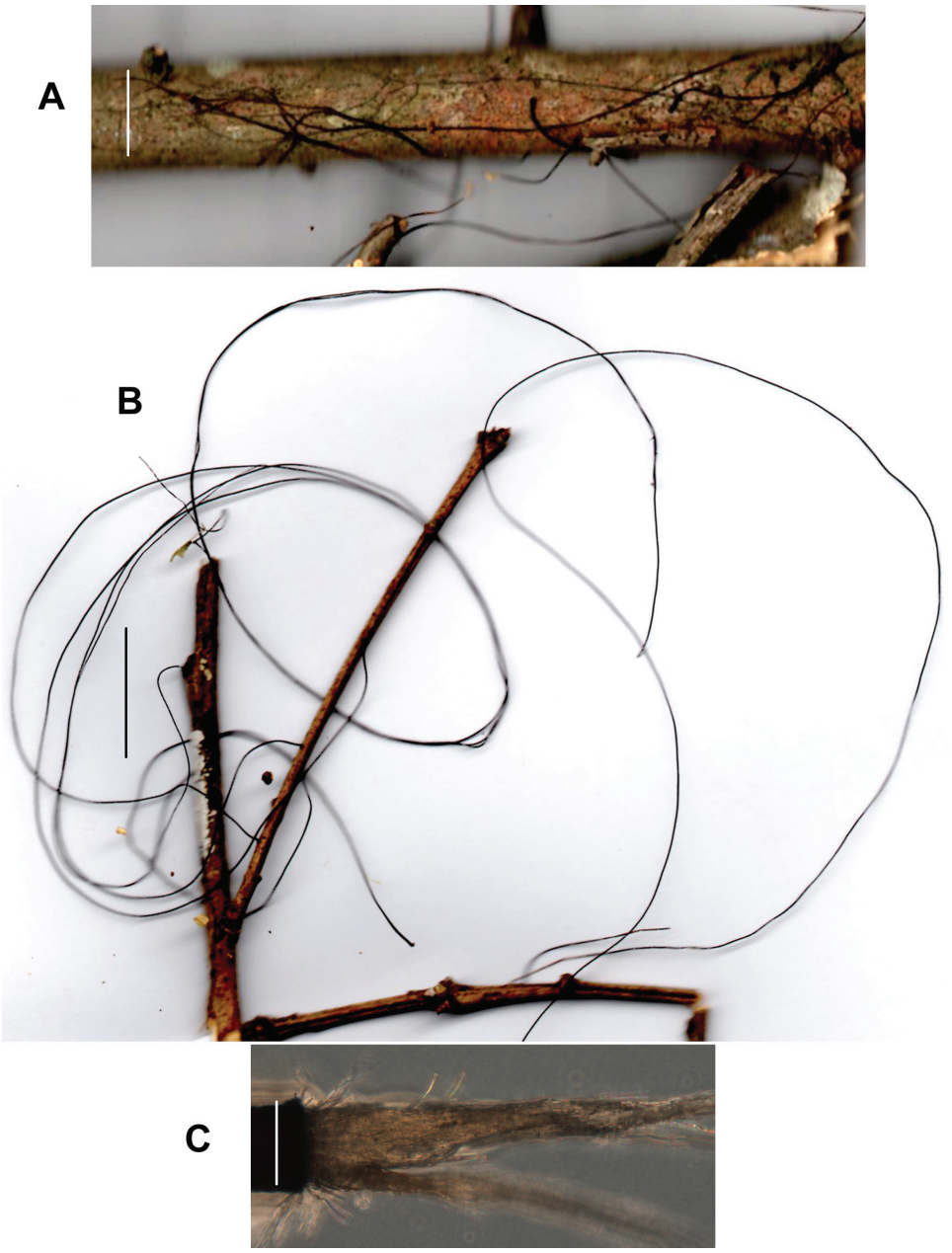

Figure 4. *Gymnopus neobrevipes*. **A** Resupinate rhizomorphs on surface of twig **B** Long aerial rhizomorphs on twig **C** Spray of hyphae from cut end of rhizomorph; 24 h. Rhizomorph on left. Scale bars: 10 mm (**A, B**); 1 mm (**C**). TFB 14607 (TENN-F-063931).

plump-ellipsoid, flattened adaxially, smooth, thin-walled, inamyloid; contents vaguely univacuolate. **Cheilocystidial structures** (Figs 5D, 9D–I) locally common to absent but apparently only close to lamellar edge, stalked or from basidiolar cells which grow

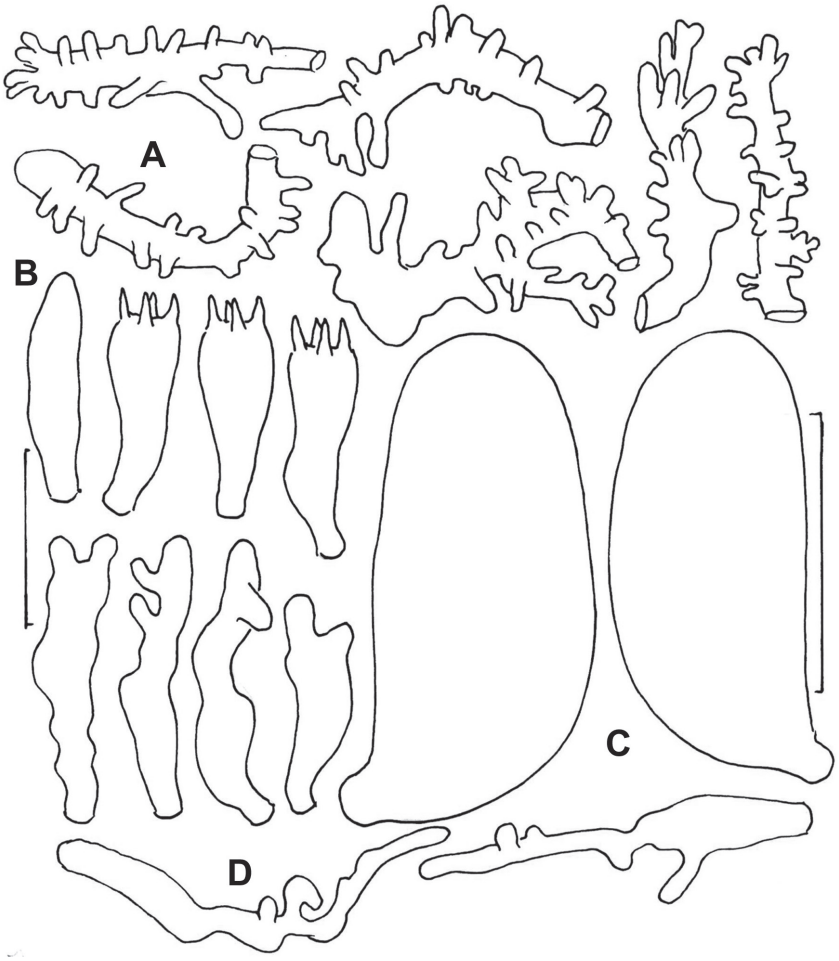

Figure 5. *Gymnopus neobrevipes*. Micromorphological structures. **A** Diverticulate hyphae of pileipellis **B** Pleurocystidium and basidia **C** Basidiospores **D** Cheilocystidia. **A–C** TFB 9087 (TENN-F-054912) **D** DED 4367 (TENN-F-047662). Scale bar: 20 μm (**A, B, D**); 5 μm (**C**).

out, often appearing as though arising deeper in lamellar trama than hymenium, lobed or subdiverticulate, 2.5–3.5 μm diam., thin-walled, hyaline, obscurely clamped. **Stipe** medullary hyphae 2–7 μm diam., hyaline, thick-walled (wall -1.5 μm thick), strictly parallel, coherent, with scattered conspicuous clamp connections. Stipe cortical hyphae 3.5–7.5 μm diam., pigmented olive-brown (PhC), subdextrinoid, thick-walled (wall -2.5 μm thick), smooth, rarely perhaps producing an ampulliform side branch with extended apex (two seen). **Rhizomorph** medullary hyphae 2–5.5(13) μm diam., thin- to firm-walled, strictly parallel and perhaps embedded in slime to be coherent, with occasional lateral branches lobate to digitate, hyaline, conspicuously clamped. Rhizomorph cortical hyphae (surface) 2–5.5(–7.5) μm diam., thick-walled (wall -0.7 μm thick to obscuring cell lumen, weakly pigmented olive tan – deep olive-brown in

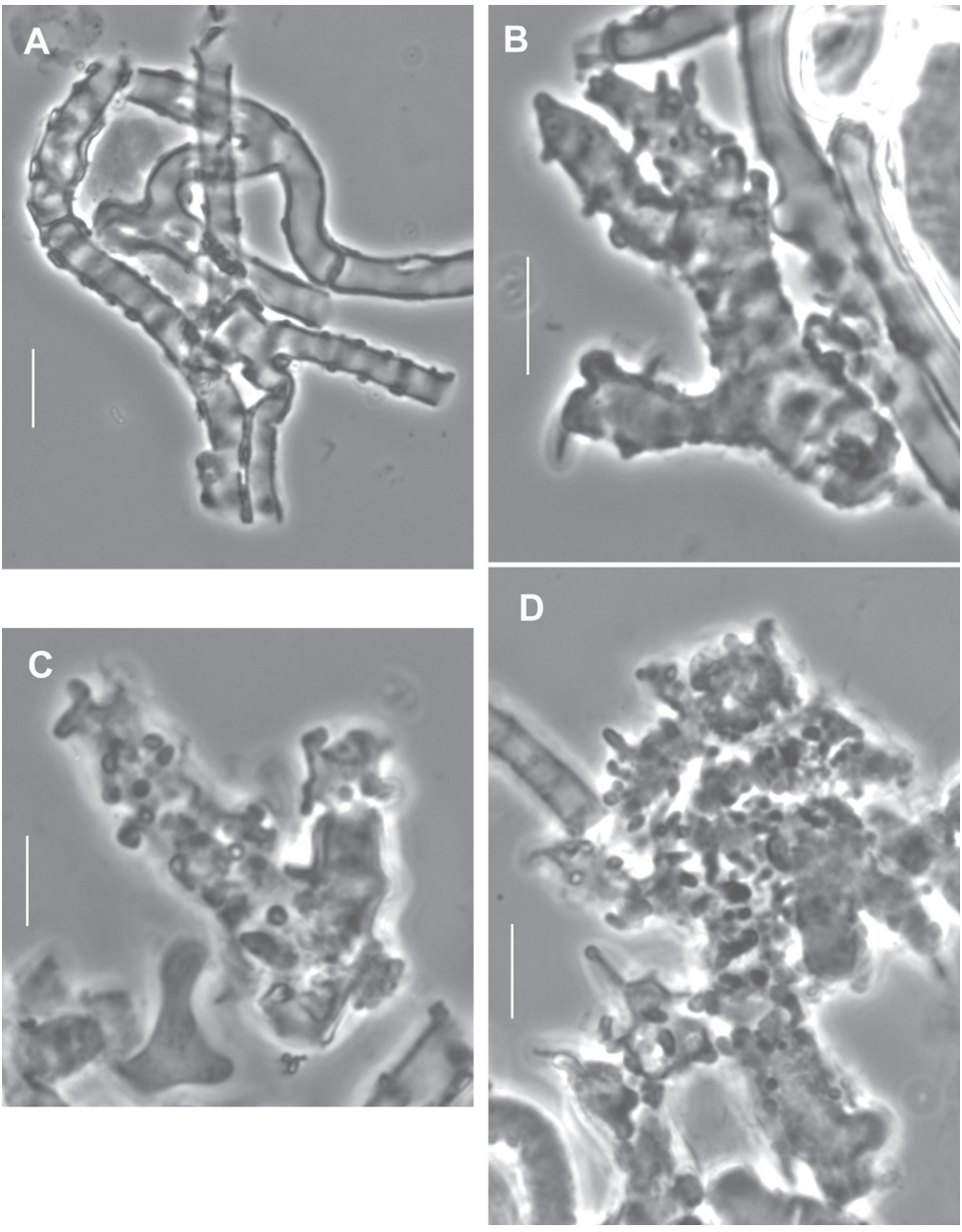

Figure 6. *Gymnopus neobrevipes*. Pileipellis elements. **A** Encrusted hyphae with banded appearance **B–D** Diverticulate hyphae of ramealis-structure. Scale bars: 5 µm. TFB 14607 (TENN-F-069310).

mass; PhC), outer wall roughened with scabs of encrustation; profile calluses -0.6 µm thick, somewhat darker than hyphal walls.

Commentary. Although collected by Ravenel, it was Curtis who conveyed the type specimen to Berkeley and Berkeley is the name-giver. The protologue (assumedly

written by Berkeley) is in Berkeley and Curtis 1853: 426. "29. *Marasmius brevipes*, Berk. & Rav. MSS. Pileo convexo estriato atro-sanguineo; stipitate brevi filiformi aterriimo nitida e mycelio repente similari enato; lamellis paucis adnatis rufis. Rav. No. 1527. On dead twigs of oak, June, Santee Canal, South Carolina, H.W. Ravenel, Esq.

"Pileus 1–2 line broad, convex, dark blood red; margin even; stem filiform, jet black, quite smooth, 1–2 line high, springing from creeping mycelial thread of the same nature with itself; gills ventricose, few, adnate, rufous.

"Allied to *M. haematocephalus*, &s, but distinguished at once by its short polished stem and dark gills. The colour of the pileus is nearly that of *M. atrorubens*. "

The pileipellis structure is similar to others described in sect. *Androsacei*. Desjardin and Petersen (1989) described pileipellis as not gelatinised (the tissue is not so), but failed to describe the gelatinisation of individual hyphae. This gelatinisation is merely a minor gelatinous sheath of individual hyphae for the outline of hyphal wall is not altered. However, the flake-like encrustation is carried on the gel surface and is seen at some small distance from the hyphal wall outline.

Amongst basidia in a mount soaked in KOH overnight, structures are seen which can be interpreted as gelatinised cheilocystidia. In rare cases, the remnants of digitate branching can be seen, but usually nothing is left of the supporting cell but some ghost-like structure. In a mount of lamellar edge only briefly in KOH, an enormous amount of debris is detected surrounding hymenial structures. It appears to be some sort of degeneration, quite possibly partial gelatinisation, but including numerous rod-shaped bacteria. This may be another indication of gelatinisation of tissues, this time of old basidia and subhymenial hyphae.

Subbasidial hyphae (subhymenium) become zig-zag in form as basidia are formed, evacuate and disappear. These hyphae are easily mistaken for some sort of cystidial structures, especially cheilocystidia.

A chronology of authoritative literature follows. Singer (in Dennis 1953) supplied a detailed description of *G. neobrevipes* (as *Mi. brevipes*) and Dennis (1953) examined type material and offered a rather uninformative illustration. Dennis (1970) offered a description of *M. brevipes* (as *Micromphale*), but perhaps as valuable is a diminutive aquarelle (Pl. 8, Fig. 4) which provides a good representation. Perhaps the best description of *G. neobrevipes* (as *Mi. brevipes*) was offered by Pegler (1983) and the description was based on more specimens than the type. Desjardin (1989: 447–449) examined the type of *M. brevipes* and Desjardin and Petersen (1989) published a species description based on numerous specimens.

Pileipellis structures, especially erect broom cell-like cells, are often gelatinised, especially in age. Likewise, cheilocystidia, while observed only occasionally, are often reduced to debris by gelatinisation or occasionally produce apical growths which can attain significant length. Lamellar tramal hyphae are often observed as thick-walled, but usually this is due to gelatinisation of the hyphal walls (inner wall boundary is clear, but outer wall boundary is obliterated and the gelatinised wall appears as though thick).

Pegler (1983) included *Mi. brevipes* as the only representative of *Micromphale* in the Lesser Antilles.

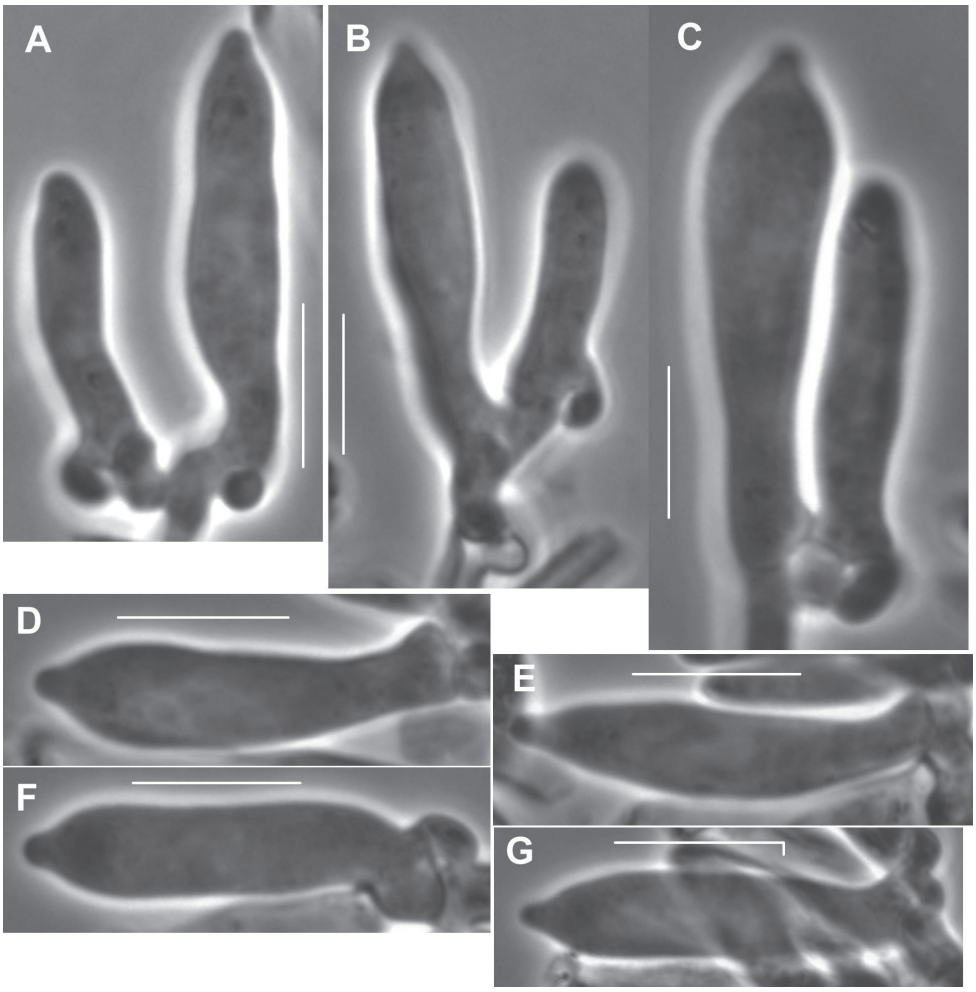

Figure 7. *Gymnopus neobrevipes*. Pleurocystidia. **A-C, F, G** showing subtending clamp connections. Note fusiform-submammilate shape. TFB 3704 (TENN-F-050692). Scale bars: 10 μm.

Rhizomorphs of *G. neobrevipes* are viable and short surface-sterilised sections (circum 1 cm) placed on malt extract agar produce sprays of mycelium from severed ends within 24 hrs. Within 72 h, the emergent mycelial sprays can be excised to establish an independent dikaryon culture which can be used for sequencing. In the case of *G. neobrevipes,* not only are sprays of mycelium produced on the cut ends (Fig. 4C), but within 72 h, many lateral hyphae emerge from the rhizomorph surface, soon resembling brownish fur. In one case, rhizomorphs of an ambient air-dried specimen were stored for over a year, yet produced mycelium as noted. In another case, a collection was heat-dried, but over one month later, rhizomorphs remained viable.

In Desjardin and Petersen (1989), a comparison was made of *M. brevipes* Berkeley & Ravenel, (1853; type, South Carolina, K) to *Marasmius porphyreticus* Petch (1947;

type, Sri Lanka, K). They concluded that *M. porphyreticus* "differs mainly in absence of cheilocystidia and in forming 'plicatosulcate' pilei." Other discriminating characters of *M. porphyreticus*: "slightly thinner pileus context, more regularly forked lamellae, and basidiomata not arising directly from rhizomorphs." Significantly, presence or absence of clamp connections was not mentioned. Plicatosulcate pilei, forked lamellae and basidiomata arising from rhizomorphs are all found in *G. neobrevipes* as well as other similar basidiomata. The comparison, despite a disparate geographic distribution, remains questionable, possibly pending phylogenetic data.

Likewise, it may be necessary to compare *G. neobrevipes* to *Marasmius tomentellus* Berk. & M.A. Curtis. "1868" (1869). J. Linnaean Soc. Bot. 10(no. 45): 298 [≡ *Gymnopus tomentellus* (Berk. & M.A. Curtis) Tkalčec & Mešec. 2013 Mycotaxon 123: 428], a taxon not mentioned by Desjardin and Petersen (1989).

Berkeley and Curtis's protologue: "Pileo convexo sulcato fulvo, stipite communi nigro albo-pubescente; stipitibus fertilibus brevibus pubescentibus; lamellis paucis pileo concoloribus. On dead wood. Pileus 1 line (~2 mm) across; fertile stems 2 lines (4–5 mm) high. Common on stems many inches long. Wright 22, Herb. Berk. This is a rhizomorphic species of *Marasmius*." (Cuba, holotype K).

Pegler (1987), with access to the type specimen of *M. tomentellus*, wrote: "This is a rhizomorphic species of *Marasmius* belonging to the section *Androsacei* Kuehner. The minute basidiomes, consisting of a pileus, 1–3 mm diam., with a short stipe, 1–4 × 0–2–0–4 mm, are borne on a common, slender rhizomorph, also about 0.2–0.4 mm diam. The stipe and rhizomorph surfaces are characterized by a white pubescence formed by numerous, short, thick-walled, hyaline hairs, 35–120 × 3–7 µm. The pileipellis is formed of irregular, diverticulate, hyaline elements, 10–17 × 4–12 µm. Only one collapsed spore, measuring 10 × 3–5 µm, could be found on the slide preparation taken from the type specimen. Singer (1976: 79) found spores on material from Louisiana, USA, which measured 11–11–5 × 4.5 µm, oblong to cylindric, but this material was not part of the type. This tiny species was well illustrated by Dennis (1951)" Presence or absence of clamp connections was not mentioned.

Pegler (1988) did not take up *M. brevipes* as part of the Cuban mycota, but did place *M. tomentellus* in the key. From this and other literature in which the type specimen of *M. tomentellus* was examined, the following characters can be gleaned: "Pileipellis with well-developed *Rameales* structure, not truly hymeniodermic; basidiome arising from a black rhizomorph; pileus 1–3 mm diam, fulvous; rhizomorph pubescent with thick-walled, hyaline hairs; spores 10 × 3.5 µm, elongate lacrymoid (see B&C 298; I: 573 (Sect. *Androsacei*)."

From Desjardin's (1989) examination of type material of *M. tomentellus*, the following can be extracted: coarse rhizomorphs with white pubescence; common short branches resembling disarticulated stipes. Only one pileus remains. Stipe and rhizomorph cortical tissue of repent hyphae -6.5 µm, thick-walled (wall -1.5 µm thick), parallel, cylindric, incrusted with granulose or amorphous brown (pigment intraparietal as well as incrusting), dextrinoid; medullary hyphae 4–8 µm diam, subparallel, cylindric,

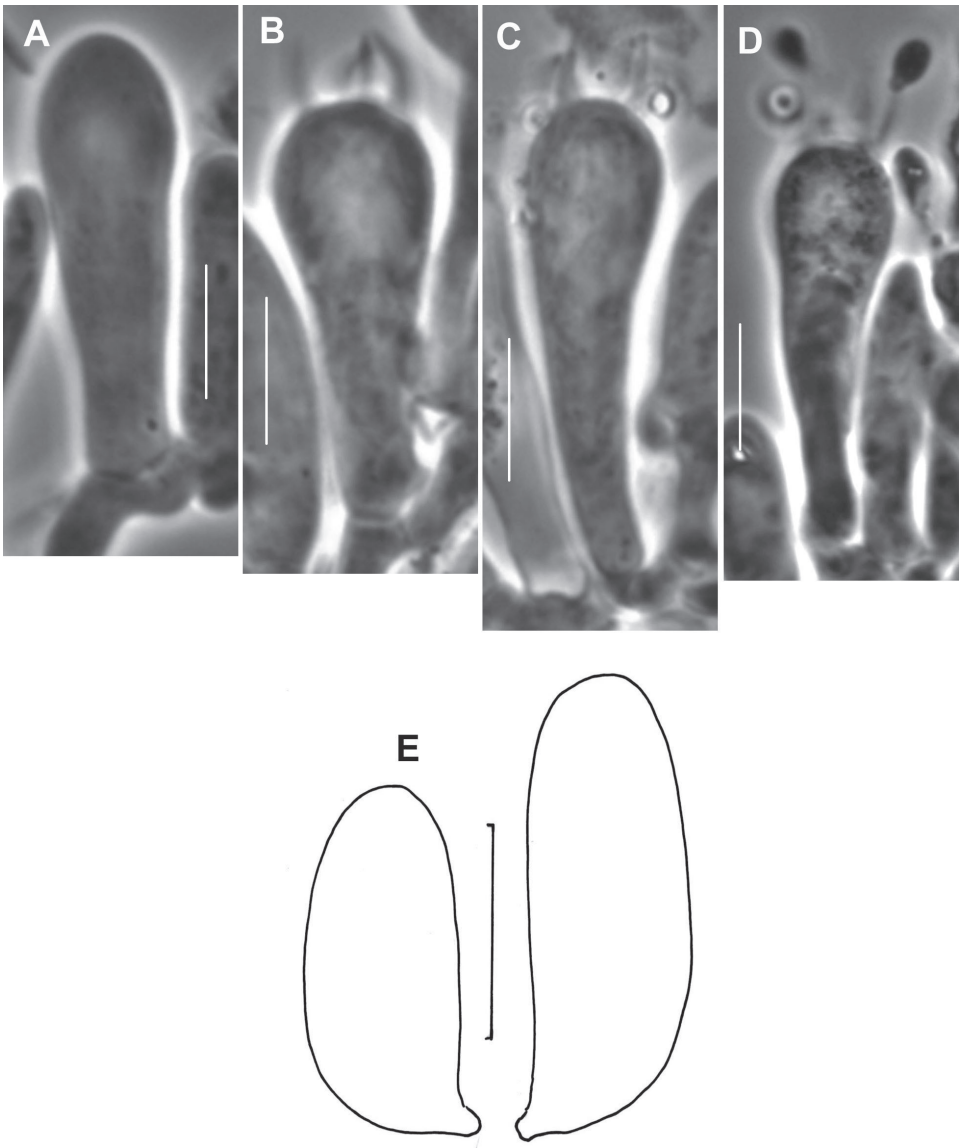

Figure 8. *Gymnopus neobrevipes*. A. Basidiole. **B–D** Basidia. E. Basidiospores. TFB 3704 (TENN-F-050692). Scale bars: 10 µm (**A–D**); 5 µm (**E**).

smooth, hyaline, weakly dextrinoid, thin-walled, unclamped. Rhizomorph vesture of numerous, erect rhizocystidia, 45–120 × (6–)8–12 µm, cylindric or lanceolate, obtuse or subacute, aseptate or with one or several secondary septa, apex of cell hyaline, base of cell hyaline, pale ochraceous or pale brown, weakly dextrinoid." This appears to be the only mention of clamp connections – absent – but confirms the tomentose surface of stipes and rhizomorphs. A thorough search for tomentosity on rhizomorphs and/or stipes of collections of G. *neobrevipes* failed to observe this.

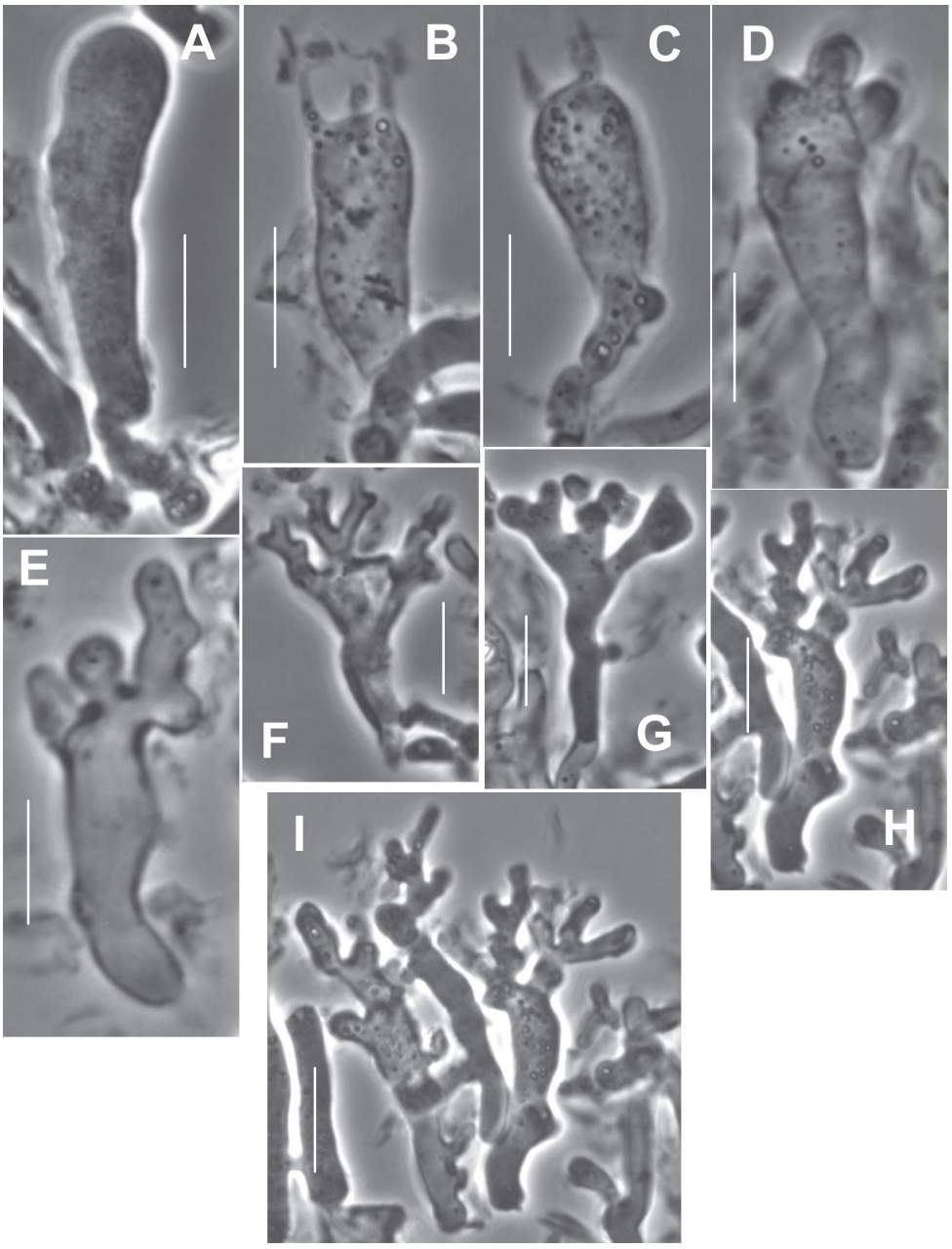

Figure 9. *Gymnopus neobrevipes*. **A** Basidiole **B, C** Basidia **D, E** Basidiiform cheilocystidia **F–H** Diverticulate cheilocystidia **I** Cluster of diverticulate cheilocystidia. DED 4367 (TENN-F-047662). Scale bars: 10 µm.

Additional species have been described in *Marasmius* sect. *Androsacei* from South-Sea Islands and at least *M. aurantiobasalis* Desjardin & Horak, (see Desjardin et al. 2000; not Desjardin and Horak 1997) exhibits several characters resembling those

of *G. neobrevipes.* Finally, Tkalčec and Mešić (2013) transferred two Corner species of *Marasmius* to *Gymnopus* sect. *Androsacei*. Several additional species epithets were transferred, including *M* (*Gymnopus*) *tomentellus.*

Specimens examined for this study. Note that the list is not related to that offered by Desjardin and Petersen (1989): **Alabama**, Baldwin Co., Blakely Historical Park, Nature Sanctuary, 30°44'36.46"N, 87°54'56.46"W, 10.VI.2005, coll J.L. Mata, JLM 1628 (USA); same data, JLM 1630 (USA); Schillingers Rd., Cottage Hill Park, 18.VI.2004, coll D.H. Nelson, det JL Mata, JLM 1564 (USA); Mobile, Univ. South Alabama North campus, forest park, 30°41'35.06"N, 88°10'55.54"W, 3.VI.2005, coll & det J.L. Mata. JLM 1616 (USA). **Louisiana**, St. Tammany Par., vic. Pearl River, Honey Island Swamp, 6.VI.1976, coll. W.B. & V.G. Cooke, Cooke no. 52125, ex DAOM 193773 [TENN-F-054662[. [no TFB number]; See also references to Singer (in Dennis 1953). **Mississippi**, George Co., Pascagoula Wildlife Management Area, vic. Boat Ramp off Rte. 26, 30°53.789'N, 88°44.848'W, 12.VII.2014, coll. RHP, TFB 14504 (TENN 69196); same data, coll. KWH, TFB 14505 (TENN 69197); Harrison Co., vic. Saucer, Tuxahatchie Hiking Trail trailhead, 30°39'43.61"N, 89°08'14.70"W, 10.VII.2014, coll. RHP, TFB 14489 (TENN-F-069182); Red Creek Wildl. Man. Area, 11.VIII.2014, coll. KWH, TFB 14498 (TENN-F-069189); Jackson Co., Parker Lake area, Pascagoula River, 17.VII.1987, coll DE Desjardin, DED 4367 (TENN-F-047662). **North Carolina**, Macon Co., vic. Highlands, Bull Pen Rd., Slick Rock campground, 27.VII.1978, coll RHP, TFB 52193 (TENN-F-041215); vic. Highlands, Bull Pen Rd., Chattooga Loop Trail, 13.VI.1987, coll RHP & E Horak, det. DE Desjardin, DED 4279 (TENN-F-047665); same location, 13.VII.1988, DED 4583 (TUNN-F-054661); vic. Highlands, Horse Cove Rd. opposite FR 401, 13.VI.1989, coll RHP, TFB 56693 (TENN-F-048667); vic. Highlands, Nantahala Nat. For., Blue Valley, first gated road on left, 24.VI.1989, coll. RHP, TFB 1827 (TENN-F-048533); same location, FS79, 8.VII.1990, coll. RHP, TFB 2895 (TENN-F-049257); same location, 10.VII.1990, coll RHP, TFB 2185 (TENN-F-048796); same location, 10.VII.1990, coll RHP, TFB 2187 (TENN-F-048794); same location, Pickelseimer's Falls trail, 18.VII.1991, coll. S.A. Gordon, TFB 3704 (TENN-F-050692; same location, junction of F.R. 83 and 83B, 14.VII.1986, coll D.E. Desjardin, DED 3813 (TENN-F-047663); same location, 13.VI.1987, coll RHP & E. Horak, det. DE Desjardin, 13.VI.1987, DED 4282 (TENN-F-047664). **Tennessee**, Cocke Co., GSMNP, Big Creek, 35°46'51.96"N, 83°12'11.74"W, 16.VI.1991, coll SA Gordon, RHP, V Antonin, HR Bhandary, TFB 3633 (TENN-F-050752); same location, 16.VI.1991, same collectors, TFB 3634 (TENN-F-050753). **Texas**, Hardin Co., Big Thicket Nat. Preserve, Lance Rosier Unit, Teel Rd., vic cypress swamp, 30°15.860'N, 94°30.75'W, coll DP Lewis, DPL 11773, TFB 14609 (TENN-F-069312); Newton Co., Co. Rd. 305, Bleakwood, Lewis Properties, 30°42.509'N, 93°49.630'W, coll & leg D.P. Lewis, DPL 11763 (DPL Herb.)

2. *Gymnopus portoricensis* R.H. Petersen, sp. nov.
Figs 10–15
Index Fungorum no. IF555347

Holotype. United States, Puerto Rico, Caribbean National Forest, El Yunque, vic. Sabana, trail 3, 1.VI.1992, coll RHP, TFB 4548 (TENN-F-051029). GenBank: KY026628-9.

Etymology. Portoricensis referring to collections made in Puerto Rico.

Diagnosis. 1) Basidiomata small, resembling those of *Gymnopus neobrevipes*, arising from rhizomorphs or from woody substrate, often in clusters of significant numbers; 2) stipe slightly eccentric or central, strongly curved, dark brown (black only at base); 3) rhizomorphs luxuriant, brown (not black); 4) spores somewhat small for the clade, (5–)6–7 × (2.5–)3–4 µm.

Description. Basidiomata (Fig. 10) marasmielloid, cespitose to imbricate, conchate when young becoming shallowly convex to applanate by maturity, stipitate. **Pileus** 2–11 mm broad, circular to broadly reniform, matt, radially rivulose outwards, thin, leathery, uniformly "light pinkish-cinnamon" (7A2) to "pinkish-cinnamon" (7B5). **Lamellae** well-defined (-0.6 mm broad and ventricose to reduced, pleated or fold-like, distant (total folds = 11–18; through folds = 7–10), concolorous to pileus or "tilleul buff" (7B2); edge entire. **Stipe** very small (1–2.5 × 0.5–0.7 mm), slender, central or eccentric, strongly curved to non-instititious attachment on substrate (wood or rhizomorph), "Mikado brown" (7C6) apically, downwards "warm sepia" (7F6), "bister" (5F8) to black; basal tuft insignificant, blond. **Rhizomorphs** extensive, slender, brown, near "tawny olive" (5C5) or "sayal brown" (6C5) to nearly black. **Odour** and **taste** negligible.

Habitat. Outer surface of old bamboo (TENN-F-051029) or rotting twigs of deciduous trees (TENN-F-050999).

Pileipellis (Figs 11A, B, 12, 13) composed of three elements involved in very thin mucoid matrix: 1) hair-like, probably erect hyphal apices (Figs 11B, 12), 30–120 × 1.5–3 µm (at widest point), subtly capitulate apically, arising as side branches of slender hyphae (not from clamps), firm- but indistinct-walled, delicately decorated with gritty deposits or a very thin mucoid sheath, tapering to 1–1.5 µm diam. and subrefringent especially at very apex; 2) repent, heavily ornamented hyphae (Figs 11A, 13B) 3–9 µm diam., firm-walled, strongly encrusted in stripes or patches with no profile calluses; contents more or less homogeneous; 3) scattered rudimentary diverticulate hyphal apices (Figs 11A, 13A) 4–7.5 µm diam., often appearing stout-tibiiform, with diverticula lobate, 2–5 × 1.5–2.5 µm; contents more or less homogeneous. Pileus trama loosely interwoven; hyphae (Fig. 13C) 3–7.5 µm diam., conspicuously clamped, appearing thick-walled but gelatinised (wall -1.5 µm thick). **Pleurocystidia** (Figs 11C, 14A–D) 21–29 × 4–5 µm, fusiform, conspicuously clamped; contents homogeneous, occasionally subtly partitioned. Basidioles clavate, clamped; **basidia** (Figs 11C, 14F, G) 20–30 × 6–8 µm, 4-sterigmate, clavate, clamped; contents with scattered, minute guttules. Effete basidia do not disappear; at least the lateral walls survive to create debris in which turgid basidia are embedded in hymenial debris.

Figure 10. *Gymnopus portoricensis*. Habit. Above: TFB 4548 (TENN-F-051029). Below: TFB 4512 (TENN-F-050999). Scale bars: 10 mm.

Basidiospores (Fig. 11D) (5–)6–7 × (2.5–)3–4 µm (Q = 1.50–2.83; Q^m = 2.08; L^m = 6.58 µm), narrowly pip-shaped to sublacrymiform (somewhat tapered towards apiculus), thin-walled, smooth, inamyloid; contents homogeneous. **Cheilocystidia** (Fig. 15) limited to well-defined lamellae, scattered, 25–35 × 7–15 µm, pedicellate, thin-walled (easily crushed), expanded distally usually with irregular lobes or apical outgrowths, obscurely clamped, hyaline; contents more or less homogeneous. Stipe

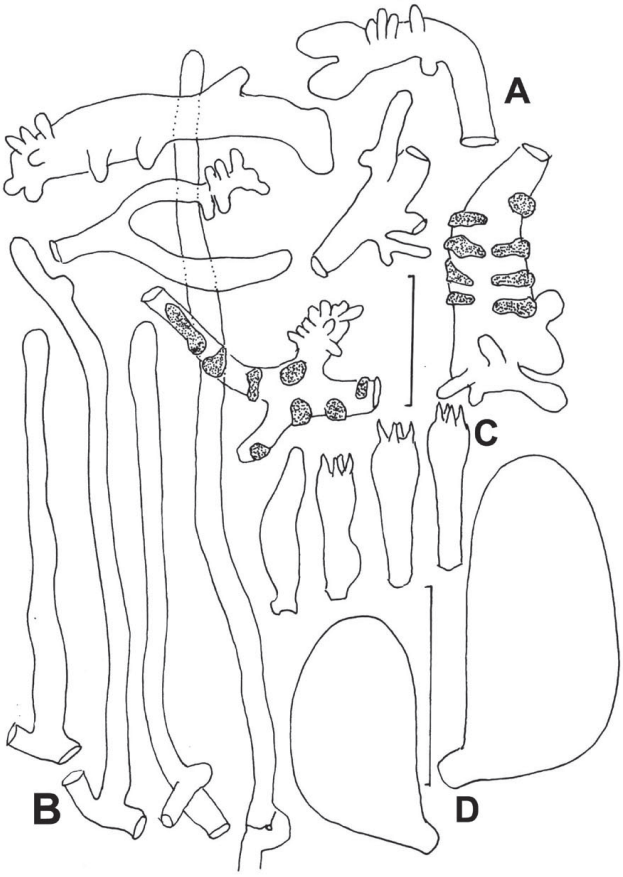

Figure 11. *Gymnopus portoricensis*. Microstructures. **A** Pileipellis structures; diverticulate and encrusted hyphal termini **B** "Pileal hairs." **C** Pleurocystidium and basidia **D** Basidiospores. Scale bars: 20 μm (**A–D**); 5 μm (**E**). TFB 4548 (TENN-F-051029).

medullary hyphae of three types: 1) 6.5–24 μm diam., thick-walled, irregularly gelatinising [wall -1.2 μm thick in H_2O, wall up to 7 μm thick in KOH and then yellowish (PhC)]; 2) 5–7.5 μm diam., thick-walled (wall -1 μm thick, not gelatinising, hyaline); clamp connections occasional, obscure; and 3) 2–4 μm diam., firm-walled, meandering through medulla; clamp connections rare, conspicuous. Stipe cortical hyphae 4–8 μm diam., strictly parallel, apparently adherent (held together adhesively and shattering under pressure), thick-walled [wall -2 μm thick, pigmented (ochraceous tan in KOH, red-brown in IKI/BF)], coarsely roughened in pigmented spicules; clamp connections not observed.

Commentary. Although basidiomata superficially resemble those of *G. neobrevipes*, the pileipellis structure is not similar. Erect, broom cell-like cells of *G. neobrevipes* are missing; diverticulate repent hyphae are rare and doubtful; erect "hairs," while clamped (and therefore assumed to belong to this organism), are more demonstrable

Figure 12. *Gymnopus portoricensis*. Pileal hairs. Note incrustation on thin slime sheath. **A** TFB 4512 (TENN-F-050999) **B, C** TFB 4548 (TENN-F-051029). Scale bars:10 μm.

in *G. neobrevipes*. Morphologically, *G. portoricensis* could be placed in *Marasmiellus* (see Retnowati 2018) based on poorly developed Ramealis-structure, no broom cells), but it equally could be interpreted as a reduced member of *Androsacei* (including *G. neobrevipes*) in which erect, broom cell-like pileipellis cells are rare to missing. Cheilocystidia are typical of the latter group. If *G. neobrevipes* is accommodated in *Gymnopus* sect. *Androsacei*, *G. portoricensis* must also be found there. ITS sequences confirm this placement (Fig. 2).

Inspection shows that almost no basidiomata originate from rhizomorphs, instead seemingly originating from woody substrate directly. Rare basidiomata, however, do arise from rhizomorphs, with stipes as side branches. Moreover, some twigs with basidiomata are devoid of rhizomorphs altogether.

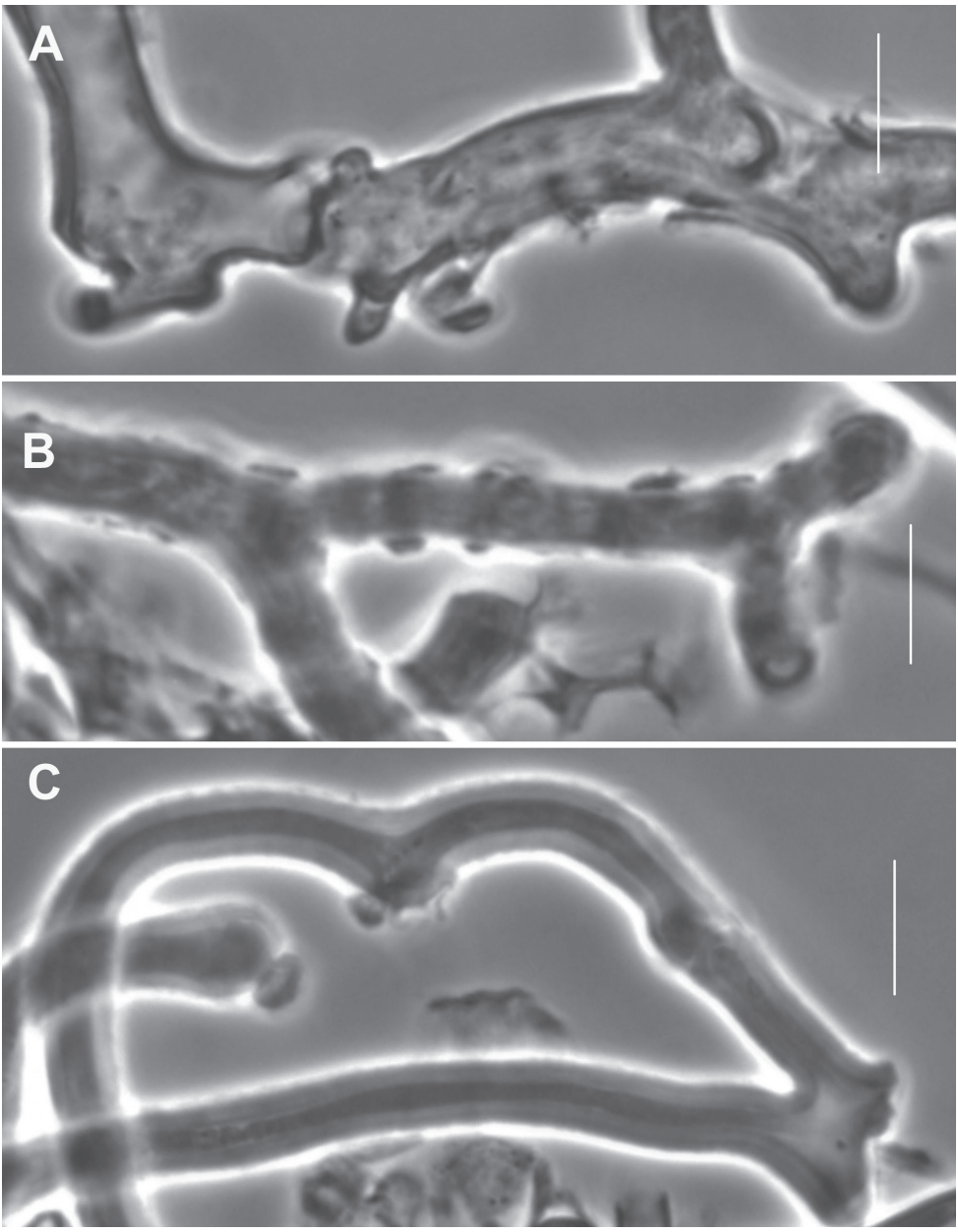

Figure 13. *Gymnopus portoricensis*. Pileipellis structures. **A** "Diverticulate" hyphal fragment **B** Encrusted hypha with thin slime sheath **C** Gelatinised hyphal walls. Scale bars: 10 µm. TFB 4548 (TENN-F-051029).

A polyspore dikaryon culture was established from TENN-F-050999 and careful examination revealed exceedingly rare (but clearly demonstrated) clamp connections. This condition is also true in cultures of *G. neobrevipes.* Desjardin (1990), while reporting clamp connections in the culture of *M. brevipes*, made no comment on their relative abundance.

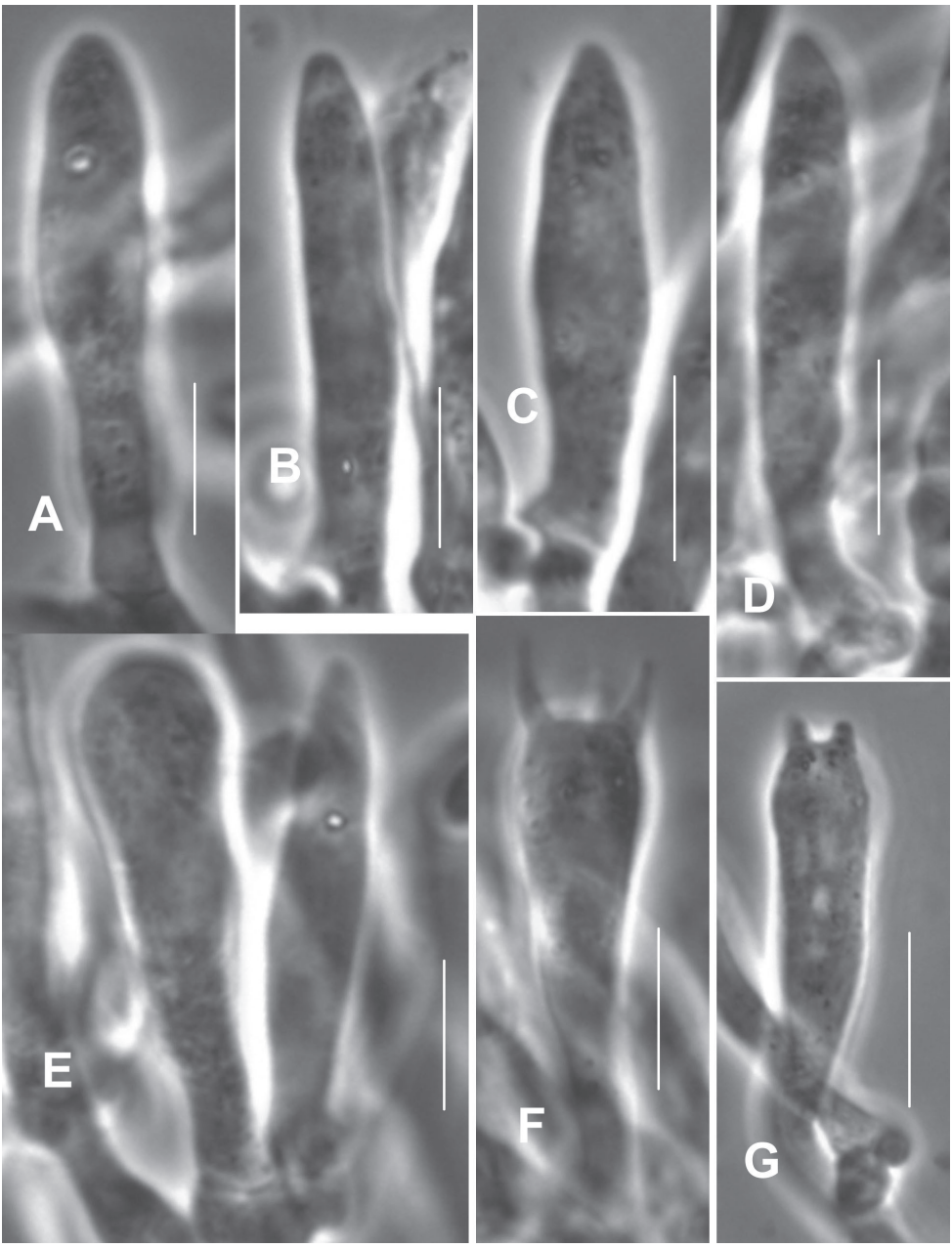

Figure 14. *Gymnopus portoricensis*. Hymenial structures. **A–D** Pleurocystidia **E** Basidiole and pleurocystidium from one clamp connection complex **F, G** Basidia. Scale bars:10 µm. TFB 4512 (TENN-F-050999).

Basidiomata are not pseudo- or eccentrically stipitate, but centrally to slightly eccentrically stipitate. The stipe, however, is usually immediately curved through the declivity in the pileus circumference. Lamellae appear to deteriorate rapidly, perhaps through insect grazing or tissue gelatinisation, but when discrete are shallow but sharp-

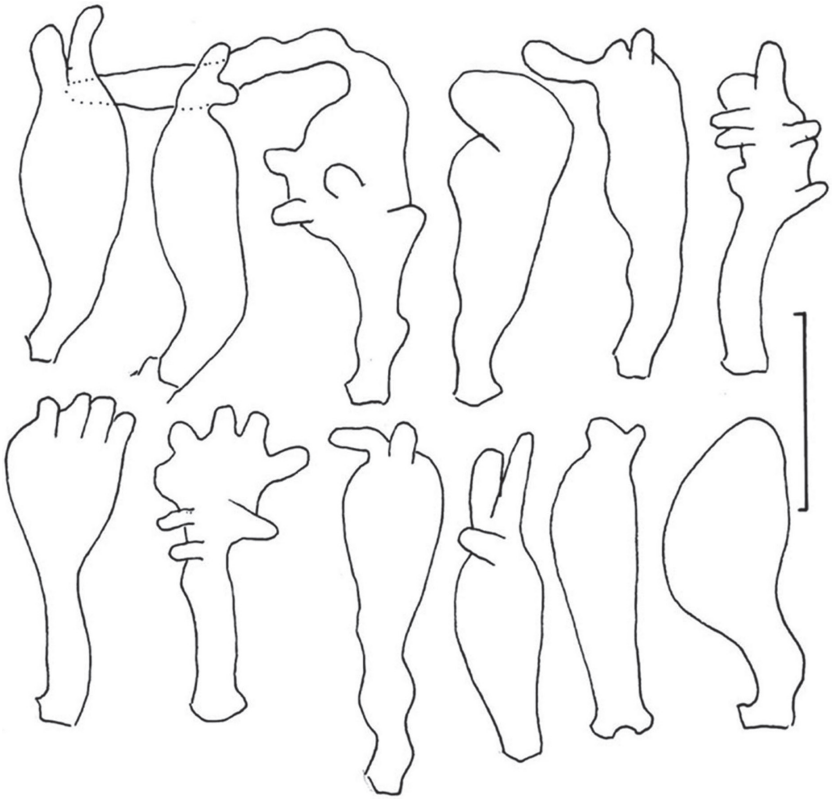

Figure 15. *Gymnopus portoricensis*. Cheilocystidia. Scale bar: 20 μm. TFB 4548 (TENN-F-051029).

ly defined (not merely as folds). Interlamellar anastomoses are absent and even lamellar buttressing is missing. Instead, the interlamellar hymenophore is smooth.

These two collections fruited on very different substrata. The origin within bamboo structures would be difficult to imagine, so perhaps basidiomata arise from a very thin, arachnoid mycelium on the bamboo surface. Rare basidiomata were seen attached to rhizomorphs, which might support typical attachment to somatic hyphae.

If *G. portoricensis* is regarded as in *Marasmius*, the epithet (*portoricensis*) is preoccupied by *Marasmius portoricensis* Murrill in Pennington. 1915. North American Flora 9(4): 262. The homonym is in *Marasmius* but not in *Gymnopus*. Described as having the longest ("longissimus") stipe – 6–8 cm × 0.5 mm – and pileus 4–10 mm broad, the holotype of *Marasmius portoricensis* is at NY (isotype MICH) and the Mycoportal record shows several long-stiped basidiomata with stipe yellow-orange and apparently several long, straight rhizomorphs of similar colour.

An ITS-based clade (Fig. 2), which includes *Gymnopus neobrevipes*, *G. portoricensis*, two environmental sequences from Okinawa and a sequence of *Gymnopus cremeostipitatus* from Korea, is sister to the rest of *Gymnopus* sect. *Androsacesi*. This section continues to expand with additional taxa yet to be determined and described.

Auxiliary specimen examined. United States, Puerto Rico, Caribbean National Forest, El Junque, road to Verada Bisley, 18°15'53"N, 65°45'13"W V.1992, coll RHP, TFB 4512 (TENN-F-050999).

Discussion

Singer (1948) proposed *Micromphale* sect. *Rhizomorphigena* based, in part, on his perception of gelatinisation of tissues in the pileus of the type species, *Marasmius westii* Murrill, (1945). Desjardin (1989) and Desjardin and Petersen (1989) concluded that diagnostic characters of *M. brevipes* matched those of *M. westii* and nomenclaturally, the epithet *brevipes* took priority. Moreover, these same characters more closely resembled those of *Marasmius* sect. *Androsacei* Kühner (1933) than those of *Micromphale* and they transferred Singer's section as *Marasmius* sect. *Rhizomorphigena*.

César et al. (2018) considered *Marasmius brevipes* and *M. westii* as taxonomic synonyms and transferred the latter as *Gymnopus westii*. Based on our current examination of the type specimen of *M. westii* (FLAS-F-17211), we reject this synonymy. Some differences: 1) Hymenial elements are without clamp connections in *M. westii* while clamp connections are common in all tissues in *M. brevipes* (Desjardin and Petersen 1989 and this study); 2) pleurocystidia are not mammilate; 3) rhizomorphs are considerably thinner than those of *G. neobrevipes*; and 4) Murrill's notes with the type of *M. westii* describe rhizomorphs as "aerial" (i.e. suspended above ground level) while those of *G. neobrevipes* are at or near ground level, predominantly bound to fallen substrate with some aerial elements.

References

Antonín V, Noordeloos ME (2010) A monograph of Marasmioid and Collybioid fungi in Europe. IHV-Verlag, Berlin, 480 pp.

Antonín V, Ryoo R, Ka K-H (2014) Marasmioid and gymnopoid fungi of the Republic of Korea. 7. *Gymnopus* sect. *Androsacei*. Mycological Progress 13: 703–718. https://doi.org/10.1007/s11557-013-0953-z

Berkeley MJ, Curtis MA (1853) Centuries of North American fungi. Ann Mag Nat Hist, ser 2 12: 417–435. https://doi.org/10.1080/03745485709495068

César E, Bandala VM, Montoya L, Ramos A (2018) A new *Gymnopus* species with rhizomorphs and its record as nesting material by birds (*Tyrannideae*) in the subtropical cloud forest from eastern Mexico. Mycokeys 42: 21–34. https://doi.org/10.3897/mycokeys.42.28894

Dennis RWG (1951) Some Agaricaceae if Trinidad and Venezuela. Leucosporae. Part. I. Transactions of the British Mycological Society 34: 411–482. https://doi.org/10.1016/S0007-1536(51)80030-5

Dennis RWG (1953) Some pleurotoid fungi from the West Indies. Kew Bull 8: 31–45. https://doi.org/10.2307/4117153

Desjardin DE (1989) The genus *Marasmius* from the southern Appalachian Mountains. PhD Theis, University of Tennessee, Knoxville, 839 pp. https://trace.tennessee.edu/utk_graddiss/2513/

Desjardin DE (1990) Culture morphology of *Marasmius* species. Sydowia 42: 17–87.

Desjardin DE, Horak E (1997) *Marasmius* and *Gloiocephala* in the South Pacific region: Papua New Guinea, New Caledonia, and New Zealand taxa. Bibliotheca Mycologica 168: 1–152.

Desjardin DE, Petersen RH (1989) Studies on *Marasmius* from eastern North America. III. *Marasmius brevipes* and *Micromphale* sect. *Rhizomorphigena*. Mycologia 81: 76–84. https://doi.org/10.1080/00275514.1989.12025628

Desjardin DE, Retnowati A, Horak E (2000) Agarics of Indonesia. 2. A preliminary monograph of *Marasmius* from Java and Bali. Sydowia 52: 92–193.

Kornerup A, Wanscher JH (1967) Methuen handbook of colour (2nd edn). Methuen Co, London, 243 pp.

Kühner R (1933) Etudes sur le genre *Marasmius*. Le Botaniste 25: 57–116.

Mata JL, Hughes KW, Petersen RH (2004) Phylogenetic placement of *Marasmiellus juniperinus*. Mycoscience 45: 214–221. https://doi.org/10.1007/S10267-004-0170-3

Mata JL, Hughes KW, Petersen RH (2007) An investigation of /omphalotaceae (Fungi: Euagarics) with emphasis on the genus *Gymnopus*. Sydowia 58(2): 191–289.

Pegler DN (1983) Agaric flora of the Lesser Antilles. Kew Bulletin, Additional Series 9.

Pegler DN (1987) A revision of the Agaricales of Cuba. I. Species described by Berkeley and Curtis. Kew Bull 42: 501–585. https://doi.org/10.2307/4110064

Pegler DN (1988) A revision of the Agaricales of Cuba. 3. Keys to families, genera and species. Kew Bulletin 43: 53–75. https://doi.org/10.2307/4118036

Petch T (1947) A revision of Ceylon Marasmii. Transactions of the British Mycological Society 31: 21–44. https://doi.org/10.1016/S0007-1536(47)80004-X

Petersen RH, Hughes KW (2016) *Micromphale* sect. *Perforantia* (Agaricales, Basidiomycetes); Expansion and phylogenetic placement. Mycokeys 18: 1–122. https://doi.org/10.3897/mycokeys.18.10007

Petersen RH, Hughes KW (2017) Corrigenda for: "*Micromphale* sect. *Perforantia* (Agaricales, Basidiomycetes); Expansion and phylogenetic placement" Mycokeys 19: 45–54. https://doi.org/10.3897/mycokeys.19.11565

Retnowati A (2018) The species of *Marasmiellus* (Agaricales: Omphalotaceae) from Java and Bali. Gardens' Bulletin Singapore 70(1): 191–258. https://doi.org/10.26492/gbs70(1).2018-17

Ridgway R (1912) Color standards and color nomenclature. Publ. Priv., Washington, DC., 53 pp. https://doi.org/10.5962/bhl.title.144788

Singer R (1948) Diagnoses fungorum novorum Agaricalium. Sydowia 2: 26–42.

Singer R (1976) *Marasmieae*. (Basidiomycetes – Tricholomataceae). Flora neotropica monog. 17: 1–347.

Tkalčec Z, A Mešic (2013) Studies of two Corner types (*Marasmius nigroimplicatus* and *M. subrigidichorda*) and new *Gymnopus* combinations. Mycotaxon 123: 419–429. https://doi.org/10.5248/123.419

Wilson AW, Desjardin DE (2005) Phylogenetic relationships in the gymnopoid and marasmioid fungi (Basidiomycetes. Euagarics clade). Mycologia 97: 667–679. https://doi.org/10.1080/15572536.2006.11832797

MycoKeys 45: 25–39 (2019)
doi: 10.3897/mycokeys.45.29964
http://mycokeys.pensoft.net

RESEARCH ARTICLE

A peer-reviewed open-access journal
MycoKeys
Launched to accelerate biodiversity research

Lactifluus bicapillus (Russulales, Russulaceae), a new species from the Guineo-Congolian rainforest

Eske De Crop[1], Jonas Lescroart[1], André-Ledoux Njouonkou[2], Ruben De Lange[1], Kobeke Van de Putte[1], Annemieke Verbeken[1]

1 *Research Group Mycology, Department of Biology, Ghent University, Ghent, Belgium* **2** *Department of Biological Sciences, Faculty of Sciences, University of Bamenda, Cameroon*

Corresponding author: *Eske De Crop* (eske.decrop@ugent.be)

Academic editor: *B. Dentinger* | Received 21 September 2018 | Accepted 18 December 2018 | Published 28 January 2019

Citation: De Crop E, Lescroart J, Njouonkou A-L, De Lange R, Van de Putte K, Verbeken A (2019) *Lactifluus bicapillus* (Russulales, Russulaceae), a new species from the Guineo-Congolian rainforest. MycoKeys 45: 25–39. https://doi.org/10.3897/mycokeys.45.29964

Abstract

The milkcap genus *Lactifluus* is one of the most common ectomycorrhizal genera within Central African rainforests. During a field trip to the Dja Biosphere Reserve in Cameroon, a new *Lactifluus* species was found. Molecular and morphological analyses indicate that the species belongs to *Lactifluus* section *Xerampelini* and we formally describe it here as *Lactifluus bicapillus* **sp. nov.**

Keywords

Ectomycorrhizal fungi, *Gilbertiodendron, Lactarius*, phylogeny, taxonomy, tropical Africa, *Uapaca*

Introduction

Rainforests occur in Central Africa and form the main vegetation type in the Guineo-Congolian region (White 1983). Large parts of southern Cameroon and northern Gabon are covered by rainforest, characterised by high humidity, closed canopies, and competition for light in the understory. Common tree species within these rainfor-

ests, such as the Dja Biosphere Reserve, include ectomycorrhizal (ECM) species from the Phyllanthaceae (e.g. *Uapaca* spp. Baill.) and the Fabaceae (i.e. *Gilbertiodendron dewevrei* (De Wild.) J.Léonard) (Sonké and Couvreur 2014). *Uapaca* species mainly occur mixed with other tree species, whereas *G. dewevrei* forms more or less monodominant stands, mixed with an occasional *Uapaca* species. These trees are typical hosts for ECM fungi and Russulaceae have been repeatedly recorded as associated with these trees (Verbeken and Walleyn 2010; De Crop et al. 2016; Delgat et al. 2017; T.W. Henkel pers. comm.).

Within Central African rainforests, the ECM Russulaceae genera *Russula* Pers. and *Lactifluus* (Pers.) Roussel are abundant (Douanla-Meli and Langer 2009; Verbeken and Buyck 2002; Verbeken et al. 2008; Verbeken and Walleyn 2010). The milkcap genus *Lactifluus* is mainly distributed in the tropics (De Crop et al. 2017). It is a species-rich genus with about 160 species distributed worldwide, of which the majority is found in tropical Asia (Le et al. 2007b; Stubbe et al. 2010; Van de Putte et al. 2010), tropical Africa (Van de Putte et al. 2009; Verbeken and Walleyn 2010; De Crop et al. 2012, 2016; Maba et al. 2014, 2015a, b; Delgat et al. 2017; De Lange et al. 2018) and the Neotropics (Henkel et al. 2000; Miller et al. 2002; Smith et al. 2011; Sá et al. 2013; Sá and Wartchow 2013). The genus is relatively understudied and many species remain undescribed due to this mainly tropical distribution. Furthermore, the genus is known for its many species complexes with morphologically cryptic species (Stubbe et al. 2010; Van de Putte et al. 2010, 2012; De Crop et al. 2014; De Crop et al. 2017).

About 20 *Lactifluus* species are known from the rainforests of Central Africa (Verbeken and Walleyn 2010). The actual diversity is expected to be higher for several reasons: (i) the ECM flora is present in most parts of the tropical African rainforest, (ii) most countries in the region are understudied due to difficult political situations or challenging sampling conditions, (iii) seasonality in the rainforest is less pronounced, which makes it difficult to assess the exact fruiting period of these fungi and the fruiting of fungi can be missed during short sampling periods, and (iv) *Lactifluus* is known for its morphologically cryptic diversity with several species complexes occurring. Traditional species descriptions were often based on morphology and this morphologically cryptic diversity makes it difficult to correctly assess the number of species based on morphology alone.

During fieldwork in Cameroon in 2012 and 2014, several *Lactifluus* specimens were found morphologically resembling yet different from the described species within *L.* subg. *Pseudogymnocarpi* (Pacioni & Lalli) De Crop. The phylogenetic results of De Crop et al. (2017), based on four nuclear genes, revealed that this species is new to science. A preliminary microscopic study confirmed the deviating morphology of the Cameroonian collections and a more detailed study of all available material was initiated. In this study, molecular and morphological examinations were performed, the collections were compared with closely related species, and a new species, *Lactifluus bicapillus*, was described based on these results.

Methods

Sampling

Sampling expeditions in Cameroon were carried out in May 2012 and May 2014, in the Guineo-Congolian rainforest of the Dja Biosphere Reserve (East Region of Cameroon), mainly in the vicinity of Somalomo and Lomié. During each expedition, four collections were made of an unknown and putative new milkcap species with characteristics of *L*. subg. *Pseudogymnocarpi*. The collections were found in either monodominant stands of *Gilbertiodendron dewevrei*, or mixed stands with *Uapaca guineensis* Müll. Arg., *U. acuminata* (Hutch.) Pax & K. Hoffm., and *U. paludosa* Aubrév. & Leandri as the main ECM hosts. Specimens were dried using a field drier and candles. The studied collections were deposited in the fungal herbarium of Ghent University (**GENT**).

Morphology

Macroscopic features were all based on fresh material described in the field. Colour codes refer to Kornerup and Wanscher (1978). Microscopic features were studied from dried material. Morphological terminology followed Verbeken and Walleyn (2010). Elements of the pileipellis and hymenium were mounted in Congo Red in L4. Sections of the pileipellis and stipitipellis were first mounted in 10% KOH to enhance cell expansion and then mounted in Congo Red dissolved in water. Basidium length excludes sterigmata length. Measurements are given as MIN–MAX, except for basidiospores. Basidiospores were measured in side view in Melzer's reagent, excluding the ornamentation, and measurements are given as described in Nuytinck and Verbeken (2005): (MIN) [Ava –2 × SDa] – *Ava* – *Avb* – [Avb + 2 × SDb] (MAX), in which Ava/b = lowest/highest mean value for the measured collections, SDa/b = standard deviation of the lowest/highest mean value. MIN/MAX = lowest/highest value measured and only given when they exceed [Ava –2 × SDa] or [Avb + 2 × SDb] respectively. Q stands for 'quotient length/width' and is given as MINQ – *Qa* – *Qb* – MAXQ, in which Qa/b = lowest/highest mean quotient for the measured specimens, MIN/MAXQ = minimum/maximum value over the quotients of all available measured basidiospores. Line drawings were made with the aid of a drawing tube at the original magnifications: 6000 × for basidiospores (Zeiss axioscop 2 microscope), 1000 × for individual elements and sections (Olympus CX31 microscope).

Phylogenetic analysis

DNA was extracted using the CTAB extraction protocol described in Nuytinck and Verbeken (2003). Protocols for PCR amplification follow Le et al. (2007a). Two nuclear markers that were previously shown to be informative within this subgenus (De

Table 1. Specimens and GenBank accession numbers of DNA sequences used in the molecular analyses. The arrangement of the subgenera and sections in the table follows their position in the concatenated phylogeny of the genus *Lactifluus* (Fig. 1).

Species	Voucher collection (herbarium)	Country	ITS accession no.	LSU accession no.
Genus *Lactifluus*				
Lactifluus* subg. *Pseudogymnocarpi				
Lactifluus* sect. *Pseudogymnocarpi				
L. cf. *longisporus*	AV 11-025 (GENT)	Tanzania	KR364054	KR364181
L. cf. *pseudogymnocarpus*	AV 05-085 (GENT)	Malawi	KR364012	KR364139
L. cf. *pumilus*	EDC 12-066 (GENT)	Cameroon	KR364067	KR364196
L. gymnocarpoides	JD 885 (BR)	Congo	KR364074	KR364203
	AV 05-184 (GENT)	Malawi	KR364024	KR364151
L. hygrophoroides	AV 05-251 (GENT)	North America	HQ318285	HQ318208
L. longisporus	AV 94-557 (Isotype, GENT)	Burundi	KR364118	KR364244
L. luteopus	AV 94-463 (Isotype, GENT)	Burundi	KR364119	None
L. medusae	EDC 12-152 (GENT)	Cameroon	KR364069	KR364198
L. pseudoluteopus	FH 12-026 (GENT)	Thailand	KR364084	KR364214
L. rugatus	EP 1212/7 (LGAM-AUA)	Greece	KR364104	KR364235
L. sudanicus	AV 11-174 (Isotype, GENT)	Togo	HG426469	KR364186
Lactifluus* sect. *Xerampelini				
L. bicapillus sp. nov.	EDC 12-176 (GENT)	Cameroon	KR364070	KR364199
	EDC 12-174 (GENT)	Cameroon	MH549201	MH549201
	EDC 14-245 (GENT)	Cameroon	MH549204	MH549204
	EDC 12-169 (GENT)	Cameroon	MH549200	MH549200
	EDC 14-249 (Holotype, GENT)	Cameroon	MH549203	MH549203
	EDC 14-284 (GENT)	Cameroon	KX499395	None
	EDC 14-238 (GENT)	Cameroon	MH549202	MH549202
	EDC 12-071 (GENT)	Cameroon	KX499396	KX622762
	L6470/Gab40 (env. seq.)	Gabon	FR731875	None
L. cf. *pseudovolemus*	ADK 2927 (GENT)	Benin	KR364113	KR364243
L. goossensiae	AB 320 (GENT)	Guinea	KR364132	KR364252
L. kivuensis	JR Z 310 (Holotype, GENT)	Congo	KR364027	KR364154
L. rubiginosus	JD 959 (BR)	Congo	KR364081	KR364210
	BB 3466 (Holotype, BR)	Zambia	KR364014	KR364250
L. persicinus	EDC 12-001 (Holotype, GENT)	Cameroon	KR364061	KR364190
L. xerampelinus	TS 1116 (Isotype, GENT)	Tanzania	KR364039	KR364166
Clade 8				
L. sp.	JN 2011-012 (GENT)	Vietnam	KR364045	KR364171
	TENN 065929 (TENN)	North America	KR364102	KR364233
L. armeniacus	EDC 14-501 (Isotype, GENT)	Thailand	KR364127	None
L. volemoides	TS 0705 (Holotype, H)	Tanzania	KR364038	KR364165
Lactifluus* sect. *Aurantiifolii				
L. aurantiifolius	AV 94-063 (Isotype, GENT)	Burundi	KR364017	KR364144
Lactifluus* sect. *Rubroviolascentini				
L. aff. *rubroviolascens*	EDC 12-051 (GENT)	Cameroon	KR364066	KR364195
L. carmineus	AV 99-099 (Holotype, GENT)	Zimbabwe	KR364131	KR364251
L. denigricans	EDC 11-218 (GENT)	Tanzania	KR364051	KR364178
L. kigomaensis	AV 11-006 (Holotype, GENT)	Tanzania	KR364052	KR364179

Species	Voucher collection (herbarium)	Country	ITS accession no.	LSU accession no.
L. subkigomaensis	EDC 11-159 (GENT)	Tanzania	KR364050	KR364177
Lactifluus* sect. *Polysphaerophori				
L. pegleri	PAM/Mart 12-091 (LIP)	Martinique	KP691416	KP691425
L. sp.	RC/Guy 09-036 (LIP)	French Guiana	KJ786645	KJ786550
	MR/Guy 13-145	French Guiana	KJ786691	KJ786595
	MCA 3937 (GENT)	Guyana	KR364109	KR364240
L. veraecrucis	M 8025 (Holotype, ENCB)	Mexico	KR364112	KR364241
Lactifluus* subg. *Lactifluus				
Lactifluus* sect. *Lactifluus				
L. corrugis s.l.	AV 05-392 (GENT)	North America	JQ753822	KR364143
L. versiformis	AV-KD-KVP 09-045 (Holotype, GENT)	India	JN388967	JN389031
L. vitellinus	KVP 08-024 (GENT)	Thailand	HQ318236	HQ318144
L. volemus	KVP 11-002 (GENT)	Belgium	JQ753948	KR364175

Crop et al. 2017) were used: (1) the internal transcribed spacer region of ribosomal DNA (ITS), comprising the ITS1 and ITS2 spacer regions and the ribosomal gene 5.8S, using primers ITS-1F and ITS4 (Gardes and Bruns 1993; White et al. 1990) and (2) a part of the ribosomal large subunit 28S region (LSU), using primers LR0R and LR5 (Moncalvo et al. 2000).

PCR products were sequenced using an automated ABI 3730 XL capillary sequencer (Life Technology) at Macrogen. Forward and reverse reads were assembled into contigs and edited where needed with the SEQUENCHER v. 5.0 software (Gene Codes Corporation, Ann Arbor, MI, USA).

A dataset was constructed, containing sequences of these recent collections, together with sequences of *L.* subg. *Pseudogymnocarpi* extracted from the dataset of De Crop et al. (2017). Furthermore, sequences were compared to sequences in the Unite database using Blastn (Abarenkov et al. 2010). One environmental sequence was found within the same Species Hypothesis and was added to the dataset. The outgroup consisted of four species of *L.* subg. *Lactifluus* (Table 1).

Sequences were aligned using the online version of the multiple sequence alignment program MAFFT v. 7 (Katoh and Standley 2013), using the E-INS-I strategy. Trailing ends of the alignment were trimmed and sequences were manually edited when necessary in MEGA 6 (Tamura et al. 2013). The alignment can be acquired from the first author and TreeBASE (S22916, http://purl.org/phylo/treebase/phylows/study/TB2:S22916).

Sequence data were divided into the following partitions: partial 18S, ITS1, 5.8S, ITS2 and partial 28S. Maximum likelihood (ML) analyses were conducted with RAxML v. 8.0.24 (Stamatakis 2014), where a ML analysis was combined with the Rapid Bootstrapping algorithm with 1000 replicates under the GTRCAT option (Stamatakis et al. 2008). All analyses were performed on the CIPRES Science Gateway (Miller et al. 2010).

Results

Our molecular results show that the recently collected specimens form a well-supported monophyletic clade within *Lactifluus* subg. *Pseudogymnocarpi*, *L.* sect. *Xerampelini* (Fig. 1). The species is sister to a well-supported clade of all other species within this section, with *L. xerampelinus* (Karhula & Verbeken) Verbeken being its closest relative. Morphological and ecological data confirm that these collections are different from all other species in *L.* sect. *Xerampelini*, therefore the new species is described here as *Lactifluus bicapillus* sp. nov.

Taxonomy

Lactifluus bicapillus **Lescroart & De Crop**
Mycobank: MB827400
Figs 2–4

Diagnosis. *Lactifluus bicapillus* differs from *L. xerampelinus* by its yellowish-orange to dark red cap, fertile lamella edge, a lampropalisade with two types of terminal elements as pileipellis type, and a distribution in the Guineo-Congolian rainforest.

Holotype. CAMEROON. East Region, Haut-Nyong division, Somalomo subdivision, Dja Biosphere Reserve, alt. ca 640 m, 3°21.83'N, 12°44.18'E, rainforest with *Uapaca paludosa* and *U. guineensis*, 14 May 2014, leg.: De Crop & Verbeken, EDC 14-249 (GENT!).

Basidiocarps medium-sized. **Pileus** 34–79 mm in diameter, firm, infundibuliform to deeply infundibuliform, planoconvex with central depression when younger; margin involute when juvenile, becoming inflexed up to reflexed when older; edge entire, sometimes eroded when older; surface felty to chamois leather-like, often slightly pruinose in the centre, often grooved, concentrically wrinkled, in young specimens completely velutinous and somewhat translucent; rubiginous (7D6–7) in centre, becoming paler and more orange towards the margin (6C5–6 to 5A5–6); young specimens dark reddish or burgundy in centre, to bright orange or yellow at the margin (8F6 to 7B6, to 6A5, 4AG); secondary velum absent. **Stipe** 16–39 × 6–12 mm, cylindrical to slightly tapering downwards, often laterally curved near the base, central to eccentric insertion to pileus, entire or bruised appearance, sometimes with white flocks near the base; surface smooth and felty, sometimes pruinose, yellowish orange (5AB5–6), becoming slightly paler and more yellow near the base and/or lamellae (5A4–5). **Lamellae** intervenose, transvenose, sparingly bifurcating; attachment adnate to decurrent with some lamellae forming a small tooth; juveniles not brittle, rather thin, older specimens brittle to very brittle, thick to very broad; edge entire and concolourous; distant, 3–5 + 6–9 L+l/cm, between 2 lamellae often 3 lamellulae, with regular short long-short pattern; creamy yellow (3A2) to yellowish orange (4A4). **Context** white, with a faint yellow tinge, colour not changing when cut, but in 1 collection (EDC 14-238) becoming brown when damaged, rather solid and full,

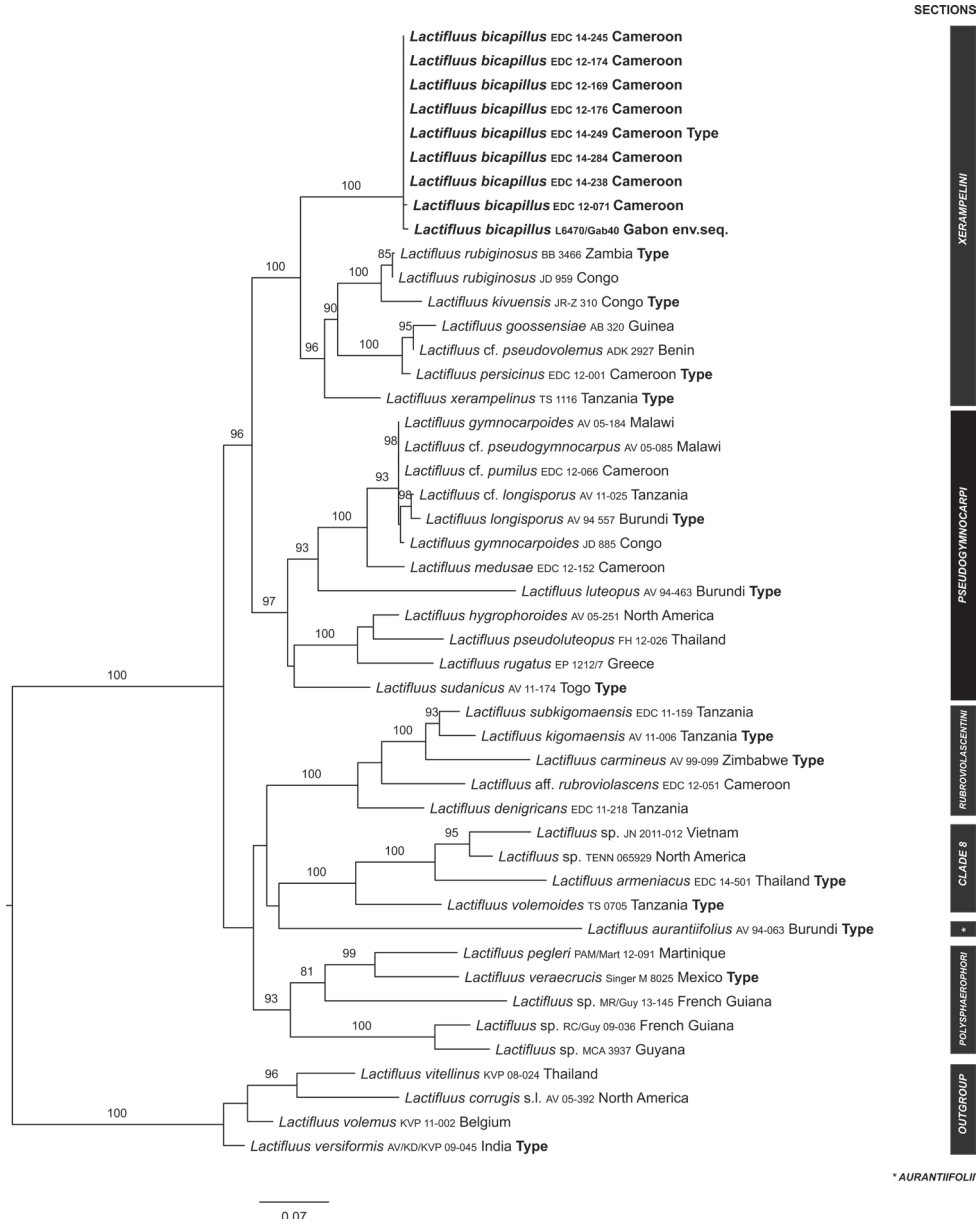

Figure 1. Overview Maximum Likelihood tree of *Lactifluus* subg. *Pseudogymnocarpi*, based on concatenated ITS and LSU sequence data. Sequences of the here described species *Lactifluus bicapillus* are written in bold. Maximum Likelihood bootstrap values > 70 are shown. Numbers of undescribed sections refer to De Crop et al. (2017).

smell sweet or not distinct, taste mild. **Latex** white, somewhat astringent, rather abundant, becomes less abundant and more watery with age, mild, colour rarely changing brownish when isolated. **Chemical reactions** unchanging with Fe_2SO_4; context faint blue after 5 sec. with guaiac.

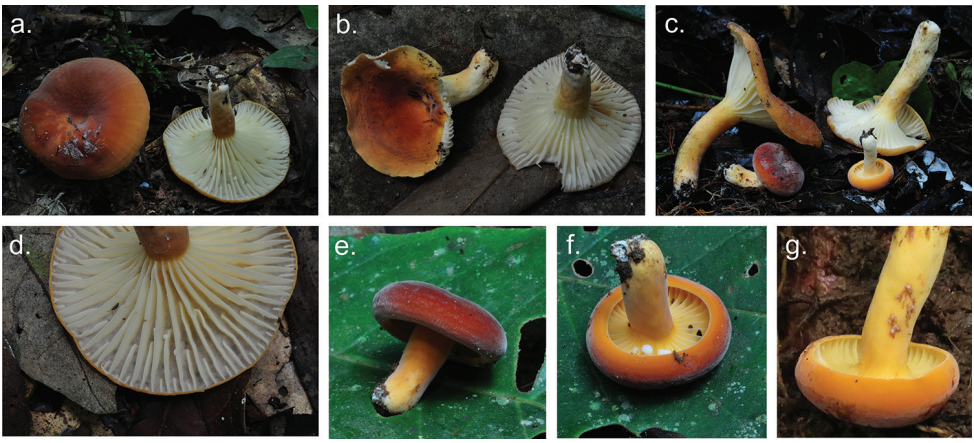

Figure 2. Basidiomata of *Lactifluus bicapillus*. **a–c** Basidiomata of *Lactifluus bicapillus* (EDC 12-176, EDC 12-174, holotype EDC 14-249 resp.) **d** Detail of lamellae (EDC 14-176), e) young specimen (EDC 12-169) **f** Detail of latex (EDC 12-169) **g** Detail of brown colour change of the latex (EDC 14-238) (photographs **a–f** by E. De Crop, **g** by A. Verbeken).

Basidiospores [6.2]–7.3–7.9–[9.6](10.3) × [4.6]–5.5–5.9–[6.8] µm; ellipsoid, with Q = (1.22)1.31–1.39(1.51); ornamentation amyloid, composed of low ridges and warts, up to 0.2 µm high, forming an incomplete to complete reticulum; plage inamyloid or centrally amyloid. **Basidia** 43–62 × 8–12 µm, rather long, narrowly subclavate, 1-, 2- or 4-spored; content oleiferic. **Sterile elements** abundant, 19.5–40 × 3.5–5.5 µm, not emergent, cylindrical, septate with clamp-like bulges under the septum, with rounded apex. **Pleurocystidia** absent. **Pleuropseudocystidia** very scarce in mature specimens, abundant in young specimens, narrowly and irregular cylindrical to flexuose, 3.3–4.6 µm diam., not emerging, apex obtuse, oleiferic content. **Lamellae-edge** fertile, consisting of basidioles with some basidia. Marginal cells absent. **Hymenophoral trama** cellular, with sphaerocytes and abundant lactifers. **Pileipellis** a lampropalisade, up to 275 µm thick; terminal elements of two types, without transitional forms: the first type long and slender, thick-walled and often septate, with a wide base, up to 7 µm, and growing thinner towards the apex, down to 1–2 µm, length 52–92 µm, often narrowing rather abruptly, and twisted; the second type short and broad, also thick-walled and often septate, not specifically narrower towards the apex, often twisted, 20–44 × 5–7 µm; subpellis composed of mostly rounded cells. **Stipitipellis** similar to pileipellis but not as thick; terminal elements of the long type 52–75 × 5–7 µm; terminal elements of the short type 22–29 × 5–7 µm. **Clamp-connections** absent.

Distribution. Known from Cameroon and Gabon.

Ecology. Guineo-Congolian rainforest, scattered on forest floor under *Gilbertiodendron dewevrei*, *Uapaca guineensis*, *U. acuminata*, and *U. paludosa.*

Etymology. A combination of 'bi' and 'capillus', referring to the two types of terminal elements in the pileipellis and stipitipellis.

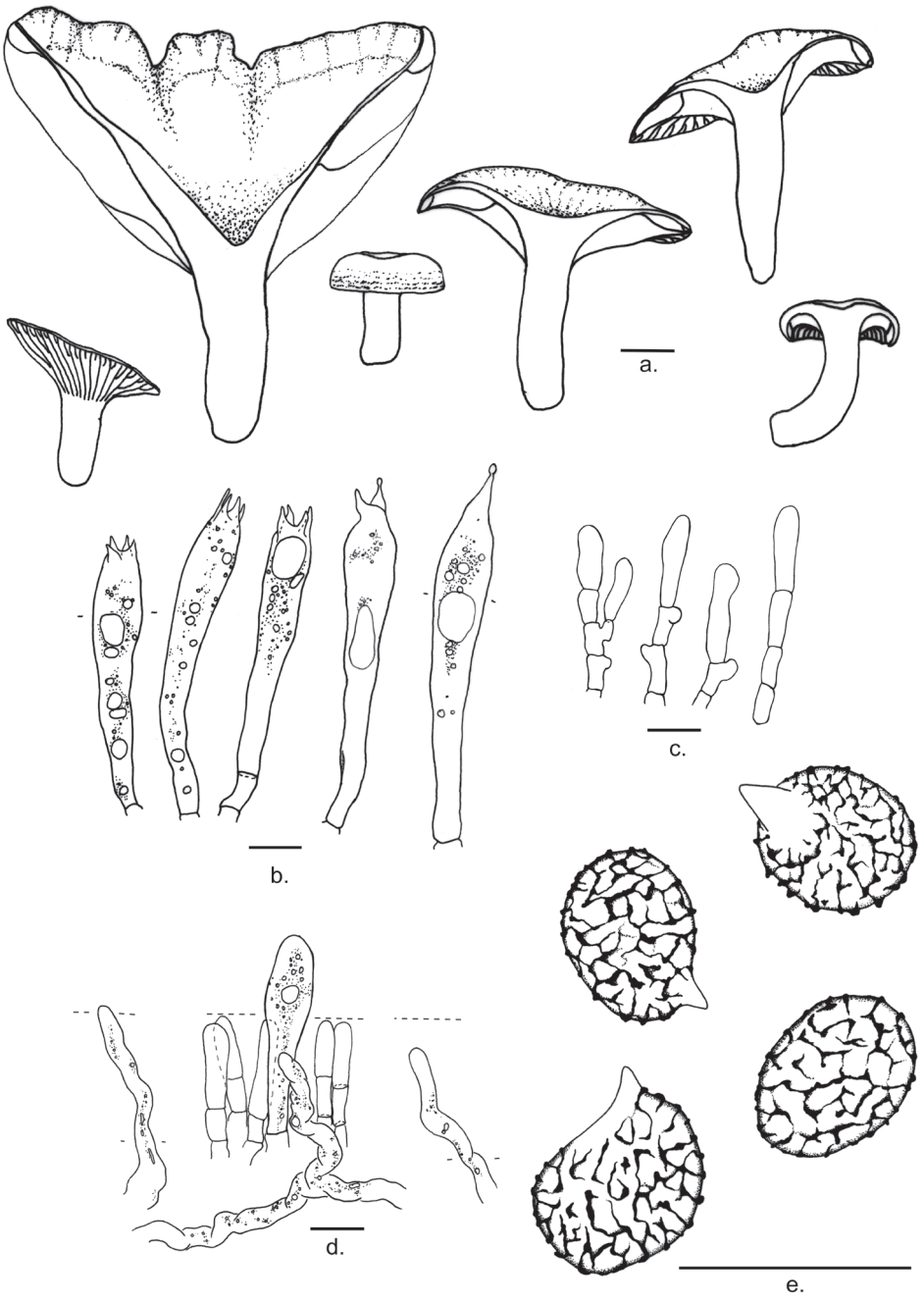

Figure 3. Microscopic features of *Lactifluus bicapillus* **a** Basidiocarps (from EDC 12-071, EDC 12-169, EDC 12-174, EDC 12-176, and EDC 14-249) **b** Basidia (from EDC 12-071, and EDC 14-249) **c** Sterile elements from the hymenium (from EDC 12-169) **d** Pleuropseudocystidia (from EDC 12-169) **e** Basidiospores (from EDC 14-249). Illustrations by E. De Crop, J. Lescroart and A. Verbeken. Scale bar: 10 μm.

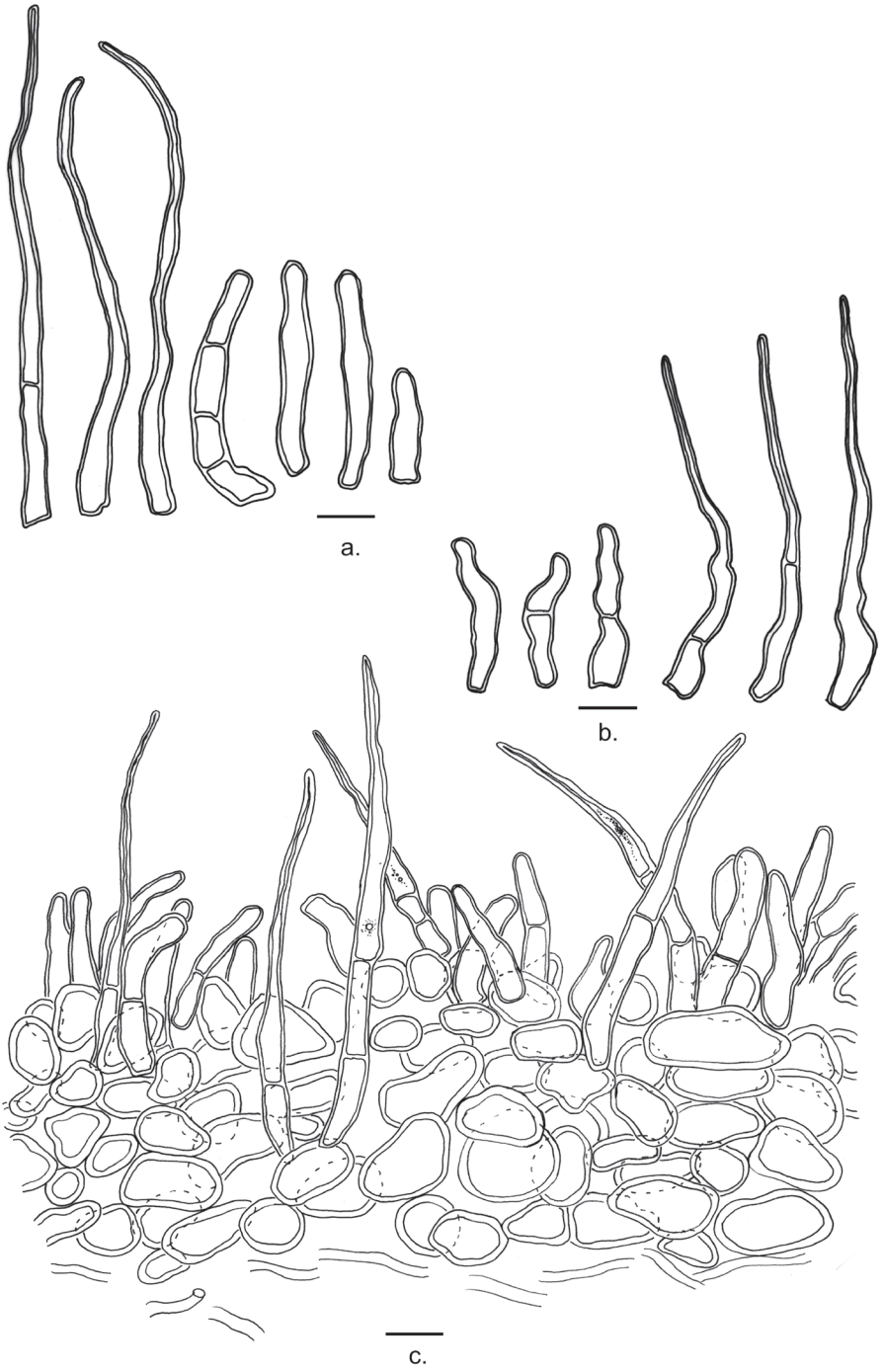

Figure 4. Microscopic features of *Lactifluus bicapillus* (continued) **a** Terminal elements of the pileipellis (from EDC 12-071) **b** Terminal elements of the stipitipellis (from EDC 12-176) **c** Section through the pileipellis (from holotype EDC 14-249). Illustrations by E. De Crop and J. Lescroart. Scale bar: 10 µm.

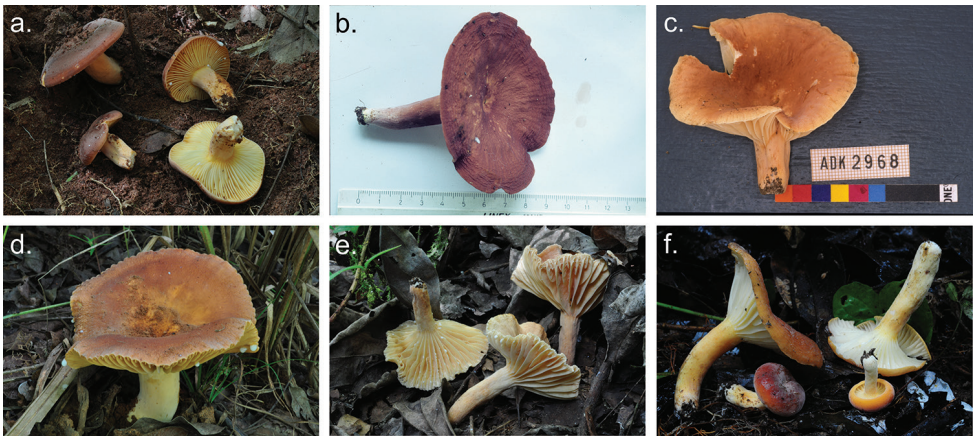

Figure 5. Basidiomata of described species of *Lactifluus* sect. *Xerampelini* **a** *L. xerampelinus* (EDC 11-113) **b** L. *kivuensis* (JR Z 233) **c** L. cf. *pseudovolemus* (ADK 2968) **d** *L. rubiginosus* (EDC 11-120) **e** *L. persicinus* (EDC 12-001, *holotypus*) **f** *L. bicapillus (*EDC 14-249, holotypus) (photographs a, **d–f** by E. De Crop, **b** by J. Rammeloo and **c** by A. De Kesel).

Conservation status. Unknown.

Specimens examined. Cameroon. East Region, Haut-Nyong division, Somalomo subdivision, Koulou village, alt. ca 650 m, 3°23.61'N, 12°44.50'E, rainforest, *Gilbertiodendron dewevrei*, *Uapaca guineensis*, *U. acuminata,* 15 May 2012, De Crop, EDC 12-071 (GENT); East Region, Haut-Nyong division, Lomié subdivision, Bosquet village, alt. ca 610 m, 3°07.82'N, 13°53.36'E, rainforest with many *Uapaca* trees, on a riverbank, *Uapaca guineensis*, 24 May 2012, De Crop, EDC 12-169 (GENT); Ibidem, *Gilbertiodendron dewevrei*, De Crop, EDC 12-174 (GENT); Ibidem, *Uapaca guineensis*, EDC 12-176 (GENT); East Region, Haut-Nyong division, Somalomo subdivision, Dja Biosphere Reserve, alt. ca 650 m, 3°21.90'N, 12°44.15'E, rainforest, *Uapaca paludosa, U. guineensis,* 14 May 2014, De Crop & Verbeken, EDC 14-238 (GENT); Ibidem, alt. ca 640 m, 3°21.83'N, 12°44.18'E, De Crop & Verbeken, EDC 14-249 (GENT); Ibidem, alt. ca 650 m, 3°19.87'N, 12°45.42'E, rainforest, near the river, *Uapaca sp.*, 17/05/2014, De Crop & Verbeken, EDC 14-284 (GENT).

Discussion

Lactifluus bicapillus is recognized in the field by its yellowish-orange to dark-red cap, a concolourous or somewhat paler stipe, yellow lamellae, and unchanging white latex. *L. bicapillus* is placed in *L.* subg. *Pseudogymnocarpi, L.* sect. *Xerampelini*. Species in this section are characterized by yellowish-orange to reddish-brown caps, a palisade-like structure as pileipellis, the absence of true pleurocystidia, and generally low ornamented basidiospores (not higher than 0.2 µm) ranging from verrucose to almost completely reticulate (De Crop et al. 2017). *Lactifluus bicapillus* perfectly concurs with

these morphological characteristics, providing additional support for its placement in *L.* sect. *Xerampelini*.

Lactifluus sect. *Xerampelini* is exclusively known from Africa and contains six described species (Fig. 5): *L. goossensiae* (Beeli) Verbeken, *L. kivuensis* (Verbeken) Verbeken, *L. persicinus* Delgat & De Crop, *L. pseudovolemus* (R. Heim) Verbeken, *L. rubiginosus* (Verbeken) Verbeken, and *L. xerampelinus* (Verbeken and Walleyn 2010; Delgat et al. 2017).

Lactifluus bicapillus differs in ecology from all but one species of *L.* sect. *Xerampelini*. Species from this section occur in woodlands, gallery forests and rainforests (Verbeken and Walleyn 2010). *Lactifluus xerampelinus* and *L. rubiginosus* are found in miombo woodland in East Africa, while *L. goossensiae* is known from both Sudanian woodland and Central African gallery forests. *Lactifluus persicinus* and *L. pseudovolemus* occur in West African gallery forests. Both *L. kivuensis* and *L. bicapillus* are found in the Guineo-Congolian rainforest, associated with *Gilbertiodendron dewevrei* and *Uapaca* species.

Macroscopically, *L. bicapillus* differs from the other species of this section by a combination of bright cap colours, which vary from dark red to bright orange near the edge, cream white lamellae and pale yellow-orange stipe colours in adult basidiocarps (Fig. 5).

All species from *L.* sect. *Xerampelini* have ellipsoid to elongate basidiospores, with amyloid ornamentation composed of very low warts and ridges (up to 0.2 µm high) that are isolated, aligned or forming an incomplete reticulum. All seven species have long and slender basidia, mostly cylindrical and 4-spored. However, 1- and 2-spored basidia are present in *L. bicapillus*, *L. persicinus*, and *L. pseudovolemus.* True cystidia are absent in all species. Pleuropseudocystidia are scarce in *L. bicapillus*, *L. persicinus*, and *L. kivuensis*, abundant in the other species. These pleuropseudocystidia are occasionally emergent in all species; however, emergent pleuropseudocystidia were not observed in *L. bicapillus*. *Lactifluus persicinus* and *L. bicapillus* have a fertile lamellar edge, whilst the others have a sterile lamellar edge (or unknown in *L. pseudovolemus* and *L. goossensiae*).

All species of this section have palisade-like structures as pileipellis. *Lactifluus bicapillus*, *L. persicinus*, and *L. goossensiae* have a lampropalisade with thick-walled terminal elements. *Lactifluus pseudovolemus* has a palisade in which the elements of the pileipellis are slightly thickened. *Lactifluus kivuensis*, *L. xerampelinus*, and *L. rubiginosus* have a palisade to trichopalisade, with only thin-walled elements of the pileipellis. Only *Lactifluus bicapillus*, *L. persicinus*, and *L. goossensiae* have terminal elements that are narrow near the apex. Furthermore, *L. bicapillus* is the only species within this section with two types of terminal elements in the pilei- and stipitipellis.

With the finding of *Lactifluus bicapillus*, *L.* sect. *Xerampelini* now contains seven described species, all from sub-Saharan Africa. Together with the recently described *L. persicinus* (Delgat et al. 2017), *L. bicapillus* was found during two sampling expeditions in Cameroon. Even though those expeditions only covered a small area of the Guineo-Congolian rainforest and gallery forests, we collected at least five species new to science (De Crop et al. 2017). This highlights the large *Lactifluus* diversity in Africa, with many areas still unexplored and probably many new species still to be found.

Acknowledgements

The first author is supported by the "Special Research Fund Ghent University" (BOF, grants B/13485/01 and BOF-PDO-2017-001201). The 2012 survey in Cameroon was financially supported by the Faculty Committee Scientific Research (FCWO) of Ghent University. The 2014 survey in Cameroon was financially supported by the Research Foundation Flanders (FWO, grant V416214N) and by the King Leopold III Fund for Nature Exploration and Conservation. We express our gratitude to all who helped during fieldwork, especially to the conservators and Ecogards in post in the Dja Biosphere Reserve (from 2012 to 2014) and Mr Tchana Tchonkui Merlin. We would like to thank Viki Vandomme for conducting lab work. We thank André De Kesel and Jan Rammeloo for providing pictures of *Lactifluus* species. We thank the reviewers and the editor for their constructive suggestions and detailed comments on the manuscript.

References

Abarenkov K, Nilsson RH, Larsson KH, Alexander IJ, Eberhardt U, Erland S, Hoiland K, Kjoller R, Larsson E, Pennanen T, Sen R, Taylor AFS, Tedersoo L, Ursing BM, Vralstad T, Liimatainen K, Peintner U, Koljalg U (2010) The UNITE database for molecular identification of fungi – recent updates and future perspectives. New Phytologist 186: 281–285. https://doi.org/10.1111/j.1469-8137.2009.03160.x

De Crop E, Nuytinck J, Van de Putte K, Lecomte M, Eberhardt U, Verbeken A (2014) *Lactifluus piperatus* (Russulales, Basidiomycota) and allied species in Western Europe and a preliminary overview of the group worldwide. Mycological Progress 13: 493–511. https://doi.org/10.1007/s11557-013-0931-5

De Crop E, Nuytinck J, Van de Putte K, Wisitrassameewong K, Hackel J, Stubbe D, Hyde KD, Roy M, Halling RE, Moreau PA, Eberhardt U, Verbeken A (2017) A multi-gene phylogeny of *Lactifluus* (Basidiomycota, Russulales) translated into a new infrageneric classification of the genus. Persoonia 38: 58–80. https://doi.org/10.3767/003158517X693255

De Crop E, Tibuhwa D, Baribwegure D, Verbeken A (2012) *Lactifluus kigomaensis* sp. nov. from Kigoma province,Tanzania. Cryptogamie Mycologie 33: 421–426. https://doi.org/10.7872/crym.v33.iss4.2012.421

De Crop E, Van de Putte K, De Wilde S, Njouonkou AL, De Kesel A, Verbeken A (2016) *Lactifluus foetens* and *Lf. albomembranaceus* sp. nov. (Russulaceae): look-alike milkcaps from gallery forests in tropical Africa. Phytotaxa 277: 159–170. https://doi.org/10.11646/phytotaxa.277.2.3

De Lange R, De Crop E, Delgat L, Tibuhwa D, Baribwegure DAV (2018) *Lactifluus kigomaensis* and *L. subkigomaensis*: two look-alikes in Tanzania. Mycoscience 59: 371–378. https://doi.org/10.1016/j.myc.2018.02.004

Delgat L, De Crop E, Njouonkou AL, Verbeken A (2017) Lactifluus persicinus sp. nov. from the gallery forests of West Cameroon. Mycotaxon 132: 471–483. https://doi.org/10.5248/132.471

Douanla-Meli C, Langer E (2009) Fungi of Cameroon II. Two new Russulales species (Basidiomycota). Nova Hedwigia 88: 491–502. https://doi.org/10.1127/0029-5035/2009/0088-0491

Gardes M, Bruns TD (1993) ITS primers with enhanced specificity for Basidiomycetes – application to the identification of mycorrhizae and rusts. Molecular Ecology 2: 113–118. https://doi.org/10.1111/j.1365-294X.1993.tb00005.x

Henkel TW, Aime MC, Miller SL (2000) Systematics of pleurotoid Russulaceae from Guyana and Japan, with notes on their ectomycorrhizal status. Mycologia 92: 1119–1132. https://doi.org/10.2307/3761479

Katoh K, Standley DM (2013) MAFFT Multiple Sequence Alignment Software version 7: improvements in performance and usability. Molecular Biology and Evolution 30: 772–780. https://doi.org/10.1093/molbev/mst010

Kornerup A, Wanscher JH (1978) Methuen Handbook of Colour. Methuen, London.

Le HT, Nuytinck J, Verbeken A, Lumyong S, Desjardin DE (2007a) *Lactarius* in northern Thailand: 1. *Lactarius* subgenus *Piperites*. Fungal Diversity 24: 173–224.

Le HT, Verbeken A, Nuytinck J, Lumyong S, Desjardin DE (2007b) *Lactarius* in northern Thailand: 3. *Lactarius* subgenus *Lactoriopsis*. Mycotaxon 102: 281–291.

Maba DL, Guelly AK, Yorou NS, Agerer R (2015a) Diversity of *Lactifluus* (Basidiomycota, Russulales) in West Africa: 5 new species described and some considerations regarding their distribution and ecology. Mycosphere 6: 737–759. https://doi.org/10.5943/mycosphere/6/6/9

Maba DL, Guelly AK, Yorou NS, Verbeken A, Agerer R (2014) Two New *Lactifluus* species (Basidiomycota, Russulales) from Fazao Malfakassa National Park (Togo, West Africa). Mycological Progress 13: 513–524. https://doi.org/10.1007/s11557-013-0932-4

Maba DL, Guelly AK, Yorou NS, Verbeken A, Agerer R (2015b) Phylogenetic and microscopic studies in the genus *Lactifluus* (Basidiomycota, Russulales) in West Africa, including the description of four new species. IMA Fungus 6: 13–24. https://doi.org/10.5598/imafungus.2015.06.01.02

Miller MA, Pfeiffer W, Schwartz T (2010) Creating the CIPRES Science Gateway for Inference of Large Phylogenetic Trees. Proceedings of the Gateway Computing Environments Workshop (GCE): 1–8. https://doi.org/10.1109/GCE.2010.5676129

Miller SL, Aime MC, Henkel TW (2002) Russulaceae of the Pakaraima Mountains of Guyana – I New species of pleurotoid *Lactarius*. Mycologia 94: 545–553. https://doi.org/10.2307/3761789

Moncalvo JM, Lutzoni FM, Rehner SA, Johnson J, Vilgalys R (2000) Phylogenetic relationships of agaric fungi based on nuclear large subunit ribosomal DNA sequences. Systematic-Biology 49: 278–305. https://doi.org/10.1093/sysbio/49.2.278

Nuytinck J, Verbeken A (2003) *Lactarius sanguifluus* versus *Lactarius vinosus* – molecular and morphological analyses. Mycological Progress 2: 227–234. https://doi.org/10.1007/s11557-006-0060-5

Nuytinck J, Verbeken A (2005) Morphology and taxonomy of the European species in *Lactarius* sect. *Deliciosi* (Russulales). Mycotaxon 92: 125–168.

Sá MCA, Baseia IG, Wartchow F (2013) *Lactifluus dunensis*, a new species from Rio Grande do Norte, Brazil. Mycosphere 4: 261–265. https://doi.org/10.5943/mycosphere/4/2/9

Sá MCA, Wartchow F (2013) *Lactifluus aurantiorugosus* (Russulaceae), a new species from Southern Brazil. Darwiniana (nueva serie) 1: 54–60.

Smith ME, Henkel TW, Aime MC, Fremier AK, Vilgalys R (2011) Ectomycorrhizal fungal diversity and community structure on three co-occurring leguminous canopy tree species in a Neotropical rainforest. New Phytologist 192: 699–712. https://doi.org/10.1111/j.1469-8137.2011.03844.x

Sonké B, Couvreur TLP (2014) Tree diversity of the Dja Faunal Reserve, southeastern Cameroon. Biodivers Data Journal 2: e1049. https://doi.org/10.3897/BDJ.2.e1049

Stamatakis A (2014) RAxML version 8: a tool for phylogenetic analysis and post-analysis of large phylogenies. Bioinformatics 30: 1312–1313. https://doi.org/10.1093/bioinformatics/btu033

Stamatakis A, Hoover P, Rougemont J (2008) A rapid bootstrap algorithm for the RAxML web servers. Systematic Biology 57: 758–771. https://doi.org/10.1080/10635150802429642

Stubbe D, Nuytinck J, Verbeken A (2010) Critical assessment of the *Lactarius gerardii* species complex (Russulales). Fungal Biology 114: 271–283. https://doi.org/10.1016/j.funbio.2010.01.008

Tamura K, Stecher G, Peterson D, Filipski A, Kumar S (2013) MEGA6: Molecular evolutionary genetics analysis version 6.0. Molecular Biology and Evolution 30: 2725–2729. https://doi.org/10.1093/molbev/mst197

Van de Putte K, De Kesel A, Nuytinck J, Verbeken A (2009) A new *Lactarius* species from Togo with an isolated phylogenetic position. Cryptogamie Mycologie 30: 39–44.

Van de Putte K, Nuytinck J, Das K, Verbeken A (2012) Exposing hidden diversity by concordant genealogies and morphology – a study of the *Lactifluus volemus* (Russulales) species complex in Sikkim Himalaya (India). Fungal Diversity 55: 171–194. https://doi.org/10.1007/s13225-012-0162-0

Van de Putte K, Nuytinck J, Stubbe D, Huyen TL, Verbeken A (2010) *Lactarius volemus* sensu lato (Russulales) from northern Thailand: morphological and phylogenetic species concepts explored. Fungal Diversity 45: 99–130. https://doi.org/10.1007/s13225-010-0070-0

Verbeken A, Buyck B (2002) Diversity and ecology of tropical ectomycorrhizal fungi in Africa. In: Watling R, Frankland JC, Ainsworth AM, Isaac S, Robinson C (Eds) Tropical Mycology. Vol. 1, 11–24.

Verbeken A, Stubbe D, Nuytinck J (2008) Two new *Lactarius* species from Cameroon. Cryptogamie Mycologie 29: 137–143.

Verbeken A, Walleyn R (2010) Monograph of *Lactarius* in Tropical Africa. National Botanic Garden, Belgium, 161 pp. [154 pls]

White JC (1983) The Vegetation of Africa. A Descriptive Memoir to Accompany the UNESCO/AETFAT/UNSO Vegetation Map of Africa. UNESCO, Paris, 356 pp.

White TJ, Bruns T, Lee S, Taylor JW (1990) Amplification and direct sequencing of fungal ribosomal RNA genes for phylogenetics. In: Innis MA, Gelfand DH, Sninsky JJ, White TJ (Eds) PCR Protocols: a Guide to Methods and Applications. Academic Press, New York, 315–322. https://doi.org/10.1016/B978-0-12-372180-8.50042-1

MycoKeys 45: 41–56 (2019)
doi: 10.3897/mycokeys.45.32549
http://mycokeys.pensoft.net

RESEARCH ARTICLE

A peer-reviewed open-access journal
MycoKeys
Launched to accelerate biodiversity research

Morphology and multigene phylogeny of *Talaromyces amyrossmaniae*, a new synnematous species belonging to the section *Trachyspermi* from India

Kunhiraman C. Rajeshkumar[1], Neriman Yilmaz[2,3], Sayali D. Marathe[1], Keith A. Seifert[2]

1 *National Fungal Culture Collection of India (NFCCI), Biodiversity and Palaeobiology (Fungi) Gr., Agharkar Research Institute, G.G. Agarkar Road, Pune, 411 004, Maharashtra, India* **2** *Biodiversity (Mycology), Ottawa Research and Development Centre, Agriculture and Agri-Food Canada, 960 Carling Ave., Ottawa, Ontario, K1A 0C6, Canada* **3** *Department of Microbiology and Plant Pathology, Forestry and Agricultural Biotechnology Institute (FABI), University of Pretoria, Pretoria, South Africa*

Corresponding author: *Kunhiraman C. Rajeshkumar* (rajeshfungi@gmail.com)

Academic editor: *P. Crous* | Received 19 December 2018 | Accepted 26 December 2018 | Published 28 January 2019

Citation: Rajeshkumar KC, Yilmaz N, Marathe SD, Seifert KA (2019) Morphology and multigene phylogeny of *Talaromyces amyrossmaniae*, a new synnematous species belonging to the section *Trachyspermi* from India. MycoKeys 45: 41–56. https://doi.org/10.3897/mycokeys.45.32549

Abstract

A new *Talaromyces* species, *T. amyrossmaniae*, isolated from decaying fruit and litter of *Terminalia bellerica*, is described and illustrated. On the natural substrate, the new species produces determinate synnemata, with a well-defined, vivid orange red to orange red cylindrical stipe, and a greyish green capitulum. Conidiophores are typically biverticillate, or sometimes have subterminal branches, with acerose phialides that produce globose to subglobose, smooth to slightly roughened conidia. Multigene phylogenetic analyses based on the internal transcribed spacer region (ITS), and partial sequences of β-tubulin (*BenA*), calmodulin (*CaM*), and DNA directed RNA polymerase second large subunit (*RPB2*) genes, along with morphological characterization, revealed that these isolates are distinct and form a unique lineage of *Talaromyces* in section *Trachyspermi*, closely allied to *T. aerius*, *T. albobiverticillius*, *T. heiheensis*, *T. erythromellis*, and *T. solicola*. The new species *T. amyrossmaniae* is the first species in section *Trachyspermi* with determinate synnemata.

Keywords

BenA, *CaM*, conidial fungi, *RPB2*, synnemata, *Trichocomaceae*, Western Ghats

Introduction

The genus *Talaromyces* was described as a teleomorph-based holomorph genus (Benjamin 1955). It is characterized by cleistothecial ascomata that have a soft hyphal exterior giving them a yellow, cream, pink or reddish coloration; its anamorphs are predominantly biverticillate or rarely terverticillate conidiophores with acerose phialides with a narrow mouth (Samson et al. 2011, Yilmaz et al. 2014). Conventionally, species of *Talaromyces* were linked with *Penicillium*, *Paecilomyces*, *Geosmithia*, and *Merimbla* anamorphs (Pitt 1980, Pitt et al. 2000). Primary phylogenetic studies of *Talaromyces* spp. revealed that they form a distinct clade that includes species formerly classified in *Penicillium* subgenus *Biverticillium*, separate from *Eupenicillium* and *Penicillium* spp. in other subgenera (LoBuglio et al. 1993; Seifert et al. 1993; Berbee et al. 1995; Peterson 2000; Heredia et al. 2001; Seifert et al. 2004). As redefined following the new single name provision of the International Code of Nomenclature of algae, fungi and plants (ICN), *Talaromyces* was expanded to include asexual species formerly included in *Penicillium* subgenus *Biverticillium* (Samson et al. 2011; Visagie and Jacobs 2012; Visagie et al. 2012; Yilmaz et al. 2012, 2014). The landmark multigene phylogeny of *Penicillium* and allied genera by Houbraken and Samson (2011) segregated the prevailing concept of the family Trichocomaceae into three families, Aspergillaceae, Thermoascaceae, and Trichocomaceae. *Talaromyces* sensu stricto is presently classified in the Trichocomaceae along with *Thermomyces*, *Sagenomella*, *Rasamsonia*, and *Trichocoma*. The molecular taxonomy and nomenclature *Talaromyces* were comprehensively revised in the recent past (Houbraken and Samson 2011; Samson et al. 2011; Seifert et al. 2012; Visagie and Jacobs 2012; Visagie et al. 2012; Yilmaz et al. 2012; Yilmaz et al. 2014). Yilmaz et al. (2014) resolved the phylogenetic positioning of *Talaromyces* species using a polyphasic taxonomic concept and placing 88 accepted species in seven well-defined sections, namely *Bacillispori*, *Helici*, *Islandici*, *Purpurei*, *Subinflati*, *Talaromyces*, and *Trachyspermi*. Subsequent to the monograph by Yilmaz et al. (2014), 54 new *Talaromyces* species have been described from all over the world (Visagie et al. 2015; Chen et al. 2016; Luo et al. 2016; Crous et al. 2016; Romero et al. 2016; Wang et al. 2016; Wang et al. 2016; Yilmaz et al. 2016a, b; Crous et al. 2017; Guevara-Suarez et al. 2017; Peterson and Jurjević 2017; Wang et al. 2017; Barbosa et al. 2018; Su and Niu 2018; Jiang et al. 2018; Varriale et al. 2018).

During the 2009 monsoon season, routine surveys were conducted to explore microfungal diversity in natural forests of Lingmala waterfalls area (17.9218N; 73.6870E) of Mahabaleshwar, northern Western Ghats, India. A previously undescribed synnema-forming fungus with penicillate conidiophores and phialidic conidiogenous cells was collected from decaying fruits and litter of *Terminalia bellerica* (*Combretaceae*) fallen onto the ground near the Lingmala waterfalls. The fungus was isolated into pure culture on different culture media, microscopic characters were recorded and its classification studied using phylogenetic analysis of aligned DNA sequences from the nuclear ribosomal ITS region and *BenA*, *CaM*, and *RPB2* partial gene sequences. This paper aims to resolve the taxonomy and phylogeny of this synnematous species, which is shown to represent a new species in *Talaromyces* section *Trachyspermi*, here named *T. amyrossmaniae.*

Materials and methods

Isolation

Conidia were removed from synnemata directly from the surface of fallen fruits under a Nikon stereomicroscope (model SMZ1500 with Digital camera; Nikon, Tokyo, Japan) and placed on malt extract agar (MEA) media containing the antibiotic Streptomycin sulphate (100 mg/L) CMS220-5G (HIMEDIA Laboratories Pvt. Ltd, Mumbai, India). Methods and media used for examining colony characters, inoculating and incubating cultures, and microscopic examination followed those of Visagie et al. (2014), with the addition of Oatmeal Agar (OA), and Potato Dextrose Agar (PDA), with incubation occurring in a Bio Multi Incubator (Model LH-30-8CT, Japan). Herbarium specimens were deposited in the Ajrekar Mycological Herbarium (AMH); cultures were accessioned and preserved in the National Fungal Culture Collection of India (NFCCI; WDCM-932), Agharkar Research Institute, Pune, India. Reference and ex-type strains used in this study are listed in Table 1.

Morphology

Colony characters were recorded after 7 d of incubation on various media, including Czapek yeast autolysate agar (CYA), Blakeslee's (1915) malt extract agar (MEAbl), yeast extract sucrose agar (YES), oatmeal agar (OA), and creatine sucrose agar (CREA). Bacto malt extract was used for MEAbl. Media preparation, inoculations, incubation conditions, and microscopic preparations followed the recommendations by Visagie et al. (2014). Colour codes and names used in descriptions are from Kornerup and Wanscher (1967). Microscopic observations were made with an Olympus (Model CX-41, Japan) dissecting microscope and Zeiss (AXIO Imager 2, Germany) compound microscope equipped with Nikon Digital sight DS-Fi1 and AxioCam MRc5 cameras driven by AxioVision Rel 4.8 software (AXIO Imager 2, Germany).

DNA extraction, amplification, and phylogenetic analyses

Colonies were grown on MEAbl plates, and genomic DNA was extracted following the rapid salt extraction method of Aljanabi and Martinez (1997). The ITS regions was amplified using primer pairs ITS5 and ITS4 (White et al. 1990). For the amplification of *RPB2* gene region, primer pairs RPB2-5F and RPB2-7cR (Liu et al. 1999) were used with touch-up PCR conditions: 5 cycles with annealing temperature 48 °C followed by 5 cycles at 50 °C and final 25 cycles at 52 °C. The partial *BenA* gene was amplified with primer pair Bt2a and Bt2b (Glass and Donaldson 1995) with 50 °C as annealing temperature. The partial *CaM* gene was amplified using primer pair CF1M

Table 1. Accession numbers for fungal strains and strains used for the phylogenetic analysis.

Species	Collection no.	Substrate and origin	GenBank accession no.			
			ITS	*BenA*	*CaM*	*RPB2*
T. aerius	CBS 140611[T]	Indoor air, China	KU866647	KU866835	KU866731	KU866991
T. albobiverticillius	CBS 133440[T]	Decaying leaves of a broad leaved tree, Taiwan	HQ605705	KF114778	KJ885258	KM023310
	CBS 140498	Air from HVAC system, China	KR855658	KR855648	KR855653	KR855663
T. amyrossmaniae	**NFCCI 1919[T]**	**Fallen decaying fruits of *Terminalia bellerica* (Combretaceae), Maharashtra, India**	**MH909062**	**MH909064**	**MH909068**	**MH909066**
	NFCCI 2351	**Fallen decaying fruits of *Terminalia bellerica* (Combretaceae), Maharashtra, India**	**MH909063**	**MH909065**	**MH909069**	**MH909067**
T. assiutensis	CBS 147.78[T]	Soil, Egypt	JN899323	KJ865720	KJ885260	KM023305
	CBS 645.80	*Gossypium*, India	JN899334	KF114802	*	*
T. atroroseus	CBS 133442[T]	House dust, South Africa	KF114747	KF114789	KJ775418	KM023288
	CBS 133449	Mouse dung, Denmark	KF114744	KF114788	*	*
T. austrocalifornicus	CBS 644.95[T]	Soil, USA	JN899357	KJ865732	KJ885261	*
T. brasiliensis	CBS 142493[T]	Honey of *Melipona scutellaris*; Recife, Pernambuco, Brazil	MF278323	LT855560	LT855563	LT855566
T. convolutus	CBS 100537[T]	Soil, Nepal	JN899330	KF114773	*	JN121414
T. diversus	CBS 320.48[T]	Leather, USA	KJ865740	KJ865723	KJ885268	KM023285
	DTO 244-E6	House dust, New Zealand	KJ775712	KJ775205	*	*
T. erythromellis	CBS 644.80[T]	Soil from creek bank, New South Wales	JN899383	HQ156945	KJ885270	KM023290
T. heiheensis	HMAS 248789[T]	Rotten wood, China	KX447526	KX447525	KX447532	KX447529
T. minioluteus	CBS 642.68[T]	Unknown	JN899346	KF114799	KJ885273	JF417443
	CBS 270.35	*Zea mays*, USA	KM066172	KM066129	*	*
	CBS 137.84	Fruit damaged by insect, Spain	KM066171	KF114798	*	*
T. minnesotensis	CBS 142381[T]	Human ear, USA	LT558966	LT559083	LT795604	LT795605
T. solicola	DAOM 241015[T]	Soil, South Africa	FJ160264	GU385731	KJ885279	KM023295
	CBS 133446	Soil, South Africa	KF114730	KF114775	*	*
T. systylus	BAFCcult3419[T]	Soil, Argentina	KP026917	KR233838	KR233837	*
T. trachyspermus	CBS 373.48[T]	Unknown, USA	JN899354	KF114803	KJ885281	JF417432
	CBS 118437	Soil, Morocco	KM066169	KM066127	*	*
T. ucrainicus	CBS 162.67[T]	Unknown	JN899394	KF114771	KJ885282	KM023289
	CBS 127.64	Soil treated with cyanimide, Germany (ex-type of *T. ohiensis*)	KM066173	KF114772	*	*
T. udagawae	CBS 579.72[T]	Soil, Japan	JN899350	KF114796	KX961260	*

[T]: ex-type strain

and CF4 (Hubka et al. 2014) subjected to 32 cycles under the following temperature regime: first cycle at 95 °C for 3 min, 55 °C for 30 seconds, and 72 °C for 1 min; followed by 30 cycles at 95 °C for 30 seconds, 55 °C for 30 seconds, 72 °C for 1 min; and a final cycle at 95 °C for 30 seconds, 55 °C for 30 seconds, and 72 °C for 10 min. PCR products were purified with StrataPrep PCR Purification Kit (Agilent Technologies, TX, USA) and sequenced using the BigDye Terminator v. 3.1 Cycle Sequencing Kit (Applied Biosystems, USA). Sequencing reactions were run on a ABI PRISM® 3100 Genetic Analyzer (Applied Biosystems, USA).

Sequence alignment and phylogenetic analysis

Reference sequences of *Talaromyces* section *Trachyspermi* were downloaded from GenBank and aligned in MAFFT v. 7.305b (Katoh and Standley 2013) with the newly generated sequences. Alignments were manually adjusted in Geneious as needed. A Maximum Likelihood analysis was done in IQtree v. 1.6 (Nguyen et al. 2015) after selecting the most suitable substitution model with the Modelfinder (Kalyaanamoorthy) algorithm built into the software. The trees were visualized in Figtree v. 1.4.3 ((http://tree.bio.ed.ac.uk/software/figtree) and edited for publication in Affinity Designer v. 1.6.1 (Serif Europe Ltd, UK). The new DNA sequences were deposited in GenBank (Table 1).

Results

Phylogenetic analyses

The phylogenetic analysis showed that the new species described below as *Talaromyces amyrossmaniae* belongs to section *Trachyspermi*. The relationships of the new species with accepted species and its genetic coherence and phylogenetic consistency were analysed with single concatenated sequence datasets based on four loci (ITS, *BenA, CaM* and *RPB2*). The length of the data sets were 540 bp for ITS, 379 bp for *BenA*, 550 bp for *CaM*, and 851 bp for *RPB2* loci. The best fitting models for the ML analysis were TPM2u+F+I+G4 for ITS, TIM2e+G4 for *BenA*, K2P+I+G4 for *CaM*, and K2P+I+G4 for *RPB2*. All trees were rooted with *T. pinophilus* (CBS 631.66). The single gene trees and the multigene phylogram are shown in Figures 1, 2.

Because of the limited resolution of the official fungal DNA barcode, the ITS (Schoch et al. 2012), in the *Trichocomaceae*, *BenA* was proposed as the secondary DNA barcode for *Talaromyces* (Yilmaz et al. 2014). The overall tree topologies of ITS and *BenA* phylogenies had relatively consistent association of species. However, the type species of section *Trachyspermi*, *T. trachyspermus* was well separated from *T. assiutensis* in the *BenA* analysis whereas strains of the two species were intermixed in the ITS analysis. *Talaromyces ucraicinus* was consistently a sister clade to *T. trachyspermus* and *T. assiutensis.* Our proposed new species, *T. amyrossmaniae*, was distinguished from other species both by ITS and other markers (Figs 1, 2). It is consistently included in a major clade along with *T. aerius*, *T. albobiverticillius*, *T. erythromellis*, *T. heiheensis*, and *T. solicola* in the ITS analysis. As with the ITS, in the concatenated phylogeny and *RPB2* analyses, *T. amyrossmaniae* clustered with *T. albobiverticillius*, *T. heiheensis*, *T. erythromellis*, *T. aerius*, and *T. solicola* (Figs 1, 2). However, in the *BenA* phylogeny, *T. amyrossmaniae* was segregated from that major-clade. *Talaromyces amyrossmaniae* is clustered with *T. austrocalifornicus in* the *CaM* analyses (Fig. 1). Yilmaz et al. (2014) mentioned that amplification of *CaM* is difficult in section *Trachyspermi*. *CaM* data

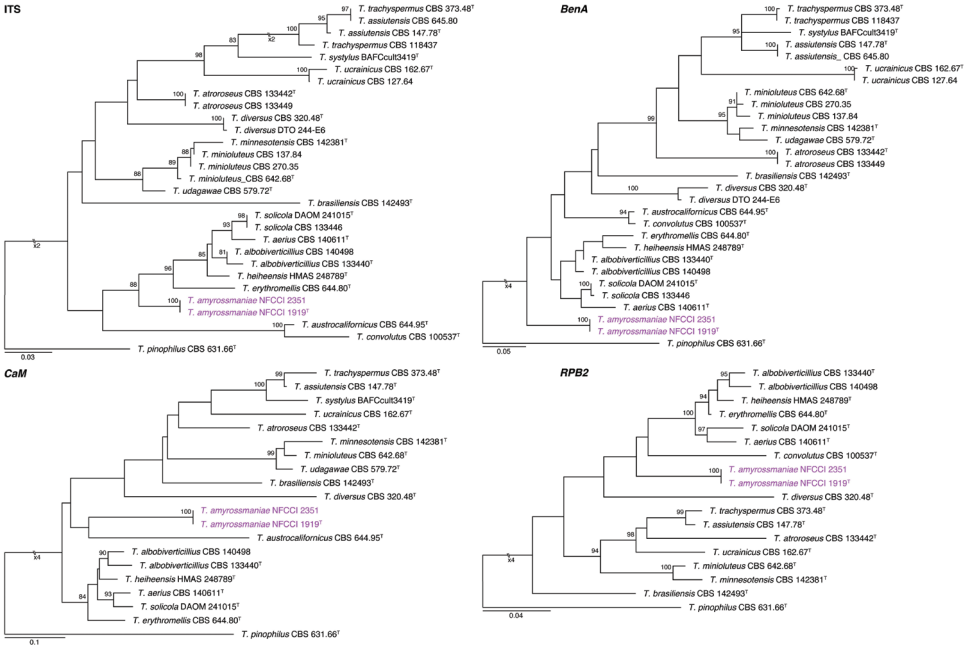

Figure 1. Maximum likelihood (ML) phylogenetic trees of ITS region, *BenA, CaM* and *RPB2* genes of strains belong *Talaromyces* section *Trachyspermi*. *Talaromyces pinophilus* (CBS 631.66^{T}) was chosen as outgroup. Bootstrap values above 70% are indicated. Purple names indicate *T. amyrossmaniae* strains. ^{T}: ex-type.

could not be analyzed critically because the new sequences generated through Sanger sequencing (ABI PRISM 3100 Genetic Analyzer) contained a homopolymer stretch of around 30 bp after base 320, resulting in poor quality and short sequences, even after many attempts using modified PCR conditions and primers.

Morphology

In this study, we introduce one new species, *Talaromyces amyrossmaniae* belonging to section *Trachyspermi*. Strains conform with the general morphological characters of this section. *Talaromyces amyrossmaniae* was compared with its close relatives, with the distinguishing characters mentioned in the note after the species description. Also, Table 2 compares the new species with the closely allied species in section *Trachyspermi*. The main character that differentiates *T. amyrossmaniae* from other synnemata-producing species in the genus *Talaromyces* is the length of the synnemata. *Talaromyces amyrossmaniae* has the shortest synnemata (up to 150 µm). A synopsis of comparative morphology and growth rate of synnema producing species of *Talaromyces* is given in Table 3.

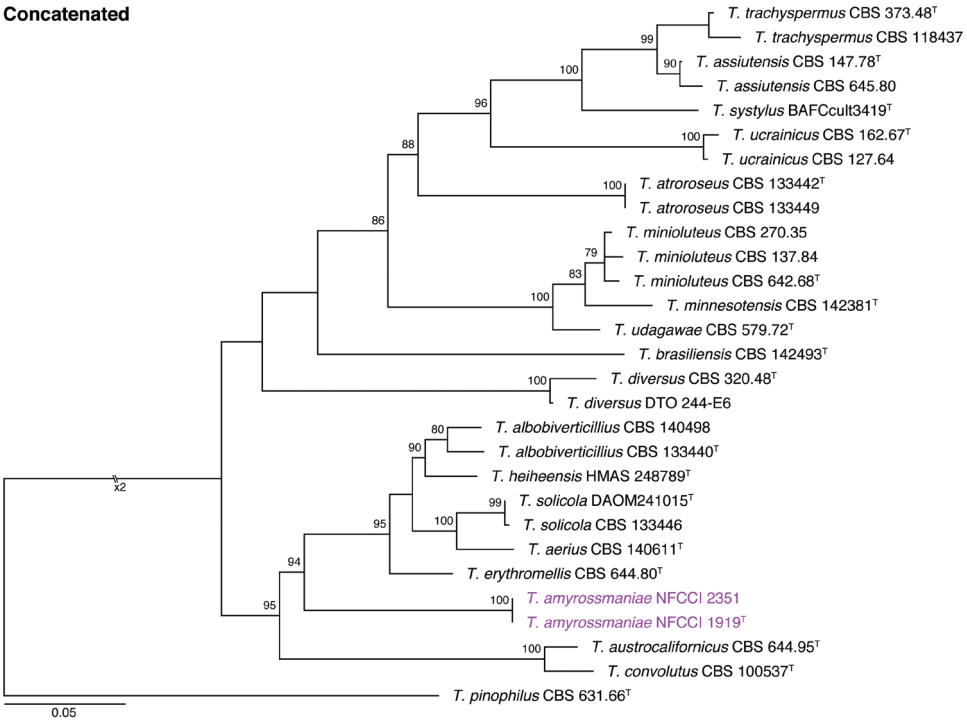

Figure 2. Maximum likelihood (ML) combined phylogenetic trees using ITS region, *BenA, CaM* and *RPB2* genes of strains belong *Talaromyces* section *Trachyspermi*. *Talaromyces pinophilus* (CBS 631.66^{T}) was chosen as outgroup. Bootstrap values above 70% are indicated. Purple names indicate *T. amyrossmaniae* strains. ^{T}: ex-type.

Taxonomy

Talaromyces amyrossmaniae **Rajeshkumar, Yilmaz & Seifert, sp. nov.**
MycoBank MB518601
Figure 3

Etymology. Latin, named after Dr Amy Y. Rossman, in honour of her career as a research leader in Systematic Mycology and Microbiology, USDA ARS, Beltsville, Maryland, USA.

Diagnosis. Synnemata abundant in nature, determinate, 90–120 µm tall, with an unbranched stalk 10–35 µm wide, base wider, up to 50–60 µm. Synnema stipe orange red or vivid orange red, capitulum terminal, compact, globose with conidiophores and a powdery grey-green conidial mass in closely packed, split columns. On MEAbl synnemata produced after 2 weeks incubation, up to 120 µm long. Conidiophores biverticillate, with sometime terverticilate sub-branches. Acerose phialides producing

Table 2. Comparative morphology of *Talaromyces* section *Trachyspermi*.

Species	Conidiophore branching	Conidia ornamentation	Conidial shape	Conidial size (µm)
T. aerius	Biverticillate, minor proportion with subterminal branches	Smooth	Ellipsoidal	2–3.5 (–4.5) × 2–3
T. albobiverticillius	Biverticillate, minor proportion with subterminal branches	Smooth to finely roughened	Globose to subglobose	2–3.5 (–4) × 1.5–2.5
T. amyrossmaniae	**Biverticillate, minor proportion with subterminal branches**	**Smooth to finely roughened**	**Globose or subglobose**	**2.5–4 (–6) × 2.5–3.5 (–8)**
T. assiutensis	Mono to biverticillate	Smooth	Ovoidal to ellipsoidal	2–4 × 1.5–2.5
T. atroroseus	Biverticillate, minor proportion with subterminal branches	Finely roughened to rough	Ellipsoidal	2–3.5 × 1.5–2.5
T. austrocalifornicus	Biverticillate	Smooth	Subglobose	1.5–3 × 1.5–2.5
T. brasiliensis	Biverticillate	Finely roughened	Globose	2 × 3
T. convolutus	Mono to biverticillate	Smooth	Ellipsoidal	(2–) 3–4 × 1.5–2 (–3)
T. diversus	Biverticillate, minor proportion with subterminal branches	Smooth to finely roughened	Subglobose to ellipsoidal	2–3 (–5) × 2–3 (–3.5)
T. erythromellis	Biverticillate having symmetrical subterminal branches,	Smooth	Subglobose to ellipsoidal	2–3.5 × 1.5–2.5
T. heiheensis	Biverticillate with subterminal branches, minor proportionquaterverticillate	Smooth	Subglobose to ellipsoidal	2.5–3 × 2–2.5
T. minioluteus	Biverticillate	Smooth	Ellipsoidal	2.5–4 × 1.5–2.5
T. minnesotensis	Biverticillate	Smooth	Ellipsoidal	2.5–3.5 × 2–3
T. solicola	Biverticillate	Rough	Globose to subglobose	2–3.5 × 2–2.5
T. systylus	Biverticillate	Rough	Globose	3.5 × 4
T. trachyspermus	Mono to biverticillate	Smooth	Ellipsoidal	2–3.5 (–5) × 1.5–2.5
T. ucrainicus	Mono to biverticillate	Smooth	Broadly ellipsoidal to ovoidal	2–4 (–5) × 1.5–2.5 (–3)
T. udagawae	Biverticillate	Smooth	Subglobose to ellipsoidal	3–4 × 2–3

smooth to slightly roughened globose to subglobose conidia. Restricted growth on all media, acid production absent on CREA.

In: *Talaromyces* section *Trachyspermi*.

Type. INDIA, Maharashtra, Mahabaleshwar, Lingmala falls; isolated from fallen decaying fruits and litter of *Terminalia bellerica* (*Combretaceae*), 9 June 2009, isolated by K.C.Rajeshkumar, holotype: AMH 9330, extype: NFCCI 1919, other culture NFCCI 2351.

Gene sequences: ex-holotype MH909062(ITS), MH909064(*BenA*), MH909068(*CaM*), MH909066(*RPB2*).

Description. Colony diameter, 7 d (mm): CYA 4–6; CYA 37 °C no growth; ME-Abl 12–14; YES 5–7; DG18 4–5; OA 10–13; CREA 3–5.

Colony characters: CYA 25 °C, 7 d: colonies low, plane; margins low, entire (< 1 mm); mycelia white; no germination; sporulation absent; soluble pigmentation absent;

Table 3. Synopsis of comparative morphology and growth rate of synnema producing species of *Talaromyces*.

Species	Section	Synnemata				Growth rates (mm)		
		Shape	Time of production	Height (µm)	Acid production on CREA	CYA 25 °C	CYA 37 °C	MEA 25 °C
T. amyrossmaniae[a]	*Trachyspermi*	Determinate	Prolonged	Up to 150	Absent	4–6	No growth	12–14
T. calidicanius[b]	*Talaromyces*	Determinate	Prolonged	Up to 6000	Moderate	27–30	No growth	47–48
T. cecidicola[b]	*Purpurei*	Determinate	Prolonged	Up to 1250	Absent	33–34	No growth	37–38
T. cholorolomа[b]	*Purpurei*	Determinate	Prolonged	Up to 1200	Weak to moderate	40–45	No growth	45–48
T. coalescens[b]	*Purpurei*	Determinate	Prolonged	Up to 1200	Very weak	32–34	2–4	43–45
T. dendriticus[b]	*Purpurei*	Determinate	Prolonged	Up to 5000	Absent	23–26	5–6	35–36
T. duclauxii[b]	*Talaromyces*	Indeterminate	After 7d	Up to 5000	Weak	25–27	3–4	48–50
T. flavovirens[b]	*Talaromyces*	Determinate, covered or masked by yellow mycelial covering	Prolonged	Up to 750	Absent	19–20	5–6	37–38
T. palmae[b]	*Subinflati*	Indeterminate	Prolonged	Up to 8000	Weak	20–25	No growth	22–26
T. panamensis[b]	*Talaromyces*	Determinate, cone shaped and often sterile	After 7d	Up to 6800	Strong	23–24	No growth	28–30
T. pittii[b]	*Purpurei*	Determinate, phototropic	Prolonged	Up to 1000	Absent	34–36	No growth	42–44
T. pseudostromaticus[b]	*Purpurei*	Determinate	Prolonged	Up to 8000	Absent	25–34	No growth	38–43
T. ramulosus[b]	*Purpurei*	Determinate	Prolonged	Up to 500	Absent	32–40	5–8	45–48
T. systylus[c]	*Trachyspermi*	Indeterminate	Prolonged	Up to 4000	Good	14–18	16–19	18–21

[a]: Data from this study. [b]: Data from Yilmaz et al. (2014). [c]: Data from Romero et al. (2016).

exudates absent; reverse Yellowish white (4A2). MEAbl 25 °C, 7 d: colonies low, slightly raised, synnemata present; margins low, entire (1 mm); mycelia white; texture velvety; sporulation dense (except margins); conidia en masse Dull green (27D4–27E4); soluble pigmentation yellow; exudates orange to reddish orange small droplets; reverse Hazel brown (6E6) at center fading into Light brown (6D8) to Light yellow (3A5). YES 25 °C, 7 d: colonies slightly raised, sulcate, sunken at center; margins low, entire (< 1 mm); mycelia pale pinkish red, with and appearance of Pastel red (7A4–7A5); texture floccose; sporulation absent; soluble pigmentation absent; exudates absent; reverse Light brown (7D6). DG18 25 °C, 7 d: colonies slightly raised, sulcate, sunken at center; margins low, entire (1 mm); mycelia pale yellow; texture floccose; sporulation moderately dense at center, margins absent; conidia en masse Greyish green to Dull green (26C4–26D4); soluble pigmentation absent; exudates absent; reverse Brownish orange to Brownish yellow (5C6) in the center, fading into Light yellow (4A5). OA 25 °C, 7 d: colonies low, plane; margins low, entire (< 1 mm); mycelia white; texture velvety; sporulation moderately dense at center, margins absent; conidia en masse Greyish green (27C4–27D4); soluble pigmentation dark red; exudates absent; reverse Brown (7E8) in the centre, fading into Copper red (7C8). CREA 25 °C, 7 d: acid production absent.

Micromorphology. Determinate synnemata formed after 2 weeks on MEAbl up to 80–150 µm long. Conidiophores biverticillate with a minor proportion having subterminal branches; stipes smooth walled 80–120 × 3–4 µm; extra branches up to 30 µm long;

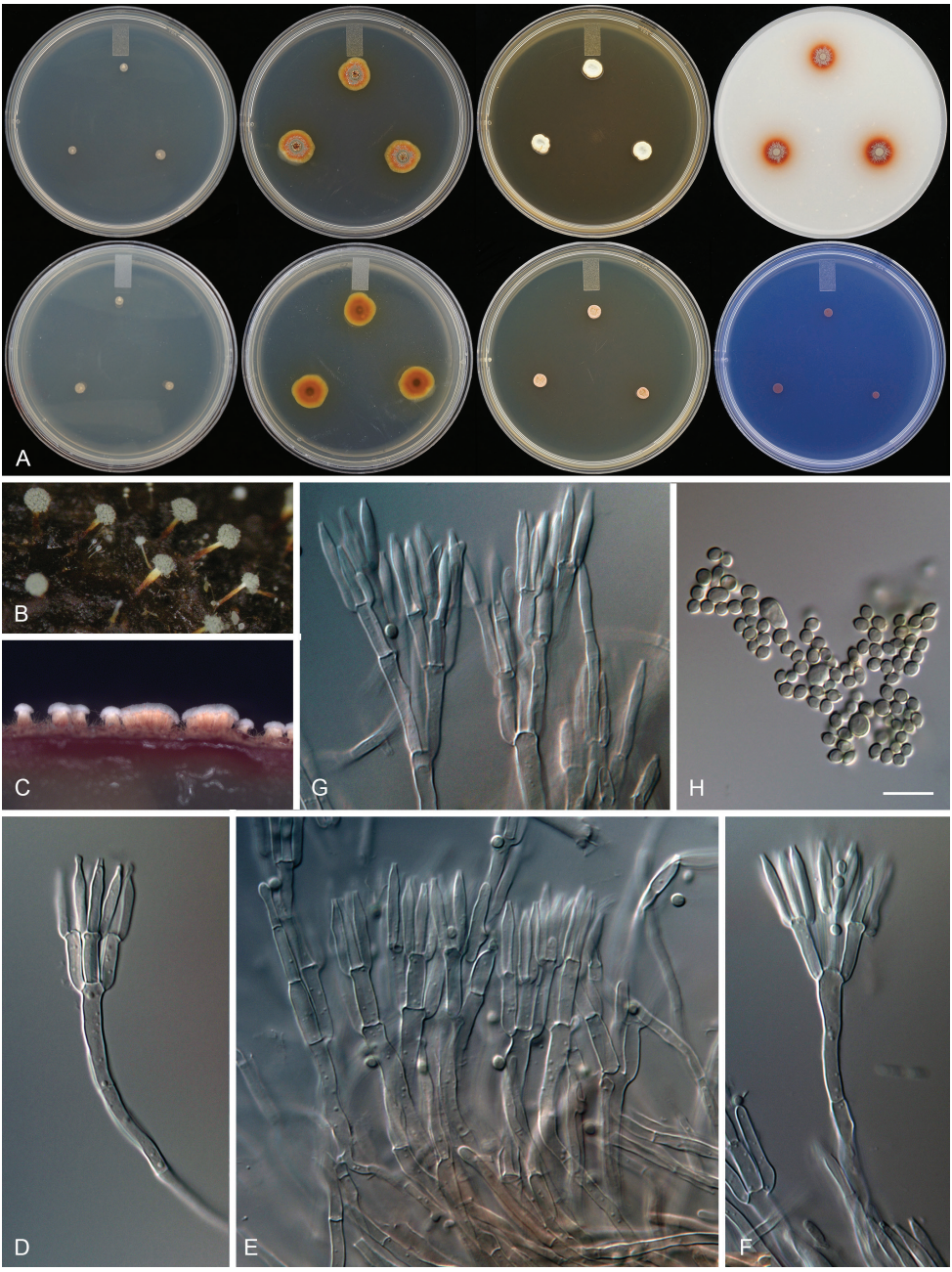

Figure 3. *Talaromyces amyrossmaniae* (NFCCI 1919) **A** Colonies on CYA, MEAbl (obverse and reverse), Colonies obverse on YES, OA, DG18, CREA **B** Synnemata on *Terminalia bellerica* fruit in nature **C** Synnema formation on MEAbl after 14 d at 25 °C **D–F** Biverticillate penicilli **G** Biverticillate penicilli with subterminal branches **H** Conidia. Scale bar: 10 µm.

metulae three to six, divergent, 10–13 × 2.5–3 µm; phialides acerose, three to six per metulae, 12–15 (–18) × 2–3 µm; conidia smooth, globose to subglobose, 2.5–4 × 2.5–3.5 µm. Sometimes it produces large-sized conidia up to 6–8 µm. Ascomata not observed.

Discussion

In our study, a novel *Talaromyces* species, *T. amyrossmaniae* is described based on two isolates from decaying fruits and litter of *Terminalia bellerica* (*Combretaceae*). We used ITS, *BenA*, *CaM* and *RPB2* sequences to apply genealogical concordance phylogenetic species recognition (GCPSR; Taylor et al. 2000) to delineate the species, and a multigene phylogenetic analysis to place *T. amyrossmaniae* in *Talaromyces* section *Trachyspermi*. *Talaromyces* section *Trachyspermi* (as '*trachyspermus*') was introduced by Yaguchi et al. (1996) based on ubiquinone systems, overriding the traditional morphology based classification of *Talaromyces*. Yilmaz et al. (2014) applied multigene phylogenies and morphology to redefine classification of *Talaromyces* and divided the genus into seven sections. They noted that *Talaromyces* section *Trachyspermi* includes species with generally biverticillate penicilli with acerose phialides and when ascomata are produced, they are creamish white or yellow. Colonies generally grow restrictedly on CYA, YES, CREA and DG18; some species have colonies with abundant red pigments.

Morphologically, *T. amyrossmaniae* resembles the other species of section *Trachyspermi* and produces dark orange to red pigmentation on MEAbl, restricted growth on MEAbl, CYA, DG18, YES and CREA, symmetrical biverticillate penicilli with a minor proportion having sub-terminal branches, and acerose phialides that form globose to subglobose, smooth to slightly roughened conidia. Although, synnematous *Talaromyces* species also are found in section *Purpurei*, section *Talaromyces*, section *Trachyspermi*, and section *Subinflati*, *T. amyrossmaniae* is the first species in section *Trachyspermi* with determinate synnemata that are seen on fallen decaying fruits in nature and also on MEAbl after 7–14 d of incubation at 25 °C. *Talaromyces systylus* is another synnema producer in section *Trachyspermi,* but it produces indeterminate synnemata up to 4000 µm and grows at 37 °C (Romero et al. 2016). *Talaromyces amyrossmaniae* has the shortest synnemata in *Talaromyces* and it grows very restrictedly compared to the other synnema producing species on CYA and MEAbl. With these key characters, it is easy to distinguish the new species from the other synnemata producing species of *Talaromyces*.

Based on ITS, *BenA, CaM*, and *RPB2* phylogenies, *T. amyrossmaniae* is part of the same clade as *T. austrocalifornicus*, *T. convolutus*, *T. heiheensis*, *T. aerius*, *T. solicola*, *T. albobiverticillius*, and *T. erythromellis*; however, it can be distinguished from all of these species by having determinate synnemata in nature and by differences in colony growth characteristics. Also, *T. amyrossmaniae* forms predominant concentric rings of synnemata on the different media used in our studies and even forms synnemata in vitro on MEAbl.

Many species of *Talaromyces* have been recorded as saprophytes, endophytes, and human pathogens from different geoclimatic regions and microhabitats across India. Most importantly, *Talaromyces marneffei* is a potentially pathogenic thermally dimorphic fungus causing systemic mycosis in HIV-infected patients; its dissemination was thoroughly studied from Manipur state of India (Singh et al. 1999; Ranjana et al. 2002). Recent studies on endophytic *T. pinophilus* isolated from the rhizomes of *Curcuma amada* from Karnataka revealed the production and partial characterization of L-asparaginase (Krishnapura and Belur 2016). Likewise, endophytic *T. radicus*, isolated from *Catharanthus roseus*, produces vincristine and vinblastine and was studied for induce apoptotic cell death (Palem et al. 2015). *Talaromyces flavus* is also recorded as an endophytic fungi isolated from ethno-medicinal plants in the sacred forests of Meghalaya having antimicrobial and antioxidant activity (Bhagobaty and Joshi 2012). Devi et al. (2014) reported a marine strain of *T. verruculosus*, from Andhra Pradesh, as a potent polyhydroxybutyrate degrader. Similarly, the stress-tolerant soil fungus *T. funiculosus,* isolated from the neem rhizosphere, was identified as a potential strain for phosphate solubilization (Kanseet al. 2015). *Talaromyces flavus* isolated from paddy rhizosphere of Darjeeling Hills exhibited phosphate solubilizing activity in vitro and positively influenced the growth of *Oryza sativa*, *Cicer arietinum*, and *Vigna radiata* under greenhouse conditions (Chakraborty et al. 2011). A keratin degrading strain of *T. trachyspermus* was isolated from the grounds of a gelatin factory in Jabalpur, Madhya Pradesh, and digested human hair in stationary culture (Rajak et al. 1991). *Talaromyces trachyspermus* was reported as a soil saprophyte in paddy fields of Orissa (Dutta and Ghosh 1965). Species identifications of these *Talaromyces* strains were mostly based on micro- and macro morphological characters in these studies. Because such approaches often underestimate species diversity, adoption of a polyphasic approach to authenticate such identifications will increase the number of *Talaromyces* species known from different eco-geographic zones of India. Further investigation is also needed to study the ecological importance of these species.

Acknowledgements

KC Rajeshkumar thanks SERB, Department of Science and Technology, Government of India for providing financial support under the project YSS/2015/001590; Dr Amy Y. Rossman for invaluable support and guidance in mycology and Dr K.M. Paknikar (Director, ARI) provided facilities and motivation in our work.

References

Aljanabi SM, Martinez I (1997) Universal and rapid salt-extraction of high quality genomic DNA for PCR-based techniques. Nucleic Acids Research 25: 4692–4693. https://doi.org/10.1093/nar/25.22.4692

Barbosa RN, Bezerra JD, Souza-Motta CM, Frisvad JC, Samson RA, Oliveira NT, Houbraken J (2018) New *Penicillium* and *Talaromyces* species from honey, pollen and nests of stingless bees. Antonie van Leeuwenhoek 13: 1–30. https://doi.org/10.1007/s10482-018-1081

Benjamin CR (1955) Ascocarps of *Aspergillus* and *Penicillium*. Mycologia 47: 669–687. https://doi.org/10.2307/3755578

Berbee ML, Yoshimura A, Sojiyamaj, Taylor JW (1995) Is *Penicillium* monophyletic? An evaluation of phylogeny in the family *Trichochomaceae* 18S, 5.8S and ITS ribosomal DNA sequence data. Mycologia 87: 201–222. https://doi.org/10.2307/3760907

Bhagobaty RK, Joshi SR (2012) Antimicrobial and antioxidant activity of endophytic fungi isolated from ethnomedicinal plants of the "Sacred forests" of Meghalaya, India. Mikologia Lekarska 19: 5–11.

Blakeslee AF (1915) Lindner's roll tube method of separation cultures. Phytopathology 5: 68–69.

Chakraborty BN, Chakraborty U, Sunar K, Dey PL (2011) RAPD profile and rDNA sequence analysis of *Talaromyces flavus* and *Trichoderma* species. Indian Journal of Biotechnology 10: 487–495.

Chen AJ, Sun BD, Houbraken J, Frisvad JC, Yilmaz N, Zhou YG, Samson RA (2016) New *Talaromyces* species from indoor environments in China. Studies in Mycology 84: 119–144. https://doi.org/10.1016/j.simyco.2016.11.003

Crous PW, Wingfield MJ, Burgess TI, Hardy GS, Crane C, Barrett S, Cano-Lira JF, Le Roux JJ, Thangavel R, Guarro J, Stchigel AM (2016) Fungal Planet description sheets 469–557. Persoonia 37: 252–253. https://doi.org/10.3767/003158516X694499

Crous PW, Wingfield MJ, Burgess TI, Carnegie AJ, Hardy GS, Smith D, Summerell BA, Cano-Lira JF, Guarro J, Houbraken J, Lombard L (2017) Fungal Planet description sheets 625–715. Persoonia 39: 460–461. https://doi.org/10.3767/persoonia.2017.39.11

Devi SS, Sreenivasulu Y, Rao KV (2014) *Talaromyces verruculosus*, a novel marine fungi as a potent polyhydroxybutyrate degrader. Research Journal of Pharmacy and Technology 7: 433–438.

Dutta BG, Ghosh GR (1965) Soil fungi from Orissa (India) IV. Soil fungi of paddy fields. Mycopathologia et Mycologia Applicata 25: 316–322. https://doi.org/10.1007/BF02049919

Glass NL, Donaldson GC (1995) Development of primer sets designed for use with the PCR to amplify conserved genes from filamentous ascomycetes. Applied and Environmental Microbiology 61: 1323–1330.

Guevara-Suarez M, Sutton DA, Gené J, García D, Wiederhold N, Guarro J, Cano-Lira JF (2017) Four new species of *Talaromyces* from clinical sources. Mycoses 60: 651–662. https://doi.org/10.1111/myc.12640

Heredia G, Rayes M, Aria RM, Bills GF (2001) *Talaromyces ocotl* sp. nov., and observation on *T. rotundus* from conifer forest soils of Veracruz State, Mexico. Mycologia 93: 528–540. https://doi.org/10.2307/3761738

Houbraken J, Samson R A (2011) Phylogeny of *Penicillium* and the segregation of *Trichocomaceae* into three families. Studies in Mycology 70: 1–51. https://doi.org/10.3114/sim.2011.70.01

Hubka V, Lyskova P, Frisvad JC, Peterson SW, Skorepova M, Kolarik M (2014) *Aspergillus pragensis* sp. nov. discovered during molecular reidentification of clinical isolates belonging to *Aspergillus* section *Candidi*. Medical Mycology 52: 565–576. https://doi.org/10.1093/mmy/myu022

Jiang XZ, Yu, ZD, Ruan YM, Wang L (2018). Three new species of *Talaromyces* sect. *Talaromyces* discovered from soil in China. Scientific Reports 8: 4932. https://doi.org/10.1038/s41598-018-23370-x

Kanse OS, Whitelaw-Weckert M, Kadam TA, Bhosale HJ (2015) Phosphate solubilization by stress-tolerant soil fungus *Talaromyces funiculosus* SLS8 isolated from the Neem rhizosphere. Annals of Microbiology 65: 85–93. https://doi.org/10.1007/s13213-014-0839-6

Katoh K, Standley DM (2013) MAFFT multiple sequence alignment software version 7: Improvements in performance and usability. Molecular Biology and Evolution 30: 772–780. https://doi.org/10.1093/molbev/mst010

Kornerup A, Wanscher JH (1967) Methuen Handbook of Colour (2nd edn). Methuen, London.

Krishnapura PR, Belur PD (2016) Partial purification and characterization of l-asparaginase from an endophytic *Talaromyces pinophilus* isolated from the rhizomes of *Curcuma amada*. Journal of Molecular Catalysis B: Enzymatic 124: 83–91. https://doi.org/10.1016/j.molcatb.2015.12.007

Liu, YJ, Whelen S, Hall BD (1999) Phylogenetic relationships among ascomycetes: Evidence from an RNA polymerse II subunit. Molecular Biology and Evolution 16: 1799–1808. https://doi.org/10.1093/oxfordjournals.molbev.a026092

LoBuglio KF, Pitt JI, Taylor JW (1993) Phylogenetic analysis of two ribosomal DNA regions indicates multiple independent losses of a sexual *Talaromyces* state among asexual *Penicillium* species in subgenus *Biverticillium*. Mycologia 85: 592–604. https://doi.org/10.2307/3760506

Luo Y, Lu X, Bi W, Liu F, Gao W (2016) *Talaromyces rubrifaciens*, a new species discovered from heating, ventilation and air conditioning systems in China. Mycologia 108: 773–779. https://doi.org/10.3852/15-233

Nguyen LT, Schmidt HA, Haeseler A Von, Minh BQ (2015) IQ-TREE: A fast and effective stochastic algorithm for estimating maximum-likelihood phylogenies. Molecular Biology and Evolution 32: 268–274. https://doi.org/10.1093/molbev/msu300

Palem PP, Kuriakose GC, Jayabaskaran C (2015) An endophytic fungus, *Talaromyces radicus*, isolated from *Catharanthus roseus*, produces vincristine and vinblastine, which induce apoptotic cell death. PloS One 10: e0144476. https://doi.org/10.1371/journal.pone.0144476

Peterson SW (2000) Phylogenic analysis of *Penicillium* species based on ITS and LSU-rDNA nucleotide sequences. In: Samson RA, Pitt JI (Eds) Integration of modern taxonomic methods for *Penicillium* and *Aspergillus.* The Netherlands: Harwood Academic Publishers, 163–178.

Peterson SW, Jurjević Ž (2017) New species of *Talaromyces* isolated from maize, indoor air, and other substrates. Mycologia 109: 537–556. https://doi.org/10.1080/00275514.2017.1369339

Pitt JI (1979) The genus *Penicillium* and its teleomorphic states *Eupenicillium* and *Talaromyces.* Academic Press, London, 634 pp.

Pitt JI, Samson RA, Frisvad JC (2000) List of accepted species and their synonyms in the family *Trichocomaceae*. In: Samson RA, Pitt JI (Eds) Integration of modern taxonomic methods for *Penicillium* and *Aspergillus* classification. Harwood Academic Press, Amsterdam, 9–79.

Rajak RC, Parwekar S, Malviya H, Hasija SK (1991) Keratin degradation by fungi isolated from the grounds of a gelatin factory in Jabalpur, India. Mycopathologia 114: 83–87. https://doi.org/10.1007/BF00436426

Ranjana KH, Priyokumar K, Singh TJ, Gupta CC, Sharmila L (2002) Disseminated *Penicillium marneffei* infection among HIV-infected patients in Manipur state, India. Journal of Infection 45: 268–271. https://doi.org/10.1053/jinf.2002.1062

Romero SM, Romero AI, Barrera V, Comerio R (2016) *Talaromyces systylus*, a new synnematous species from Argentinean semiarid soil. Nova Hedwigia 102: 241–256. https://doi.org/10.1127/nova_hedwigia/2015/0306

Samson RA, Yilmaz N, Houbraken J, Spierenburg H, Seifert KA, Peterson SW, Varga J, Frisvad JC (2011) Phylogeny and nomenclature of the genus *Talaromyces* and taxa accommodated in *Penicillium* subgenus *Biverticillium*. Studies in Mycology 70: 159–184. https://doi.org/10.3114/sim.2011.70.04

Schoch CL, Seifert KA, Huhndorf S, Robert V, Spouge JL, Levesque CA, Chen W, Bolchacova E, Voigt K, Crous PW, Miller AN (2012) Nuclear ribosomal internal transcribed spacer (ITS) region as universal DNA barcode marker for Fungi. Proceedings of the National Academy of Sciences of the United States of America 109: 6241–6246. https://doi.org/10.1073/pnas.1117018109

Seifert KA, Frisvad JC, Houbraken J, Llimona X, Peterson SW, Samson RA, Visagie CM (2012) (2051) Proposal to conserve the name *Talaromyces* over *Lasioderma* (Ascomycota). Taxon 61: 461–462.

Seifert KA, Frisvad JC, McLean MA (1993) *Penicillium kananaskense*, a new species from Alberta soil. Canadian Journal of Botany 72: 20–24. https://doi.org/10.1139/b94-004

Seifert KA, Hoekstra ES, Frisvad JC, Louis-Seize G (2004) *Penicillium cecedicola*, a new species on cynipid insect galls on *Quercus pacifica* in the western United States. Studies in Mycology 50: 517–523.

Singh PN, Ranjana K, Singh YI, Singh KP, Sharma SS, Kulachandra M, Nabakumar Y, Chakrabarti A, Padhye AA, Kaufman L, Ajello L (1999) Indigenous disseminated *Penicillium marneffei* infection in the State of Manipur, India: Report of four autochthonous cases. Journal of Clinical Microbiology 37: 2699–2702.

Su L, Niu YC (2018) Multilocus phylogenetic analysis of *Talaromyces* species isolated from curcurbit plants in China and description of two new species, *T. curcurbitiradicus* and *T. endophyticus.* Mycologia 110(2): 375–386. https://doi.org/10.1080/00275514.2018.1432221

Taylor JW, Jacobson DJ, Kroken S, Kasuga T, Geiser DM, Hibbett DS, Fisher MC (2000) Phylogenetic species recognition and species concepts in fungi. Fungal Genetics and Biology 31: 21–32. https://doi.org/10.1006/fgbi.2000.1228

Varriale S, Houbraken J, Granchi Z, Pepe O, Cerullo G, Ventorino V, Chin-A-Woeng T, Meijer M, Riley R, Grigoriev IV, Henrissat B, de Vries RP, Faraco V (2018). *Talaromyces borbonicus* sp. nov., a novel fungus from biodegraded *Arundo donax* with potential abilities in lignocellulose conversion. Mycologia 27: 1–9. https://doi.org/10.1080/00275514.2018.1456835

Visagie CM, Houbraken J, Frisvad JC, Hong S-B, Klaassen CH, Perrone G, Seifert KA, Varga J, Yaguchi T, Samson RA (2014) Identification and nomenclature of the genus *Penicillium*. Studies in Mycology 78: 343–371. https://doi.org/10.1016/j.simyco.2014.09.001

Visagie CM, Jacobs K (2012) Three new additions to the genus *Talaromyces* isolated from Atlantis sandveld fynbos soils. Persoonia 28: 14–24. https://doi.org/10.3767/003158512X632455

Visagie CM, Llimona X, Vila J, Louis-Seize G, Seifert KA (2012) Phylogenetic relationships and the newly discovered sexual state of *Talaromyces flavovirens*, comb. nov. Mycotaxon 122: 399–411. https://doi.org/10.5248/122.399

Visagie CM, Yilmaz N, Frisvad JC, Houbraken J, Seifert KA, Samson RA, Jacobs K (2015) Five new *Talaromyces* species with ampulliform-like phialides and globose rough walled conidia resembling *T. verruculosus*. Mycoscience 56: 486–502. https://doi.org/10.1016/j.myc.2015.02.005

Wang QM, Zhang YH, Wang B, Wang L (2016) *Talaromyces neofusisporus* and *T. qii*, two new species of section *Talaromyces* isolated from plant leaves in Tibet, China. Scientific Reports 6: 18622. https://doi.org/10.1038/srep18622

Wang XC, Chen K, Xia YW, Wang L, Li T, Zhuang WY (2016) A new species of *Talaromyces* (*Trichocomaceae*) from the Xisha Islands, Hainan, China. Phytotaxa 267: 187–200. https://doi.org/10.11646/phytotaxa.267.3.2

Wang XC, Chen K, Qin WT, Zhuang WY (2017) *Talaromyces heiheensis* and *T. mangshanicus,* two new species from China. Mycological Progress 16: 73–81. https://doi.org/10.1007/s11557-016-1251-3

White TJ, Bruns T, Lee J, Taylor J (1990) Amplification and direct sequencing of fungal ribosomal RNA genes for phylogenetics. In: Innis MA, Gelfand DH, Sninsky JJ, White TJ (Eds) PCR protocols: a guide to methods and applications. Academic Press, San Diego, 315–322. https://doi.org/10.1016/B978-0-12-372180-8.50042-1

Yaguchi T, Someya A, Udagawa SI (1996) A reappraisal of intrageneric classification of *Talaromyces* based on the ubiquinone systems. Mycoscience 37: 55–60. https://doi.org/10.1007/BF02461457

Yilmaz N, Houbraken J, Hoekstra ES, Frisvad JC, Visagie CM, Samson RA (2012) Delimitation and characterization of *Talaromyces purpurogenus* and related species. Persoonia 29: 39–54. https://doi.org/10.3767/003158512X659500

Yilmaz N, López-Quintero CA, Vasco-Palacios AM, Frisvad JC, Theelen B, Boekhout T, Samson RA, Houbraken J (2016a) Four novel *Talaromyces* species isolated from leaf litter from Colombian Amazon rain forests. Mycological Progress 15: 1041–1056. https://doi.org/10.1007/s11557-016-1227-3

Yilmaz N, Visagie CM, Frisvad JC, Houbraken J, Jacobs K, Samson RA (2016b) Taxonomic re-evaluation of species in *Talaromyces* section *Islandici*, using a polyphasic approach. Persoonia 36: 37–56. https://doi.org/10.3767/003158516X688270

Yilmaz N, Visagie CM, Houbraken J, Frisvad JC, Samson RA (2014) Polyphasic taxonomy of the genus *Talaromyces*. Studies in Mycology 78: 175–341. https://doi.org/10.1016/j.simyco.2014.08.001

MycoKeys 45: 57–73 (2019)
doi: 10.3897/mycokeys.45.31799
http://mycokeys.pensoft.net

RESEARCH ARTICLE

A peer-reviewed open-access journal
MycoKeys
Launched to accelerate biodiversity research

Description of Aeminiaceae fam. nov., *Aeminium* gen. nov. and *Aeminium ludgeri* sp. nov. (Capnodiales), isolated from a biodeteriorated art-piece in the Old Cathedral of Coimbra, Portugal

João Trovão[1], Igor Tiago[1], Fabiana Soares[1], Diana Sofia Paiva[2], Nuno Mesquita[1], Catarina Coelho[1], Lídia Catarino[3], Francisco Gil[4], António Portugal[1]

1 *Centre for Functional Ecology, Science for People and the Planet, University of Coimbra, Coimbra, Portugal* **2** *Laboratory for Plant Health (Fitolab), Instituto Pedro Nunes, Coimbra, Portugal* **3** *Geosciences Center, University of Coimbra, Coimbra, Portugal* **4** *Center for Physics of the University of Coimbra (CfisUC), Coimbra, Portugal*

Corresponding author: *João Trovão* (jtrovaosb@gmail.com)

Academic editor: *C. Gueidan* | Received 21 November 2018 | Accepted 6 January 2019 | Published 28 January 2019

Citation: Trovão J, Tiago I, Soares F, Paiva DS, Mesquita N, Coelho C, Catarino L, Gil F, Portugal A (2019) Description of Aeminiaceae fam. nov., *Aeminium* gen. nov. and *Aeminium ludgeri* sp. nov. (Capnodiales), isolated from a biodeteriorated art-piece in the Old Cathedral of Coimbra, Portugal MycoKeys 45: 57–73. https://doi.org/10.3897/mycokeys.45.31799

Abstract

When colonizing stone monuments, microcolonial black fungi are considered one of the most severe and resistant groups of biodeteriorating organisms, posing a very difficult challenge to conservators and biologists working with cultural heritage preservation. During an experimental survey aimed to isolate fungi from a biodeteriorated limestone art piece in the Old Cathedral of Coimbra, Portugal (a UNESCO World Heritage Site), an unknown microcolonial black fungus was retrieved. The isolated fungus was studied through a complete examination based on multilocus phylogeny of a combined dataset of ITS rDNA, LSU and *rpb2*, in conjunction with morphological, physiological, and ecological characteristics. This integrative analysis allows for the description of a new family, Aeminiaceae fam. nov., a new genus *Aeminium* gen. nov., and a new species, *Aeminium ludgeri* sp. nov., in the order Capnodiales.

Keywords

Biodeterioration, Capnodiales, microcolonial black fungi, phylogeny, taxonomy

Introduction

Microcolonial black fungi (MCBF) are a remarkably diverse fungal group characterized by unique phenotypic features, such as strongly melanized cell walls, slow growth, ability to shift from a mycelial to a meristematic state, high morphological plasticity, and predominant asexual reproduction (Butinar et al. 2005, Sterflinger 2006, Selbmann et al. 2015). They exhibit several physiological adaptations allowing their tolerance to various stress factors, including extreme temperatures, high solar and ultraviolet radiation, osmotic changes, and severe drought (Sterflinger 2006; Zakharova et al. 2013, Selbmann et al. 2015). This set of unique characteristics results from their adaptation to oligotrophic lifestyles, which are achieved through the production of protective molecules such as mycosporines and carotenoids (Gorbushina et al. 2003, 2008), restricted compacted growth, predominant specialized survival structures, and simple life cycles (Selbmann et al. 2005). Understandably, the ecology of MCBF reflects their resistance, as they occur in extreme environments such as hot and cold deserts, saltpans, acidic and hydrocarbon-contaminated sites, and exposed rocks surfaces (Selbmann et al. 2015). When colonizing stone monuments and art pieces, they deepen fissures and cracks through hyphal penetration (biopitting) (Sterflinger and Krumbein 1997; Lombardozzi et al. 2012) and the production of corrosive extracellular polysaccharides (Sterflinger 2006; Selbmann et al. 2014), synergistically promoting aesthetic, biophysic, and biochemical dismantlement of the material. Due to their powerful destructive potential and their high resistance to many types of restoration treatments, they are one of the major challenges for conservators and biologists working with biodeterioration of cultural heritage materials (Isola et al. 2013).

Classical morphological approaches used to identify MCBF are largely inefficient due to their extremely poor differentiation and, in some cases, to the existence of polymorphic traits (Sterflinger et al. 2006). Phylogenetic analyses have revealed that their ability to grow on rock substrates is a polyphyletic trait and these organisms are mainly classified in class Dothideomycetes (orders Capnodiales, Dothideales, and Pleosporales) and class Eurotiomycetes (order Chaetotyriales) (Selbmann et al. 2013, 2014). Phylogenetic studies of MCBF belonging to order Capnodiales (collected by Friedmann (1982), Selbmann et al. (2005, 2008), Ruibal et al. (2005, 2009, 2011) and Egidi et al. (2014)), have shown that several genera of slow-growing MCBF belonged to family Teratosphaeriaceae and/or to closely associated and unclassified families, initially referred to as Teratosphaeriaceae “1” and “2”. These two families were further resolved by Quaedvlieg et al. (2014) by applying the consolidated species concept (CSC) to circumcise the majority of these organisms in two novel families, Neodevriesiaceae and Extremaceae. Neodevriesiaceae and Extremaceae were further arranged and expanded by Crous et al. (2015), Isola et al. (2016), Wang et al. (2017), and Delgado et al. (2018), deepening the available knowledge of fungi in this order.

In 2013, UNESCO recognized the University of Coimbra, Alta and Sofia (Coimbra, Portugal) as a World Heritage Site. Inside this area, several monuments exhibit clear signs of biodeterioration, including microcolonial black fungi proliferation. During one

experimental survey performed in the Old Cathedral of Coimbra (Sé Velha de Coimbra), an unknown slow-growing microcolonial black fungi with late melanization was retrieved. Therefore, we aim to determine, through a multi-gene analysis (ITS rDNA, LSU and *rpb2*) coupled with a morphological, physiological and ecological examination, the taxonomic status and position of this fungus in the order Capnodiales.

Materials and methods

Site description, sample collection and fungal isolation

The Old Cathedral of Coimbra is the only Portuguese Romanesque cathedral from the Reconquista times to have survived relatively intact until now. The Romanesque church is located on a hillside in the historic city center and was constructed between the 12th and early 13th centuries. The single-floored cloister is arranged laterally to the south of the church and is surrounded by five chapels carved in yellow dolomitic limestone. Samples were collected using sterile scalpels by scrapping small areas (3 cm^2) into a collection tube, from a deteriorated art-piece in the Santa Maria chapel (40°12'32"N, 8°25'38"W) (Suppl. material 1: Figure S1). All sampling procedures were performed with the permission of the local government authority (Direcção Regional de Cultura do Centro) and supervised by technicians from the cathedral. From the 10 retrieved isolates, one was obtained through the suspension of the retrieved sample in 1.5 ml of sterile 0.9% (w/v) NaCl solution, vortexing and plating over Malt Extract Agar (MEA) (Difco, USA) supplemented with NaCl (10%) and streptomycin (0.5 g L^{-1}) and nine originated by the spread plate technique on solid DSMZ 372- Halobacteria medium (DSMZ, Germany), NaCl 20% (w/v), pH 8, of an aliquot of a 7 days enrichment culture obtained in the same liquid medium. Inoculated plates were incubated aerobically, in the dark at room temperature (28±1 °C) and the different colonies were isolated to axenic cultures in Potato Dextrose Agar medium (PDA), (Difco, USA).

DNA extraction, PCR amplification and sequencing

DNA from pure fungal cultures was obtained using the Extract-N-Amp Plant PCR Kit (Sigma-Aldrich, USA) with several modifications. A small portion of the colonies was scraped from the agar surface using a sterile scalpel, submerged in 10 µl of extraction solution and incubated in an ABI GeneAmp 9700 PCR System (Applied Biosystems, USA), with the following protocol: 65 °C for 10 min, followed by 95 °C for 15 min. After the incubation, reactions were stopped by adding 10 µl of elution solution. The obtained genomic DNA was subjected to PCR amplification with a final volume of 25 µl, with 12.5 µl of NZYTaq Green Master Mix (NZYTech, Portugal), 1 µl of each primer (10 mM), 9.5 µl of ultra-pure water and 1 µl of template DNA. Primer pairs ITS1-F/ITS4 (White et al. 1990; Gardes and Bruns 1993), LSU1fd/LR5 (Vilgalys and

Hester 1990; Crous et al. 2009) and f*rpb2*-5F/f*rpb2*-414R (Liu et al. 1999; Quaedvlieg et al. 2011) were used to amplify the ITS, LSU and *rpb2* regions, respectively. PCR reactions were performed using an ABI GeneAmp 9700 PCR System (Applied Biosystems, USA), with the following conditions: initial denaturation temperature of 96 °C for 2 min, followed by 40 cycles of denaturation temperature of 96 °C for 45 s, primer annealing at 54 °C (ITS), 52 °C (LSU), 49 °C (*rpb2*), primer extension at 72 °C for 90 s, and a final extension step at 72 °C for 2 min. Obtained amplicons were purified using the NZYGelpure DNA purification kit (NZYTech, Portugal) and sequenced using an ABI 3730xl DNA Analyzer system (96 capillary instruments) using the BigDye v. 3.1 Terminator Cycle Sequencing Ready Reaction Kit (Applied Biosystems, USA) at GATC-Biotech, Germany.

Phylogenetic analysis

DNA sequences were assembled using the Geneious R11.0.02 software (https://www.geneious.com), deposited in GenBank and compared with sequences from the National Center of Biotechnology Information nucleotide databases using NCBIs Basic Local Alignment Search Tool (BLAST), with the option Standard nucleotide BLAST of BLASTN v. 2.6 (Altschul et al. 1997). For construction of the datasets, additional representative sequences of the different families of the order Capnodiales were retrieved from GenBank based on the studies of Quaedvlieg et al. (2014), Isola et al. (2016), Wang et al. (2017), Delgado et al. (2018), (Suppl. material 2: Table S1). Because the ITS region BLAST analysis was the only gene providing a reasonable match (> 95%) with six environmental sequences obtained from a biodeteriorated limestone studied by Vázquez-Nion and colleagues (2016) in Spain, these sequences were also included in the final analysis (best scores for LSU: 95% *Devriesia* sp. ZWY45 (KP010375.1) and *Devriesia* sp. ZWY38 (KP010374.1); best score for *rpb2*: 86% *Hortaea thailandica* CBS 125423 (KF902206.1)). Sequences of each gene were individually aligned using ClustalX[2] (Larkin et al. 2007) and manually adjusted using UGENE v. 1.26.3 (Okonechnikov et al. 2012). The resulting individual alignments were concatenated using SeaView v. 4 (Gouy et al. 2010). Prior to the phylogenetic analysis, the model of nucleotide substitution for each individual partition was estimated using TOPALi v. 2.5 (Milne et al. 2009) under the Akaike Information Criterion (AIC). In all partitions the best-fit model was determined to be GTR+I+G. A Bayesian Markov Chain Monte Carlo (MCMC) analysis was performed with MrBayes v. 3.2.6 (Ronquist et al. 2012), with four runs over an initial number of 10 million generations. Trees were saved after each 100 generations and the MCMC heated chain "temperature" was set to the value of 0.15. The run was set to stop automatically when the average standard deviation of split frequencies fell below 0.01. After the analysis has stopped, the distribution of log-likelihood scores was confirmed with the Tracer v. 1.5 software (Rambaut and Drummond 2007) to ensure that the stationary phase and convergence in the analysis had been reached. The sampled topologies below the asymptote (25%) were rejected as part of the burn-in phase and the lasting

trees were used to calculate the Bayesian posterior probabilities (BP) in an 50% majority rule consensus tree. The resulting phylogenetic tree was viewed in FigTree v. 1.2.2 (Rambaut and Drummond 2008). The obtained alignment and respective phylogenetic tree were deposited in TreeBASE with the submission ID 23164.

Physiological analysis

To examine heat resistance, mycelia from grown cultures on PDA were homogenized and heated at 75 °C for 30 min, in a shaking water bath. A small aliquot of the heated suspension was plated on fresh PDA culture medium and examined periodically to evaluate fungal growth (according to Seifert et al. 2004). Colonies were considered heat resistant if growth was observed after a period of 3 months after exposure to the protocol described. To determine NaCl tolerance, strains were cultivated on Malt Extract Agar supplemented with NaCl at different concentrations (5, 10, 15, 20, 25, 30% [w/v]) (adapted from Sterflinger 1998). To determine pH tolerance, strains were cultivated on MEA with pH adjustments from 5 to 11, according to Tiago et al. (2004). In all cases, diameters of the colonies were assessed by measuring two perpendicular diameters per colony, weekly during 4 weeks. For all tests, each case study was evaluated in triplicate.

Morphological analysis

For morphological characterization, strains were cultivated on PDA (Difco, USA), Malt Extract Agar (MEA), (Difco, USA) with 10% NaCl (w/v) and Dichloran Glycerol Agar (DG-18), (Sigma-Aldrich, USA) for up to 6 months. Morphological analysis was performed directly on the cultured media plates or using the slide culture technique. Preparations were transferred into slides, observed with a light microscope (Leica DM 4000B (Leica, Germany)), and photographed (Leica DFC 490 digital camera (Leica, Germany)). At least 30 measurements per structure were considered. Representative drawings of microscopic morphological characteristics were obtained with Adobe Illustrator CC (Adobe, USA).

Results

Phylogenetic analysis

The phylogenetic analysis was performed using the aligned sequences of the concatenated three-gene dataset with 1301 characters (627 for LSU, 204 for *rpb2* and 470 for ITS), encompassing 133 representative sequences belonging to the different families of the order Capnodiales (Fig. 1). From the obtained gene alignments, we were able to verify 260, 143

and 304 unique patterns present in the LSU, *rpb2* and ITS partitions respectively. The MCMC analysis of the three concatenated genes run for 3430000 generations, resulting in 137204 trees. The initial 34300 trees, representative of the analysis burn-in phase was discarded, while the remaining trees were used to calculate posterior probabilities in the majority rule consensus tree. From the phylogenetic data obtained in this study, we were able to verify that the isolated fungi clustered in a monophyletic group with strong support (100% Bayesian posterior probability), distinctly placed from other families in the order Capnodiales but related to the families Extremaceae and Neodevriesiaceae. Thus, this novel lineage is proposed here as a new family Aeminiaceae fam. nov., a new genus, *Aeminium* gen. nov., and a new species *Aeminium ludgeri* sp. nov.

Physiological studies

Preliminary physiological analysis comprised all the isolates obtained in this study (data not shown). However, as no significant statistical difference was observed among the isolates under the different tested conditions, the final analysis consisted only of data regarding a copy of the culture DSM 106916. No growth was observed for the fungus after exposure to the heat tolerance protocol and therefore, it was classified as non-heat tolerant and non-heat activated. Results for NaCl tolerance test are shown in Suppl. material 3: Figure S2. The fungus was able to grow in NaCl concentrations up to 20% NaCl, with optimal growth occurring at 10% NaCl concentration. No growth was observed for 25% and 30% NaCl concentrations. Nonetheless, the fungus was considered halotolerant, due to the ability to grow in various NaCl concentrations. Results for the pH tolerance test are shown in Suppl. material 4: Figure S3. The fungus showed optimal growth at pH 7 and 9; equal growth values for pH 6 and 8; and no growth was registered for pH 5, 10 and 11. Due to unnecessary pH adjustments for proliferation, strains were considered facultative alkaliphiles. Due to the ability to grown on DG-18 culture media, the fungus was also considered xerophilic.

Morphological studies

Taxonomy

Aeminiaceae J. Trovão, I. Tiago & A. Portugal, fam. nov.
MycoBank: MB824975

Description. Asexual morph: mycelium consisting of septate, smooth hyphae, gradually becoming widen, thick-walled, darker and developing into meristematic chains of conidia. Conidia dark brown, thick-walled, smooth, rugose, globose with single central septa resulting from the differentiation of toruloid-like hyphal cells. Sexual morph: unknown.

Type genus. *Aeminium* J. Trovão, I. Tiago & A. Portugal.

Type species. *Aeminium ludgeri* J. Trovão, I. Tiago & A. Portugal.

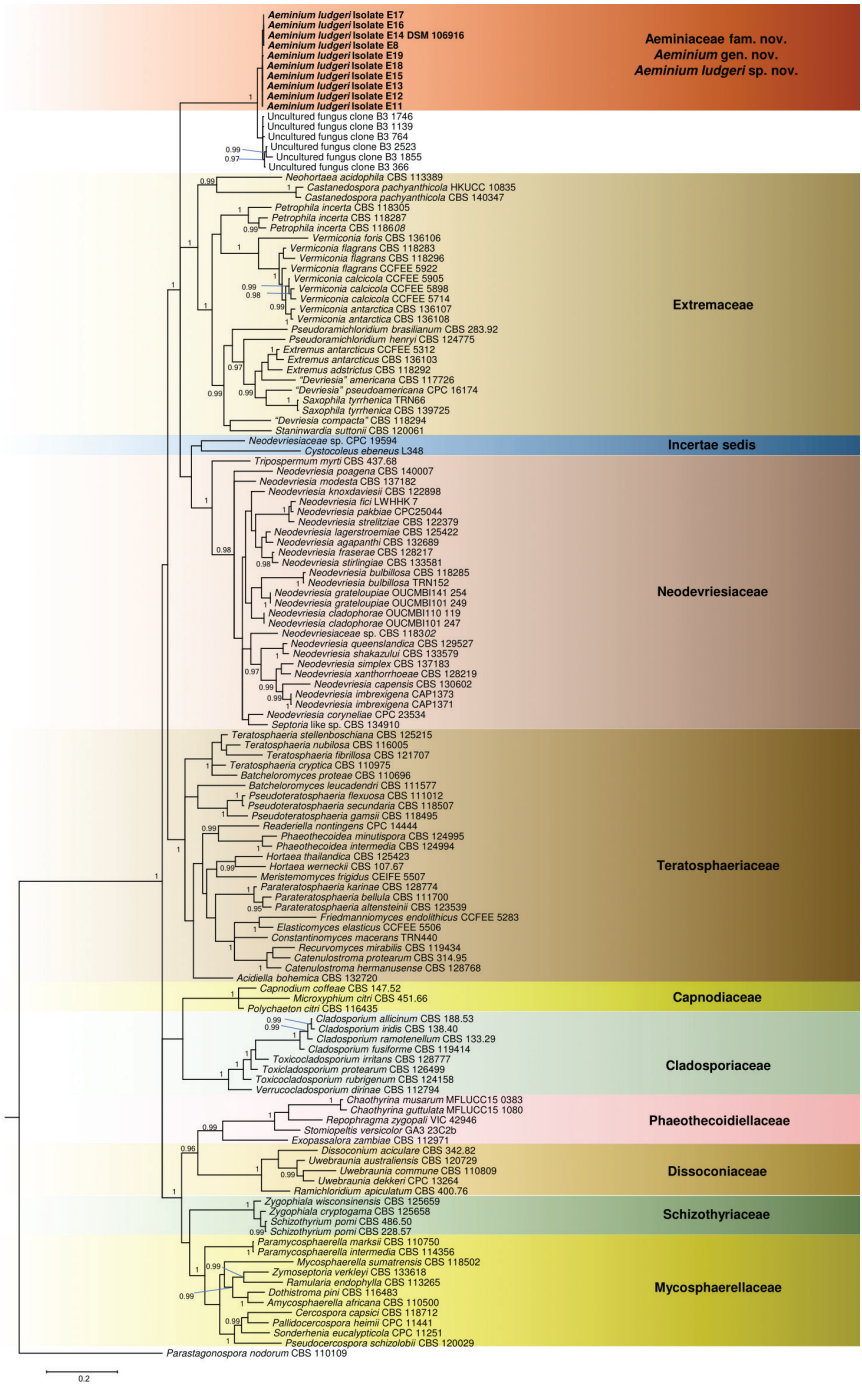

Figure 1. Bayesian 50% majority rule consensus tree based on an LSU/*rpb2*/ITS concatenated alignment, containing representative sequences from the order Capnodiales. The new strains are shown in bold. Bayesian posterior probabilities (PP) ≥ 0.95 are presented at the nodes. The tree was rooted to *Parastagonospora nodorum* CBS 110109. The scale bar specifies 0.2 expected changes per site.

Notes. Members of Aeminiaceae encompass microcolonial black fungi occurring in deteriorated limestones and are classified as halotolerant, xerophilic, and facultative alkaliphiles. They exhibit slow growth and late melanization, derived from the late differentiation of intercalary or terminal hyphal cells into arthroconidia, that turn olivaceous brown to dark. Fully maturation of the arthroconidia occurs after at least a 2-month incubation period. Their geographical distribution seems to be confined, for now, to limestones in the Iberian Peninsula, although further sampling is necessary to fully highlight their complete geographical and ecological spectrum.

Aeminium **J. Trovão, I. Tiago & A. Portugal, gen. nov.**
MycoBank: MB824976

Description. Asexual morph: mycelium consisting of septate, smooth hyphae, gradually becoming widen, thick-walled, darker and developing into meristematic chains of conidia. Conidia dark brown, thick-walled, smooth, rugose, globose with single central septa resulting from the differentiation of toruloid-like hyphal cells. Chlamydospores not observed in culture. Sexual morph: unknown.

Etymology. Named after the old Latin name of Coimbra (Aeminium), the city where the strains were isolated.

Type species. *Aeminium ludgeri* J. Trovão, I. Tiago & A. Portugal.

Aeminium ludgeri **J. Trovão, I. Tiago & A. Portugal, sp. nov.**
MycoBank: MB824977
Figure 2 and Suppl. material 5: Figure S4.

Type. Portugal, Coimbra (40°12'32"N, 8°25'38"W), isolated from a biodeteriorated limestone art piece in the Old Cathedral of Coimbra, 22 November 2016, Igor Tiago, (holotype: permanently preserved in metabolically inactive state DSM 106916).

Etymology. In memory of our late colleague Ludgero Avelar.

Diagnosis. Phylogenetic analysis based on the concatenated ITS rDNA, LSU and *rpb2* dataset considered in the present study clustered the retrieved strains in a monophyletic separate lineage related to the families Neodevriesiaceae and Extremaceae. Therefore, a new family Aeminiaceae fam. nov, a new genus *Aeminium* gen. nov., and a new species *Aeminium ludgeri* sp. nov. in the order Capnodiales are here proposed.

Description. Mycelium initially consisting of branched, septate, smooth, subhyaline to pale green, 2–3 µm wide hyphae. Hyphae moniliform, gradually becoming widen, thick-walled, darker and developing into meristematic conidial chains. Conidiophores micronematous. Arthroconidia dark brown, thick-walled, smooth, sometimes rugose, globose, measuring 3.5–6 × 4.5–6 µm, single central septa, resulting from the differentiation of intercalary or terminal toruloid-like hyphal cells. Sexual morph unknown.

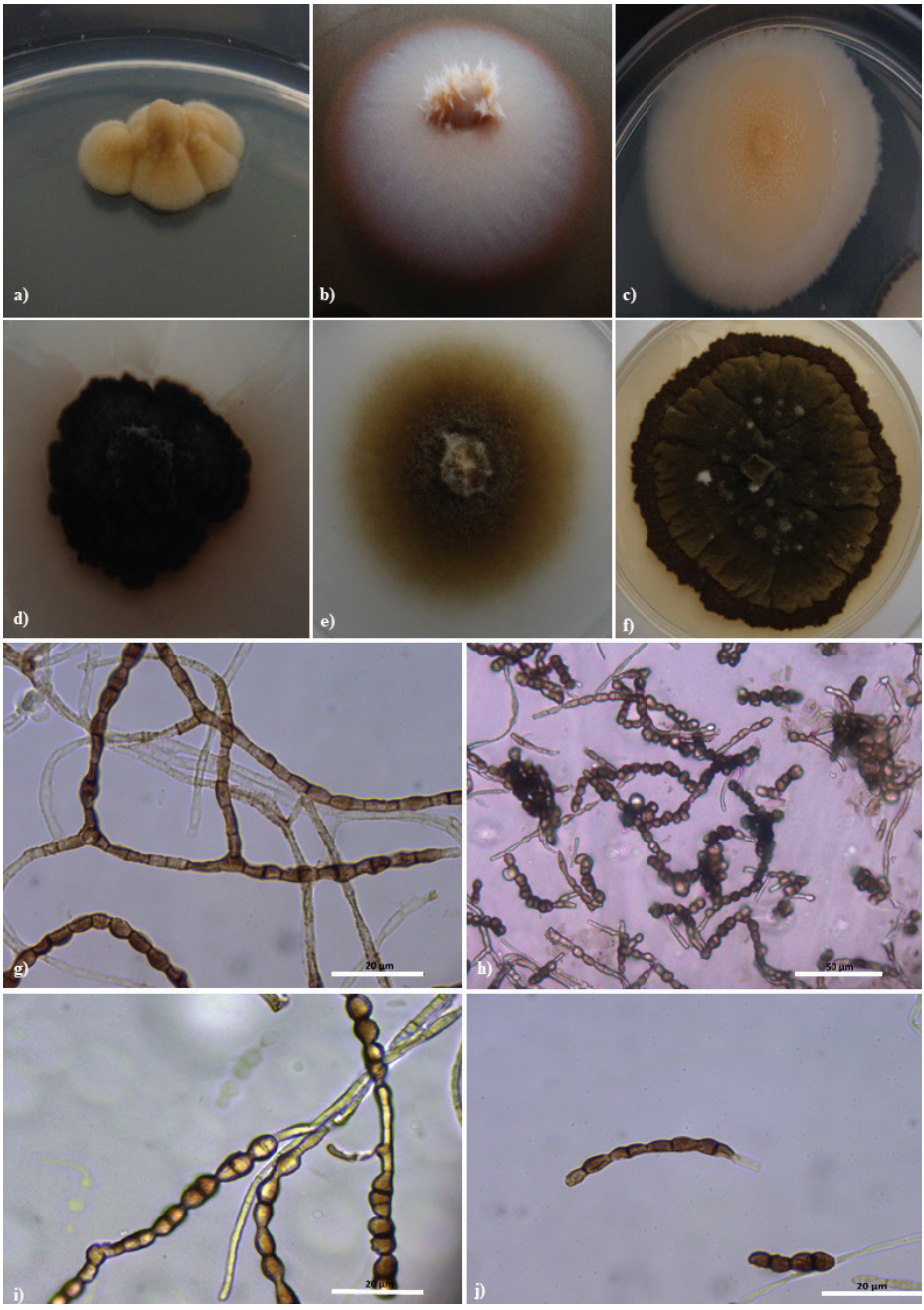

Figure 2. *Aeminium ludgeri* **a** Colony appearance on PDA **b** Colony appearance on MEA+10% NaCl (w/v) **c** Colony appearance on DG-18 **d** Colony appearance on PDA after maturation **e** Colony appearance on MEA+10% NaCl (w/v) after maturation **f** Colony appearance on DG-18 after maturation **g** Initial simple, branched, septate hyphae becoming toruloid-like (scale 20 µm) **h** Differentiated, toruloid-like hyphae and mature chains of arthroconidia (scale 50 µm) **i** Intercalary and terminal conidial chains (scale 20 µm); **j** typical aspect of arthroconidia (scale 20 µm)

Culture characteristics. On 6 weeks old PDA plates, colonies growing slowly, to 8 mm in diameter, cerebriform, irregular, raised centrally, often moist, deeply immersed into agar, pale pink, with scarce velvety, pale pink-hyaline, aerial, short hyphae and well-defined, small, white, and glossy margin; pale pink on reverse. After at least 2 months, colonies become fully mature and melanized, olivaceous brown-black on top and on reverse. On 6 weeks old MEA+10% NaCl plates, colonies growing slowly, to 25 mm in diameter, flat, circular, moist, pale pink, with prominent velvety pale pink-hyaline aerial short hyphae and with undulate margin; pale pink in reverse. After at least 2 months, colonies become fully mature and melanized, with velvety grey-white aerial short hyphae, filiform margin, olivaceous brown on top and in reverse. On 6-weeks-old DG-18 plates, colonies growing slowly, to 20 mm in diameter, flat, irregular, often moist, deeply immersed into agar, with velvety yellow-pale brown aerial short hyphae and with irregular undulate white margin; yellow-pale brown in reverse. After at least 2 months, colonies become fully mature and melanized, raised, rugose, olivaceous brown-black on top and in reverse.

Distribution. Portugal.

Additional specimens examined. Portugal, Coimbra (40°12'32"N, 8°25'38"W), isolated from a biodeteriorated limestone art piece in the Old Cathedral of Coimbra, I. Tiago, living culture E8, ibid. living culture E11, ibid. living culture E12, ibid. living culture E13, ibid. living culture E14, ibid. living culture E15, ibid. living culture E16, ibid. living culture E17, ibid. living culture E18; ibid. living culture E19.

Discussion

Here we describe *Aeminium ludgeri*, a new MCBF species, as well as establish a new genus and family within the order Capnodiales to accommodate this fungus. Phylogenetic analyses, based on ITS rDNA, LSU and *rpb2* molecular data, revealed that the retrieved isolates cluster in a separate lineage strongly supported at a family-level, related to the families Extremaceae and Neodevriesiaceae. Although some molecular variance can be observed among the studied isolates, when dealing with MCBF, larger degrees of sequence heterogeneity for species delimitation are accepted due to the lack of sexual recombination, predominance of clonality, and perpetuation of super-adapted genotypes (Egidi et al. 2014). Additionally, due to ITS sequence heterogeneity among the retrieved strains being 1%, a sole new genus and species were considered in Aeminiaceae.

The clustering of the environmental sequences obtained by Vázquez-Nion et al. (2016) with the sequences obtained during this study provides valuable information on the ecology, habitat, and geographical distribution of the new family. So far, Aeminiaceae has only been identified on deteriorated limestones monuments on the Iberian Peninsula. This ecological characteristic is clearly distinct when compared to the related Extremaceae ("epiphyllous, endophytic, saprobic or plant pathogenic") and Neodevriesiaceae ("foliicolous, saprobic or plant pathogenic") (Quaedvlieg et al. 2014).

The limestones used in the construction of the Old Cathedral of Coimbra hail from unique areas of Portugal (namely Ançã and Portunhos, near Coimbra), and simi-

lar stone structures were exported and used on several "Our Ladies of the O" statues and in the portal of the Royal Hospital in Santiago de Compostela (Spain). We hypothesize that the transportation of limestone to such places might have contributed to the dispersion of this organism and, thus, explain the detection of Aeminiaceae environmental clones in the Cathedral of Santiago de Compostela by Vázquez-Nion et al. (2016). Nonetheless, we also consider that this fungus might be endemic to limestone quarries on the Iberian Peninsula, although acknowledging that additional sampling may further expand the full geographical and ecological spectrum of this fungus.

Physiological tests allowed us to characterize the retrieved isolates as non-heat tolerant, non-heat activated, xerophilic, halotolerant (enduring NaCl concentrations up to 20%), and facultative alkaliphiles. Ecologically, these traits are somewhat more similar to those of Extremaceae (except for pH values, as Aeminiaceae is an alkaliphile and Extremaceae is an acidophile). Regarding heat-tolerance, the isolates are somewhat more similar to Neodevriesiaceae because they do not exhibit heat tolerance. To the best of our knowledge, data regarding heat tolerance for Extremaceae is scarce and could not be further compared. Furthermore, information regarding NaCl tolerance is still poorly described for both Extremaceae and Neodevriesiaceae, but future studies related to stress tolerance in these organisms could provide a valuable character in strain typification.

Although MCBF morphology-based distinction is particularly difficult to accomplish, it can be easily verified that Aeminiaceae differs from the closely related Extremaceae and Neodevriesiaceae due to the necessary period for conidia maturation. Additionally, the verified globose arthroconidia, with single central septa, are distinct from the "subcylindrical to narrowly fusoid-ellipsoidal or obclavate conidia with rarely 1–2 transverse septa" described for Extremaceae and the "rarely septate, solitary conidia composed of a central stalk and two lateral arms with 1–2 transverse septa", when compared to Neodevriesiaceae (Quaedvlieg et al. 2014). In the five known *Neodevriesia* MCBF species (*N. bulbillosa*, *N. imbrexigena*, *N. modesta*, *N. sardiniae*, and *N. simplex*), production of reproductive cells may occur both through budding (e.g. *N. simplex*) or through meristematic growth (*N. sardiniae*). When considering *A. ludgeri*, only meristematic growth was observed and the new species can be easily distinguished from *N. sardiniae* by the type and much smaller conidia dimensions. Furthermore, no exuded pigments in the agar could be detected in contrast with *N. modesta*, and no chlamydospores were noticed as found in *N. imbrexigena*. When compared with the seven known Extremaceae MCBF species (*Extremus adstrictus*, *E. antarcticus*, *Saxophila tyrrhenica*, *Petrophila incerta*, *Vermiconia foris*, *V. flagrans*, and *V. antarctica*), *A. ludgeri* is distinctive from *E. antarcticus* and *V. flagrans* by the presence of arthroconidia, and from *V. foris* due to the absence of holoblastic reproductive structures. Moreover, *A. ludgeri* exhibits arthroconidia emerging from meristematic development similar to *E. adstrictus*, *S. tyrrhenica*, *P. incerta*, and *V. antarctica*. Arthroconidia from *A. ludgeri* are, however, clearly distinct from *E. adstrictus* catenate, ellipsoidal conidia, *S. tyrrhenica* thallic-arthric conidia, and *P. incerta* pyriform/ovoidal ramoconidia.

Regarding stone monuments exposed to the environment, microcolonial black fungi are one of the main culprits of stone biodeterioration and are responsible for severe aesthetic, biochemical, and biophysical alterations (Sterflinger 2000, 2010; Sterflinger and Piñar

2013). It is, therefore, crucial to gather a deeper knowledge of the biodiversity of MCBF, and their biological, ecological, and physiological unique characteristics, to allow the development and improvement of tools to protect stone monuments from deterioration.

Acknowledgments

We are grateful to the Direcção Regional de Cultura do Centro (DRCC), the staff and technicians from the Old Cathedral of Coimbra (Sé Velha) and the University of Coimbra for their kind collaborations. We also thank Miguel Mesquita, for kindly providing the photographs of the sampling site. This work was financed by FEDER- Fundo Europeu de Desenvolvimento Regional funds through the COMPETE 2020- Operational Programme for Competitiveness and internationalization (POCI) and by Portuguese funds through Fundação para a Ciência e a Tecnologia (FCT) in the framework of the project POCI-01-0145-FEDER-PTDC/EPH-PAT/3345/2014. João Trovão was supported by Programa Operacional Capital Humano (POCH; co-funding by the European Social Fund and national funding by MCTES), through a "FCT- Fundação para a Ciência e Tecnologia" PhD research grant (SFRH/BD/132523/2017). Fabiana Soares was supported by POCH (co-funding by the European Social Fund and national funding by MCTES), through a "FCT- Fundação para a Ciência e Tecnologia" PhD research grant (SFRH/BD/139720/2018). Nuno Mesquita was supported by POCH (co-funding by the European Social Fund and national funding by MCTES), with a Post-Doc Research grant (SFRH/BPD/112830/2015). Catarina Coelho was supported by Portuguese funds through "FCT – Fundação para a Ciência e a Tecnologia" in project IN0756 - INV.EXPLORATORIA - IF/01061/2014. Igor Tiago acknowledges an Investigator contract reference IF/01061/2014.

References

Altschul SF, Madden TL, Schäffer AA, Zhang J, Zhang Z, Miller W, Lipman DJ (1997) Gapped BLAST and PSI-BLAST: a new generation of protein database search programs. Nucleic Acids Research 25: 3389–3402. https://doi.org/10.1093/nar/25.17.3389

Butinar L, Sonjak S, Zalar P, Plemenitaš A, Gunde-Cimerman N (2005) Melanized halophilic fungi are eukaryotic members of microbial communities in hypersaline waters of solar salterns. Botanica Marina 48: 73–79. https://doi.org/10.1515/BOT.2005.007

Crous PW, Schumacher RK, Wingfield MJ, Lombard L, Giraldo A, Christensen M, Gardiennet A, Nakashima C, Pereira O, Smith AJ, Groenewald JZ (2015) Fungal Systematics and Evolution: FUSE 1. Sydowia 67: 81–118. http://dx.doi.org/10.12905/0380.sydowia67-2015-0081.

Crous PW, Schoch CL, Hyde KD, Wood AR, Gueidan C, de Hoog GS, Groenewald JZ (2009) Phylogenetic lineages in the Capnodiales. Studies in Mycology 64: 17–47. https://doi.org/10.3114/sim.2009.64.02

Delgado G, Miller AN, Piepenbring M (2018) South Florida microfungi: *Castanedospora*, a new genus to accommodate *Sporidesmium pachyanthicola* (Capnodiales, Ascomycota). Cryptogamie Mycologie 39: 109–127. https://doi.org/10.7872/crym/v39.iss1.2018.109

Egidi E, Hoog GS de, Isola D, Onofri S, Quaedvlieg W, Vries M de, Verkley GJM, Stielow JB, Zucconi L, Selbmann L (2014) Phylogeny and taxonomy of meristematic rock-inhabiting black fungi in the Dothideomycetes based on multi-locus phylogenies. Fungal Diversity 65: 127–165. https://doi.org/10.1007/s13225-013-0277-y

Friedmann EI (1982) Endolithic microorganisms in the antarctic cold desert. Science 215: 1045–1053. https://doi.org/10.1126/science.215.4536.1045

Gardes M, Bruns TD (1993) ITS primers with enhanced specificity for basidiomycetes-application to the identification of mycorrhizae and rusts. Molecular Ecology 2: 113–118. https://doi.org/10.1111/j.1365-294X.1993.tb00005.x

Gorbushina AA, Kotlova ER, Sherstneva OA (2008) Cellular responses of microcolonial rock fungi to long-term desiccation and subsequent rehydration. Studies in Mycology 61: 91–97. https://doi.org/10.3114/sim.2008.61.09

Gorbushina AA, Whitehead K, Dornieden T, Niesse A, Schulte A, Hedges JI (2003) Black fungal colonies as units of survival: hyphal mycosporines synthesized by rock-dwelling microcolonial fungi. Canadian Journal of Botany 81: 131–138. https://doi.org/10.1139/b03-011

Gouy M, Guindon S, Gascuel O (2010) SeaView version 4: A multiplatform graphical user interface for sequence alignment and phylogenetic tree building. Molecular Biology and Evolution 27: 221–224. https://doi.org/10.1093/molbev/msp259

Isola D, Selbmann L, Meloni P, Maracci E, Onofri S, Zucconi L (2013) Detrimental rock black fungi and biocides: a study on the Monumental Cemetery of Cagliari. In: Rogerio-Candelera MA, Lazzari M, Cano E (Eds) Science and Technology for the Conservation of Cultural Heritage. CRC Press, London, 83–86. https://doi.org/10.1201/b15577-21

Isola D, Zucconi L, Onofri S, Caneva G, Hoog GS de, Selbmann L (2016) Extremotolerant rock inhabiting black fungi from Italian monumental sites. Fungal Diversity 76: 75–96. https://doi.org/10.1007/s13225-015-0342-9

Larkin MA, Blackshields G, Brown NP, Chenna R, McGettigan PA, McWilliam H, Valentin F, Wallace IM, Wilm A, Lopez R, Thompson JD, Gibson TJ, Higgins DG (2007) Clustal W and Clustal X version 2.0. Bioinformatics 23: 2947–2948. https://doi.org/10.1093/bioinformatics/btm404

Liu YJ, Whelen S, Hall BD (1999) Phylogenetic relationships among Ascomycetes: evidence from an RNA polymerase II subunit. Molecular Biology and Evolution 16: 1799–1808. https://doi.org/10.1093/oxfordjournals.molbev.a026092

Lombardozzi V, Castrignanò T, D'Antonio M, Casanova Municchia A, Caneva G (2012) An interactive database for an ecological analysis of stone biopitting. International Biodeterioration & Biodegradation 73: 8–15. https://doi.org/10.1016/j.ibiod.2012.04.016

Milne I, Lindner D, Bayer M, Husmeier D, McGuire G, Marshall DF, Wright F (2009) TOPALi v2: a rich graphical interface for evolutionary analyses of multiple alignments on HPC clusters and multi-core desktops. Bioinformatics 25: 126–127. https://doi.org/10.1093/bioinformatics/btn575

Okonechnikov K, Golosova O, Fursov M, UGENE team (2012) Unipro UGENE: a unified bioinformatics toolkit. Bioinformatics 28: 1166–1167. https://doi.org/10.1093/bioinformatics/bts091

Quaedvlieg W, Binder M, Groenewald JZ, Summerell BA, Carnegie AJ, Burgess TI, Crous PW (2014) Introducing the Consolidated Species Concept to resolve species in the Teratosphaeriaceae. Persoonia 33: 1–40. https://doi.org/10.3767/003158514X681981

Quaedvlieg W, Kema GHJ, Groenewald JZ, Verkley GJM, Seifbarghi S, Razavi M, Mirzadi Gohari A, Mehrabi R, Crous PW (2011) *Zymoseptoria* gen. nov.: a new genus to accommodate Septoria-like species occurring on graminicolous hosts. Persoonia 26: 57–69. https://doi.org/10.3767/003158511X571841

Rambaut A, Drummond AJ (2007) Tracer v. 1.4. http://beast.bio.ed.ac.uk/Tracer

Rambaut A, Drummond AJ (2008) FigTree: Tree figure drawing tool, v. 1.2.2. http://tree.bio.ed.ac.uk/software/figtree/

Ronquist F, Teslenko M, van der Mark P, Ayres DL, Darling A, Höhna S, Larget B, Liu L, Suchard MA, Huelsenbeck JP (2012) MrBayes 3.2: Efficient Bayesian Phylogenetic Inference and Model Choice Across a Large Model Space. Systematic Biology 61: 539–542. https://doi.org/10.1093/sysbio/sys029

Ruibal C, Gueidan C, Selbmann L, Gorbushina AA, Crous PW, Groenewald JZ, Muggia L, Grube M, Isola D, Schoch CL, Staley JT, Lutzoni F, de Hoog GS (2009) Phylogeny of rock-inhabiting fungi related to Dothideomycetes. Studies in Mycology 64: 123–133 https://doi.org/10.3114/sim.2009.64.06

Ruibal C, Millanes AM, Hawksworth DL (2011) Molecular phylogenetic studies on the lichenicolous *Xanthoriicola physciae* reveal Antarctic rock-inhabiting fungi and *Piedraia* species among closest relatives in the Teratosphaeriaceae. IMA Fungus 2: 97–103. https://doi.org/10.5598/imafungus.2011.02.01.13

Ruibal C, Platas G, Bills GF (2005) Isolation and characterization of melanized fungi from limestone formations in Mallorca. Mycological Progress 4: 23–38. https://doi.org/10.1007/s11557-006-0107-7

Seifert KA, Nickerson NL, Corlett M, Jackson ED, Louis-Seize G, Davies RJ (2004) *Devriesia*, a new hyphomycete genus to accommodate heat-resistant, *Cladosporium*-like fungi. Canadian Journal of Botany 82: 914–926. https://doi.org/10.1139/b04-070

Selbmann L, De Hoog GS, Mazzaglia A, Friedmann EI, Onofri S (2005) Fungi at the edge of life: cryptoendolithic black fungi from Antarctic desert. Studies in Mycology 51: 1–32.

Selbmann L, de Hoog GS, Zucconi L, Isola D, Ruisi S, van den Ende AHGG, Ruibal C, De Leo F, Urzì C, Onofri S (2008) Drought meets acid: three new genera in a dothidealean clade of extremotolerant fungi. Studies in Mycology 61: 1–20. https://doi.org/10.3114/sim.2008.61.01

Selbmann L, Egidi E, Isola D, Onofri S, Zucconi L, de Hoog GS, Chinaglia S, Testa L, Tosi S, Balestrazzi A, Lantieri A, Compagno R, Tigini V, Varese GC (2013) Biodiversity, evolution and adaptation of fungi in extreme environments. Plant Biosystems 147: 237–246. https://doi.org/10.1080/11263504.2012.753134

Selbmann L, de Hoog GS, Zucconi L, Isola D, Onofri S (2014) Black yeasts in cold habitats. In: Buzzini P, Margesin R (Eds) Cold-adapted Yeasts. Springer, Berlin, Heidelberg, 173–189. https://doi.org/10.1007/978-3-642-39681-6_8

Selbmann L, Zucconi L, Isola D, Onofri S (2015) Rock black fungi: excellence in the extremes, from the Antarctic to space. Current Genetics 61: 335–345. https://doi.org/10.1007/s00294-014-0457-7

Sterflinger K, Piñar G (2013) Microbial deterioration of cultural heritage and works of art-tilting at windmills? Applied Microbiology Biotechnology 97: 9637–9646. https://doi.org/10.1007/s00253-013-5283-1

Sterflinger K (2010) Fungi: their role in biodeterioration of cultural heritage. Fungal Biology Reviews 24: 1–2. https://doi.org/10.1016/j.fbr.2010.03.003

Sterflinger K (2000) Fungi as geologic agents. Geomicrobiology Journal 17 (2): 97–124. https://doi.org/10.1080/01490450050023791

Sterflinger K (2006) Black yeasts and meristematic fungi: ecology, diversity and identification. In: Péter G, Rosa C (Eds) Biodiversity and Ecophysiology of Yeasts. The Yeast Handbook. Springer, Berlin, Heidelberg, 501–514. https://doi.org/10.1007/3-540-30985-3_20

Sterflinger K (1998) Temperature and NaCl-tolerance of rock-inhabiting meristematic fungi. Antonie Van Leeuwenhoek 74: 271–281.

Sterflinger K, Krumbein WE (1997) Dematiaceous fungi as a major agent for biopitting on Mediterranean marbles and limestones. Geomicrobiology Journal 14: 219–230. https://doi.org/10.1080/01490459709378045

Tiago I, Chung AP, Veríssimo A (2004) Bacterial Diversity in a Nonsaline Alkaline Environment: Heterotrophic Aerobic Populations. Applied Environmental Microbiology. 70: 7378–7387. https://doi.org/10.1128/AEM.70.12.7378-7387.2004

Vázquez-Nion D, Rodríguez-Castro J, López-Rodríguez MC, Fernández-Silva I, Prieto B (2016) Subaerial biofilms on granitic historic buildings: microbial diversity and development of phototrophic multi-species cultures. Biofouling 32 (6): 657–669. https://doi.org/10.1080/08927014.2016.1183121

Vilgalys R, Hester M (1990) Rapid genetic identification and mapping of enzymatically amplified ribosomal DNA from several *Cryptococcus* species. Journal of Bacteriology 172: 4238–4246.

Wang MM, Shenoy BD, Li W, Cai L (2017) Molecular phylogeny of *Neodevriesia*, with two new species and several new combinations. Mycologia 109: 965–974. https://doi.org/10.1080/00275514.2017.1415075

White T, Burns T, Lee S, Taylor J (1990) Amplification and direct sequencing of ribosomal RNA genes for phylogenetics. In: Innis MA (Ed.) PCR Protocols: A Guide to Methods and Applications. Academic Press, New York, 315–322.

Zakharova K, Tesei D, Marzban G, Dijksterhuis J, Wyatt T, Sterflinger K (2013) Microcolonial fungi on rocks: a life in constant drought? Mycopathologia 175: 537–547. https://doi.org/10.1007/s11046-012-9592-1

Supplementary material 1

Figure S1. Sampling site

Authors: João Trovão, Igor Tiago, Fabiana Soares, Diana Sofia Paiva, Nuno Mesquita, Catarina Coelho, Lídia Catarino, Francisco Gil, António Portugal

Data type: species data

Explanation note: a) Cloister of the Old Cathedral of Coimbra; b) lateral view of the Santa Maria Chapel; c) Particular art-piece from where the studied fungi were retrieved (photos by Miguel Mesquita)

Link: https://doi.org/10.3897/mycokeys.45.31799.suppl1

Supplementary material 2

Table S1. Fungal strains used in the phylogenetic analysis

Authors: João Trovão, Igor Tiago, Fabiana Soares, Diana Sofia Paiva, Nuno Mesquita, Catarina Coelho, Lídia Catarino, Francisco Gil, António Portugal

Data type: phylogenetic data

Link: https://doi.org/10.3897/mycokeys.45.31799.suppl2

Supplementary material 3

Figure S2. Growth of *Aeminium ludgeri* incubated at different NaCl concentrations after 4 weeks

Authors: João Trovão, Igor Tiago, Fabiana Soares, Diana Sofia Paiva, Nuno Mesquita, Catarina Coelho, Lídia Catarino, Francisco Gil, António Portugal

Data type: statistical data

Link: https://doi.org/10.3897/mycokeys.45.31799.suppl3

Supplementary material 4

Figure S3. Growth of *Aeminium ludgeri* incubated at different pHs levels after 4 weeks

Authors: João Trovão, Igor Tiago, Fabiana Soares, Diana Sofia Paiva, Nuno Mesquita, Catarina Coelho, Lídia Catarino, Francisco Gil, António Portugal

Data type: statistical data

Link: https://doi.org/10.3897/mycokeys.45.31799.suppl4

Supplementary material 5

Figure S4. Representative drawing of *Aeminium ludgeri*

Authors: João Trovão, Igor Tiago, Fabiana Soares, Diana Sofia Paiva, Nuno Mesquita, Catarina Coelho, Lídia Catarino, Francisco Gil, António Portugal

Data type: species data

Explanation note: a) initial simple, branched, septate hyphae becoming toruloid-like and strongly melanized; b) differentiated, toruloid-like hyphae with chains of arthroconidia; c) and d) arthroconidia (scale 10 μm).

Link: https://doi.org/10.3897/mycokeys.45.31799.suppl5

MycoKeys 45: 75–92 (2019)
doi: 10.3897/mycokeys.45.30813
http://mycokeys.pensoft.net

RESEARCH ARTICLE

A peer-reviewed open-access journal
MycoKeys
Launched to accelerate biodiversity research

Apophysomyces thailandensis (Mucorales, Mucoromycota), a new species isolated from soil in northern Thailand and its solubilization of non-soluble minerals

Surapong Khuna[1,2], Nakarin Suwannarach[1,3], Jaturong Kumla[1,3], Jomkhwan Meerak[1], Wipornpan Nuangmek[4], Tanongkiat Kiatsiriroat[5], Saisamorn Lumyong[1,3,5,6]

1 *Department of Biology, Faculty of Science, Chiang Mai University, Chiang Mai 50200, Thailand* **2** *PhD Degree Program in Applied Microbiology, Department of Biology, Faculty of Science, Chiang Mai University, Chiang Mai 50200, Thailand* **3** *Center of Excellence in Microbial Diversity and Sustainable Utilization, Chiang Mai University, Chiang Mai 50200, Thailand* **4** *Faculty of Agriculture and Natural Resources, University of Phayao, Phayao 56000, Thailand* **5** *Center of Excellence for Renewable Energy, Chiang Mai University, Chiang Mai 50200, Thailand* **6** *Academy of Science, The Royal Society of Thailand, Bangkok 10300, Thailand*

Corresponding author: *Saisamorn Lumyong* (saisamorn.l@cmu.ac.th)

Academic editor: *Maarja Öpik* | Received 24 October 2018 | Accepted 2 January 2019 | Published 29 January 2019

Citation: Khuna S, Suwannarach N, Kumla J, Meerak J, Nuangmek W, Kiatsiriroat T, Lumyong S (2019) *Apophysomyces thailandensis* (Mucorales, Mucoromycota), a new species isolated from soil in northern Thailand and its solubilization of non-soluble minerals. MycoKeys 45: 75–92. https://doi.org/10.3897/mycokeys.45.30813

Abstract

A new species of soil fungi, described herein as *Apophysomyces thailandensis*, was isolated from soil in Chiang Mai Province, Thailand. Morphologically, this species was distinguished from previously described *Apophysomyces* species by its narrower trapezoidal sporangiospores. A physiological determination showed that *A. thailandensis* differs from other *Apophysomyces* species by its assimilation of D-turanose, D-tagatose, D-fucose, L-fucose, and nitrite. A phylogenetic analysis, performed using combined internal transcribed spacers (ITS), the large subunit (LSU) of ribosomal DNA (rDNA) regions, and a part of the histone 3 (H3) gene, lends support to our the finding that *A. thailandensis* is distinct from other *Apophysomyces* species. The genetic distance analysis of the ITS sequence supports *A. thailandensis* as a new fungal species. A full description, illustrations, phylogenetic tree, and taxonomic key to the new species are provided. Its metal minerals solubilization ability is reported.

Keywords

Apophysomyces, mineral solubilization, soil fungi, taxonomy

Introduction

The genus *Apophysomyces*, proposed by Misra et al. (1979) with *A. elegans* as type species, belongs to the family Saksenaeaceae of the order Mucorales (Hoffmann et al. 2013). This genus is mainly characterized by pyriform sporangia, conspicuous funnel- and/or bell-shaped apophyses, and subhyaline, smooth-walled sporangiospores (Misra et al. 1979; Cooter et al. 1990; Alvarez et al. 2010). *Apophysomyces* is commonly found in soil, decaying vegetation, and detritus, and it has been reported to cause severe human infections in temperate and tropical regions (Misra et al. 1979; Cooter et al. 1990; Chakrabarti et al. 2003; Alvarez et al. 2010; Bonifaz et al. 2014). Currently, there are five known *Apophysomyces* species including *A. elegans* P.C. Misra, K.J. Srivast. & Lata (Misra et al. 1979), *A. ossiformis* E. Álvarez, Stchigel, Cano, Deanna A. Sutton & Guarro (Alvarez et al. 2010), *A. trapeziformis* E. Álvarez, Stchigel, Cano, Deanna A. Sutton & Guarro (Alvarez et al. 2010), *A. variabilis* E. Álvarez, Stchigel, Cano, Deanna A. Sutton & Guarro (Alvarez et al. 2010), and *A. mexicanus* A. Bonifaz, Cano, Stchigel & Guarro (Bonifaz et al. 2014).

During the isolation of non-soluble mineral solubilizing fungi from agricultural soil in northern Thailand, we found a particular population of *Apophysomyces* which we describe here as a new species based on morphological, molecular, and physiological characteristics. To confirm its taxonomic status, the phylogenetic relationship was determined by analysis of the combined sequence dataset of the ITS and LSU of rDNA, and part of the histone 3 gene.

Materials and methods

Fungal isolation

Soil samples were collected from agricultural areas of Mae Wang District, Chiang Mai Province, Thailand. The samples were air-dried at room temperature for 3 d, sieved and mixed through a 2 mm mesh prior to isolation of fungi by serial dilution. The dilution spread plate method was used with three serial dilutions in 0.5% NaCl solution. After dilution, 0.1 ml of suspension was spread on modified Aleksandrov agar (5.0 g glucose, 0.5 g $MgSO_4 \bullet 7H_2O$, 0.1 g $CaCO_3$, 0.005 g $FeCl_3$, 2.0 g Ca_3PO_4, 3.0 g K_2HPO_4, and 15.0 g agar, pH 7.0, in 1 L of deionized water) for detection of non-soluble mineral solubilizing fungi. The plates were incubated at 30 °C in darkness for 5 d. Colonies which produced clear zones were considered mineral solubilizing strains and were selected for further studies.

Morphological studies and growth observation

The colonies' morphology on potato dextrose agar (PDA; CONDA, Spain), Czapek agar (CZA; Difco, France), and malt extract agar (MEA; Difco, France) was observed

after 5 d of incubation in darkness at 37 °C. Three replicates were made in each medium. The colony diameter was measured. Micromorphological features were examined using a light microscope (Olympus CX51, Japan) following the methods described by Alvarez et al. (2010). The anatomical features were from at least 50 measurements of each structure.

Physiological studies

Carbon source assimilation profiles were determined with the API 50CH commercial kit (bioMérieux, France), following the methods described by Schwarz et al. (2007). To obtain sufficient sporulation, all isolates were cultured for 1 week on CZA at 37 °C. A final concentration of 5×10^5 spores/ml was prepared in 20 ml of yeast nitrogen base containing 0.5 g/l of chloramphenicol and 0.1% Bacto agar, and each well of the strips was inoculated with 300 µl of the spore containing medium. The inoculated API 50CH strips were incubated for 48–72 h at 37 °C in darkness. After incubation, the strips were read visually and growth or lack of growth was noted. Weak growth was considered as a positive result.

For nitrogen source assimilation we prepared inoculum as described above, but the yeast nitrogen base broth was replaced by carbon nitrogen base broth, and testing was performed in sterile, disposable, multiwell microplates. The medium with the nitrogen sources was dispensed into the wells in 150 µl, and each well was inoculated with 50 µl of the spore containing medium. The microplates were incubated at 37 °C in darkness for 48–72 h. Growth on NaCl (2%, 5%, 7%, and 10%), 2% $MgCl_2$ and 0.1% cycloheximide was determined. All tests were performed in three replicates.

Molecular studies

Genomic DNA of five day-old fungal mycelia on CZA was extracted using the fungal Genomic DNA Extraction Mini Kit (FAVOGEN, Taiwan). The ITS region of DNA was amplified by polymerase chain reactions (PCR) using ITS4 and ITS5 primers (White et al. 1990), the LSU of rDNA gene were amplified with NL1 and NL4 primers (Kurtzman and Robnett 1998), and histone 3 (H3) gene was amplified with the H3-1a and H3-1b primers (Glass and Donaldson 1995). The amplification program for these three domains were performed in separated PCR reaction and consisted of an initial denaturation at 95 °C for 5 min, followed by 35 cycles of denaturation at 95 °C for 30 s, annealing at 52 °C for 30 s (ITS); 52 °C for 45 s (LSU), and 54 °C for 1 min (H3), and extension at 72 °C for 1 min. Negative controls lacking fungal DNA were run for each experiment to check for any contamination of the reagents. PCR products were checked on 1% agarose gels stained with ethidium bromide under UV light and purified using NucleoSpin Gel and PCR Clean-up Kit (Macherey-Nagel, Germany). The purified PCR products were directly sequenced. Sequencing reactions were performed and sequences were automatically determined

in a genetic analyzer at 1st Base Company (Kembangan, Malaysia) using the same PCR primers mentioned above. Sequences were used to query GenBank via BLAST (http://blast.ncbi.nlm.nih.gov).

Details of the sequences used for phylogenetic analysis obtained from this study and from previous studies are provided in Table 1. The multiple sequence alignment was carried out using MUSCLE (Edgar 2004), and a combined ITS, LSU, and H3 alignments were deposited in TreeBASE under the study ID 23168. The combined ITS, LSU and H3 sequences dataset consisted of 28 taxa and the aligned dataset comprised 1991 characters including gaps (ITS: 1–942, LSU: 943–1620, and H3: 1621–1991). A maximum likelihood (ML) phylogenetic tree was constructed using RAxML v. 7.0.3 (Stamatakis 2006), applying the rapid bootstrapping algorithm for 1000 replications. *Saksenaea vasiformis* ATCC 60625 and *S. erythrospora* UTHSC 08-3606 were used as the outgroup. The ML trees were plotted with TreeView32 (Page 2001). Clades with bootstrap values (BS) ≥ 70% were considered as significantly supported (Hillis and Bull 1993). The best-fit substitution model for Bayesian inference algorithm was estimated by jModeltest v. 2.1.10 (Darriba et al. 2012) using Akaike information criterion. Bayesian phylogenetic analyses were carried out using the Metropolis-coupled Markov chain Monte Carlo (MCMCMC) method in MrBayes v. 3.2 (Ronquist et al. 2012), under a GRT+I+G model. Markov chains were run for one million generations, with six chains and random starting trees. The chains were sampled every 100 generations. Among these, the first 2000 trees were discarded as the burn-in phase of each analysis and the resulting trees were used to calculate Bayesian posterior probabilities. Bayesian posterior probabilities (PP) ≥ 0.95 were considered as a significant support (Alfaro et al. 2003). Pairwise genetic distances (proportions of variable sites) within and between five *Apophysomyces* species were computed using MEGA v. 6 (Tamura et al. 2013), with pairwise deletion of gaps and missing data.

The non-soluble minerals solubilization ability

This experiment was carried out using basal medium (10.0 g glucose, 0.5 g $(NH)_4SO_4$, 0.2 g NaCl, 0.1 g $MgSO_4 \bullet 7H_2O$, 0.2 g KCl, 0.5 g yeast extract, 0.002g $MnSO_4 \bullet H_2O$, and 15.0 g agar per liter of deionized water, pH 7.0) with addition of non-soluble metal minerals including $Ca_3(PO_4)_2$, $CaCO_3$, $CuCO_3 \bullet Cu(OH)_2$, CuO, $CoCO_3$, $FePO_4$, $MgCO_3$, MnO, $ZnCO_3$, ZnO, feldspar ($KAlSi_3O_8$), and kaolin ($Al_2Si_2O_5(OH)_4$) to the desired final concentration of 0.5% according to the method described by Fomina et al. (2005). The medium was autoclaved at 121 °C for 15 min. After autoclaving, for each experiment, 25 ml of test media was poured into Petri dishes. Mycelial inocula were prepared by growing the fungus on CZA at 30 °C in darkness for 7 d. Mycelial plugs (5 mm in diameter) from the periphery of the growing colony were then used to inoculate the center of the tested media. All plates were incubated at 30 °C in darkness

Table 1. Sequences used for phylogenetic analysis. Type species of *Apophysomyces* are in bold.

Taxa	Strain/isolate	GenBank accession number			References
		ITS	D1/D2 domain	H3	
Apophysomyces elegans	CBS 476.78	FN556440	FN554249	FN555155	Alvarez et al. 2010
Apophysomyces elegans	CBS 477.78	FN556437	FN554250	FN555154	Alvarez et al. 2010
Apophysomyces elegans	FMR 12015	HE664070	–	–	Da Cunha et al. 2012
Apophysomyces variabilis	CBS 658.93	FN556436	FN554258	FN555161	Alvarez et al. 2010
Apophysomyces variabilis	UTHSC 06-4222	FN556428	FN554255	FN555162	Alvarez et al. 2010
Apophysomyces variabilis	UTHSC 03-3644	FN556431	FN554259	FN555158	Alvarez et al. 2010
Apophysomyces variabilis	GMCH 480/07	FN556442	FN554253	FN555163	Alvarez et al. 2010
Apophysomyces variabilis	IMI 338332	FN556438	FN554257	FN555159	Alvarez et al. 2010
Apophysomyces variabilis	IMI 338333	FN556439	FN554256	FN555160	Alvarez et al. 2010
Apophysomyces variabilis	GMCH 211/09	FN556443	FN554254	FN555164	Alvarez et al. 2010
Apophysomyces variabilis	FMR 13881	LT837923	LT837927	–	Unpublished
Apophysomyces variabilis	FMR 13217	LT837922	LT837926	–	Unpublished
Apophysomyces variabilis	FMR 12016	HE664071	–	–	Da Cunha et al. 2012
Apophysomyces variabilis	GMCH M333/05	FN813491	–	–	Guarro et al. 2011
Apophysomyces variabilis	GMCH M52/05	FN813490	–	–	Guarro et al. 2011
Apophysomyces trapeziformis	UTHSC 08-1425	FN556429	FN554261	FN555168	Alvarez et al. 2010
Apophysomyces trapeziformis	UTHSC 08-2146	FN556430	FN554260	FN555169	Alvarez et al. 2010
Apophysomyces trapeziformis	UTHSC 06-2356	FN556427	FN554262	FN555167	Alvarez et al. 2010
Apophysomyces trapeziformis	UTHSC 04-891	FN556433	FN554264	FN555165	Alvarez et al. 2010
Apophysomyces trapeziformis	UTHSC R-3841	FN556434	FN554263	FN555166	Alvarez et al. 2010
Apophysomyces ossiformis	UTHSC 04-838	FN556432	FN554252	FN555157	Alvarez et al. 2010
Apophysomyces ossiformis	UTHSC 07-204	FN556435	FN554251	FN555156	Alvarez et al. 2010
Apophysomyces mexicanus	CBS 136361	HG974255	HG974256	HG974254	Bonifaz et al. 2014
Apophysomyces thailandensis	SDBR-CMUS24	MH733250	MH733253	MH733256	This study
Apophysomyces thailandensis	SDBR-CMUS26	MH733251	MH733254	MH733257	This study
Apophysomyces thailandensis	SDBR-CMUS219	MH733252	MH733255	MH733258	This study
Saksenaea vasiformis	ATCC 60625	FR687323	HM776675	–	Alvarez et al. 2010
Saksenaea erythrospora	UTHSC 08-3606	FR687328	HM776680	–	Alvarez et al. 2010

for 4 d. Colony diameter and solubilization zone (halo zone) were measured. Solubilization index (SI) was calculated as the halo zone diameter divided by the fungal colony diameter (Vitorino et al. 2012, Kumla et al. 2014). SI values of less than 1.0, between 1.0 and 2.0, and more than 2.0 were regarded as low, medium, and high solubilization activities, respectively. Three replications were made in each treatment.

Statistical analysis

The data were analyzed by one-way analysis of variance (ANOVA) by SPSS program version 16.0 (SPSS Inc., USA) for Windows, and Tukey's range test was used for significant differences (P <0.05) between treatments.

Table 2. Growth rate of *Apophysomyces thailandensis* on different media and at different temperatures.

Medium	Temperature (°C)	Isolate/growth rate (mm/day)		
		SDBR-CMUS24	SDBR-CMUS26 (Holotype)	SDBR-CMUS219
PDA	4	–	–	–
	20	5.78 ± 0.51 i	5.78 ± 0.19 jk	5.67 ± 0.67 i
	25	8.58 ± 0.76 g	8.67 ± 0.76 g	8.83 ± 0.88 f
	30	28.33 ± 0.00 b	28.33 ± 0.00 b	28.33 ± 0.00 b
	37	40.64 ± 0.00 a	45.04 ± 0.00 a	42.64 ± 0.00 a
	42	16.73 ± 0.47 d	17.00 ± 0.00 d	16.89 ± 0.19 d
	45	–	–	–
	50	–	–	–
MEA	4	–	–	–
	20	3.64 ± 0.62 k	3.55 ± 0.16 l	3.69 ± 0.36 k
	25	5.89 ± 019 i	6.11 ± 0.19 ij	6.00 ± 0.33 hi
	30	7.00 ± 0.71 h	7.57 ± 0.74 h	6.95 ± 0.70 gh
	37	9.80 ± 1.00 f	9.93 ± 1.10 f	9.07 ± 0.99 f
	42	6.13 ± 0.63 i	6.38 ± 0.57 i	6.08 ± 0.62 hi
	45	–	–	–
	50	–	–	–
CZA	4	–	–	–
	20	4.60 ± 0.20 j	4.93 ± 0.76 k	4.67 ± 0.99 j
	25	7.89 ± 0.35 g	8.33 ± 0.76 gh	7.28 ± 0.19 g
	30	17.00 ± 0.00 d	17.00 ± 0.00 d	17.00 ± 0.00 d
	37	21.25 ± 0.00 c	21.25 ± 0.00 c	21.25 ± 0.00 c
	42	13.79 ± 0.46 e	14.09 ± 0.13 e	13.94 ± 0.39 e
	45	–	–	–
	50	–	–	–

PDA = potato dextrose agar, MEA = malt extract agar and CZA = Czapek agar. "-" = no growth.
Value with the different letters with in the same column indicated the significant difference at P <0.05 according to Tukey's range test

Results

Growth observation and physiological studies

Mycelial growth of the three *A. thailandensis* isolates on three different agar media and at different temperatures is presented in Table 2. PDA promoted the best mycelial growth followed by CZA, and MEA. All isolates grew at temperatures ranging from 20–42 °C. The highest growth rate was observed on PDA at 37 °C.

Carbon assimilation profiles of the three strains of *A. thailandensis* are shown in Table 3. Assimilation patterns of all strains were positive for 23 carbon sources (amidon, D-adonitol, D-arabitol, D-fructose, D-fucose, D-glucose, D-lyxose, D-maltose, D-mannitol, D-mannose, D-melezitose, D-ribose, D-sorbitol, D-tagatose, D-trehalose, D-turanose, D-xylose, glycerol, glycogen, L-arabinose, L-fucose, *N*-acetyl-glucosamine and xylitol). Variability in nitrogen assimilation and tolerance to NaCl, $MgCl_2$, and cycloheximide of the three strains of *A. thailandensis* are presented in Table 4. All strains were positive for 10 nitrogen sources (arginine, creatine, L-cysteine, L-leucine,

Table 3. Carbon assimilation profiles for *Apophysomyces* species obtained with API 50 CH strips.

Carbon source	*A. thailandensis*[a]			*A. elegans*[b]	*A. mexicanus*[c]	*A. ossiformis*[b]	*A. trapeziformis*[b]	*A. variabilis*[b]
	SDBR-CMUS24	**SDBR-CMUS26^T**	**SDBR-CMUS219**	**CBS 476.78^T**	**CBS 136361^T**	**UTHSC 04-838^T**	**UTHSC 08-1425^T**	**CBS 658.93^T**
GLY (glycerol)	+	+	+	+	+	+	+	+
ERY (erythritol)	–	–	–	–	–	–	–	–
DARA (D-arabinose)	–	–	–	–	–	–	–	–
LARA (L-arabinose)	+	+	+	+	–	+	+	+
RIB (D-ribose)	+	+	+	+	+	+	+	+
DXYL (D-xylose)	+	+	+	+	+	+	+	+
LXYL (L-xylose)	–	–	–	–	–	–	–	–
ADO (D-adonitol)	+	+	+	+	+	+	+	+
MDX (*methyl*-ß-D-xylopyranoside)	–	–	–	–	–	–	–	–
GAL (D-galactose)	–	–	–	–	–	–	–	–
GLU (D-glucose)	+	+	+	+	+	+	+	+
FRU (D-fructose)	+	+	+	+	+	+	+	+
MNE (D-mannose)	+	+	+	+	+	+	+	+
SBE (L-sorbose)	–	–	–	–	–	–	–	–
RHA (L-rhamnose)	–	–	–	–	–	–	–	–
DUL (dulcitol)	–	–	–	–	–	–	–	–
INO (inositol)	–	–	–	–	–	–	–	–
MAN (D-mannitol)	+	+	+	+	+	+	+	+
SOR (D-sorbitol)	+	+	+	+	+	+	+	+
MDM (*methyl*-D-mannopyranoside)	–	–	–	–	–	–	–	–
MDG (*methyl*-D-glucopyranoside)	–	–	–	–	–	–	–	–
NAG (*N*-acetyl-glucosamine)	+	+	+	+	+	+	+	+
AMY (amygdalin)	–	–	–	–	–	–	–	–
ARB (arbutin)	–	–	–	–	–	–	–	–
ESC (esculin)	–	–	–	+	–	–	–	–
SAL (salicin)	–	–	–	–	–	–	–	–
CEL (D-cellobiose)	–	–	–	+	–	+	+	+
MAL (D-maltose)	+	+	+	+	+	+	+	+
LAC (D-lactose)	–	–	–	–	–	–	–	–
MEL (D-melibiose)	–	–	–	–	–	–	–	–
SAC (D-saccharose)	–	–	–	–	–	–	–	–
TRE (D-trehalose)	+	+	+	+	+	+	+	+
INU (inulin)	–	–	–	–	–	–	–	–
MLZ (D-melezitose)	+	+	+	+	–	+	+	+
RAF (D-raffinose)	–	–	–	–	–	–	–	–
AMD (amidon)	+	+	+	+	–	+	+	+
GLYG (glycogen)	+	+	+	+	+	+	+	+
XLT (xylitol)	+	+	+	+	+	+	+	+
GEN (gentiobiose)	–	–	–	–	–	–	–	–
TUR (D-turanose)	+	+	+	–	–	–	–	–
LYX (D-lyxose)	+	+	+	–	+	+	–	–

Carbon source	*A. thailandensis*[a]			*A. elegans*[b]	*A. mexicanus*[c]	*A. ossiformis*[b]	*A. trapeziformis*[b]	*A. variabilis*[b]
	SDBR-CMUS24	SDBR-CMUS26^T	SDBR-CMUS219	CBS 476.78^T	CBS 136361^T	UTHSC 04-838^T	UTHSC 08-1425^T	CBS 658.93^T
TAG (D-tagatose)	+	+	+	–	–	–	–	–
DFUC (D-fucose)	+	+	+	–	–	–	–	–
LFUC (L-fucose)	+	+	+	–	–	–	–	–
DARL (D-arabitol)	+	+	+	+	+	+	+	+
LARL (L-arabitol)	–	–	–	+	+	+	+	+
GNT (potassium gluconate)	–	–	–	–	+	–	–	–
2KG (potassium 2-keto- gluconate)	–	–	–	–	–	–	–	–
5KG (potassium 5-keto- gluconate)	–	–	–	–	–	–	–	–

[a]This study, [b]Alvarez et al. (2010) and [c]Bonifaz et al. (2014)

Table 4. Nitrogen assimilation and tolerance to chemical compounds for *Apophysomyces* species.

Nitrogen source and other tests	*A. thailandensis*[a]			*A. elegans*[b]	*A. mexicanus*[c]	*A. ossiformis*[b]	*A. trapeziformis*[b]	*A. variabilis*[b]
	SDBR-CMUS24	SDBR-CMUS26^T	SDBR-CMUS219	CBS 476.78^T	CBS 136361^T	UTHSC 04-838^T	UTHSC 08-1425^T	CBS 658.93^T
Creatine	+	+	+	+	+	+	+	+
L-lysine	+	+	+	+	+	+	+	+
Nitrate	+	+	+	+	+	+	+	+
Nitrite	+	+	+	–	–	–	–	–
L-tryptophan	+	+	+	+	+	+	+	+
L-proline	+	+	+	+	+	+	+	+
L-leucine	+	+	+	+	+	+	+	+
L-ornithine	+	+	+	+	+	+	+	+
L-cysteine	+	+	+	+	+	+	+	+
Arginine	+	+	+	+	+	+	+	+
2% NaCl	–	–	–	+	+	+	+	+
5% NaCl	–	–	–	–	–	–	–	–
7% NaCl	–	–	–	–	–	–	–	–
10% NaCl	–	–	–	–	–	–	–	–
2% $MgCl_2$	+	+	+	+	+	+	+	+
Cycloheximide 0.1%	–	–	–	–	–	–	–	–

[a]This study, [b]Alvarez et al. (2010) and [c]Bonifaz et al. (2014)

L-lysine, L-ornithine, L-proline, L-tryptophan, nitrate and nitrite). All strains were able to grow on 2% $MgCl_2$, but could not grow on 2%, 5%, 7%, and 10% NaCl, and on 0.1% cycloheximide.

Phylogenetic results

The topologies of each single-gene and the multi-gene (ITS, LSU, and H3 genes) trees were similar. Therefore, we show only the multi-gene tree (Fig. 1). Our phylogenetic analysis separated *Apophysomyces* into three main clades. Clade I contained two species (*A. variabilis* and *A. elegans*). *Apophysomyces trapeziformis*, *A. mexicanus*, and *A. ossiformis* were assigned to clade II. *Apophysomyces thailandensis* was clearly separated from the other *Apophysomyces* species and formed a separate monophyletic clade (clade III) with high BS (100%) and PP (1.0) support.

The percentage of nucleotide distances of ITS (ITS1+5.8S+ITS2) sequence between *A. thailandensis* and other *Apophysomyces* species is shown in Table 5. The percentage nucleotide distance of *A. thailandensis* ranged from 4.53–15.60% from other *Apophysomyces* species.

Metal minerals solubilization ability

The ability of *A. thailandensis* to solubilize metal minerals depended on the type of minerals and strain. In some cases, *A. thailandensis* produced a solubilization zone in agar that was larger than the fungal colonies (Fig. 2A–D), while in other cases the solubilization zones were found beneath the fungal colonies (Fig. 2E–H). The solubilization activities were expressed in terms of a solubilization index (SI) and are shown in Figure 3. The solubilization activity of all *A. thailandensis* strains in the presence of $CaCO_3$, $Ca_3(PO_4)_2$, $CuCO_3$•$Cu(OH)_2$, CuO, $ZnCO_3$, and ZnO was characterized as medium (SI value between 1.0 and 2.0) activity. All strains showed a low solubilization activity (SI value less than 1.0) for $CoCO_3$, $FePO_4$, MnO, feldspar, and kaolin.

Taxonomy

Apophysomyces thailandensis **S. Khuna, N. Suwannarach & S. Lumyong, sp. nov.**
MycoBank No.: MB827677
Fig. 4

Etymology. For '*thailandensis*', referring to Thailand, where soil containing the new fungus was collected.

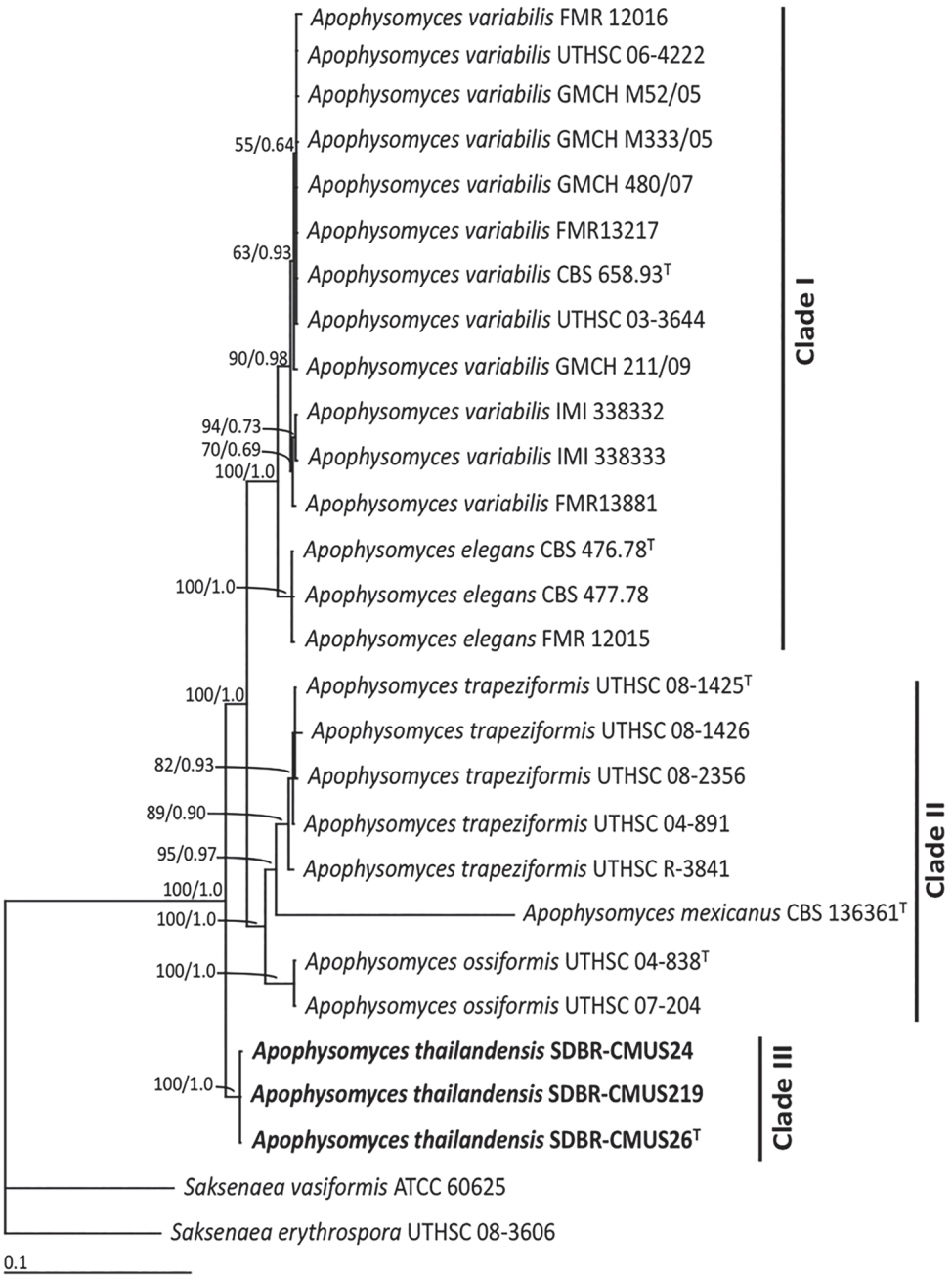

Figure 1. Phylogenetic tree derived from maximum likelihood analysis of a combined ITS, LSU, and H3 genes of 28 sequences. *Saksenaea vasiformis* and *S. erythrospora* were used as outgroup. Numbers above branches are the bootstrap statistics percentages (left) and Bayesian posterior probabilities (right). Branches with bootstrap values ≥ 50% are shown at each branch and the bar represents 0.1 substitutions per nucleotide position. The fungal isolates from this study are in bold. Superscript T = type species.

Table 5. Mean percentage nucleotide *p*-distances of ITS (ITS1+5.8S+ITS2) sequences compared between *Apophysomyces* species.

Number	***Apophysomyces* species**	**Within species**	**1**	**2**	**3**	**4**	**5**
1	*A. thailandensis* (n=3)	0.0 ± 0.00					
2	*A. trapeziformis* (n=5)	1.15±0.31	4.53±0.43				
3	*A. ossiformis* (n=2)	0.10±0.00	5.25±0.07	4.70±0.28			
4	*A. variabilis* (n=12)	0.55±0.26	4.96±0.05	5.85±0.24	5.95±0.13		
5	*A. mexicanus* (n=1)	–	15.60±0.00	16.30±0.00	15.30±0.00	16.10±0.00	
6	*A. elegans* (n=3)	0.10±0.00	4.56±0.26	6.18±0.17	5.75±0.21	3.00±0.10	16.75±0.38

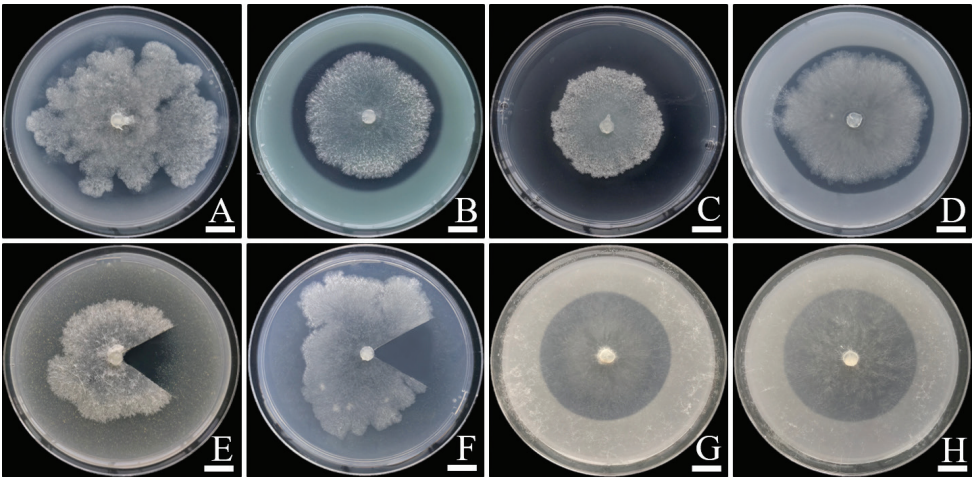

Figure 2. Solubilization of non-soluble minerals in agar media by *Apophysomyces thailandensis* SDBR-CMUS26 (holotype). **A** $Ca_3(PO_4)_2$ **B** $CuCO_3$•$Cu(OH)_2$ **C** CuO **D** $ZnCO_3$ **E** $FePO_4$ **F** MnO **G** Feldspar **H** Kaolin. Scale bars: 10 mm. Fungal colonies in **E** and **F** were cut for the solubilization area (halo zone) observation.

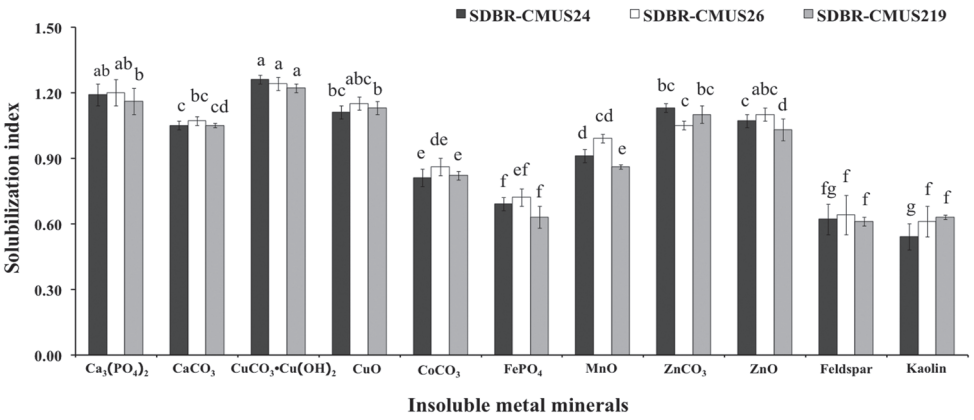

Figure 3. Solubilization index of the ability to solve non-soluble mineral by *Apophysomyces thailandensis*. Data are means of three replicates. Error bar at each point indicates ± SD. Different letters above each graph indicate that the means are significantly different by Tukey's test ($P < 0.05$)

Holotype. THAILAND. Chiang Mai Province: Mae Wang District, (18°36'46"N, 98°46'30"E), isolated from soil in agricultural area, 8 August 2017, S. Khuna, dried cultures: SDBR-CMUS26; ex-type living culture: TBRC9299

Gene sequences (from holotype). MH733251 (ITS), MH733254 (LSU), MH733257 (H3).

Diagnosis. Distinguished from other *Apophysomyces* species by the slightly trapezoidal sporangiospores, and from *A. elegans*, *A. trapeziformis*, and *A. mexicanus* by its narrower sporangiospores.

Colonies on PDA attaining a diameter of 90 mm after 2 d at 37 °C, whitish at first, becoming white to cream-colored, reverse concolorous (Fig. 4A). Colonies on MEA attaining a diameter of 90 mm after 5 d at 37 °C, flat, whitish, reverse concolorous (Fig. 4B). Colonies on CZA attaining a diameter of 90 mm after 4 d at 37 °C, whitish at first, becoming white to cream-colored, with scarce aerial mycelium, reverse concolorous (Fig. 4C). On all agar media the hyphae are branched, hyaline, smooth-walled, and have 5–15 µm in diameter (Fig. 4D). Sporulation was observed only on CZA. Sporangiophores erect, usually arising singly, emerging from aerial hyphae, at first hyaline but soon becoming light brown, usually straight, slightly tapered towards the apex, unbranched, 60–890 µm in length, 3.75–7.5 µm wide, and smooth-walled. Sporangia apophysate, terminal, pyriform, multispored, white at first, becoming light greyish brown when mature, and 25–58 µm in diameter. Apophyses short, funnel to bell shaped, 21–52 × 19–46 µm (Fig. 4E). Sporangiospores slightly trapezoidal in side view, cylindrical in front view, with flattened to slightly concave lateral walls, hyaline to light brown in mass, smooth- and thin-walled, 5–6(9) × 2–3 µm (Fig. 4F).

Other cultures examined. THAILAND. Chiang Mai Province: Mae Wang District, (18°36'46"N, 98°46'30"E), isolated from soil in agricultural areas, 8 August 2017, S. Khuna, living cultures: SDBR-CMUS24 and SDBR-CMUS219.

Key to *Apophysomyces* species*

1	Sporangiospores trapezoid, ellipsoid, subtriangular or claviform in shape..... ***A. variabilis***
–	Sporangiospores less variable in shape **2**
2	Sporangiospores slightly trapezoidal to trapezoidal in shape **3**
–	Sporangiospores other shapes **5**
3	Sporangiospores 2–3 µm wide ..... ***A. thailandensis***
–	Sporangiospores 3–5 µm wide **4**
4	Apophyses cup-funnel shape, 8–15 µm long ..... ***A. mexicanus***
–	Apophyses funnel-shaped, 15–20 µm long..... ***A. trapeziformis***
5	Sporangiospores bone-like in shape..... ***A. ossiformis***
–	Sporangiospores ovoid, broadly ellipsoidal to barrel-shaped ..... ***A. elegans***

* Sporangiospores and apophyses observed on Czapek agar in culture.

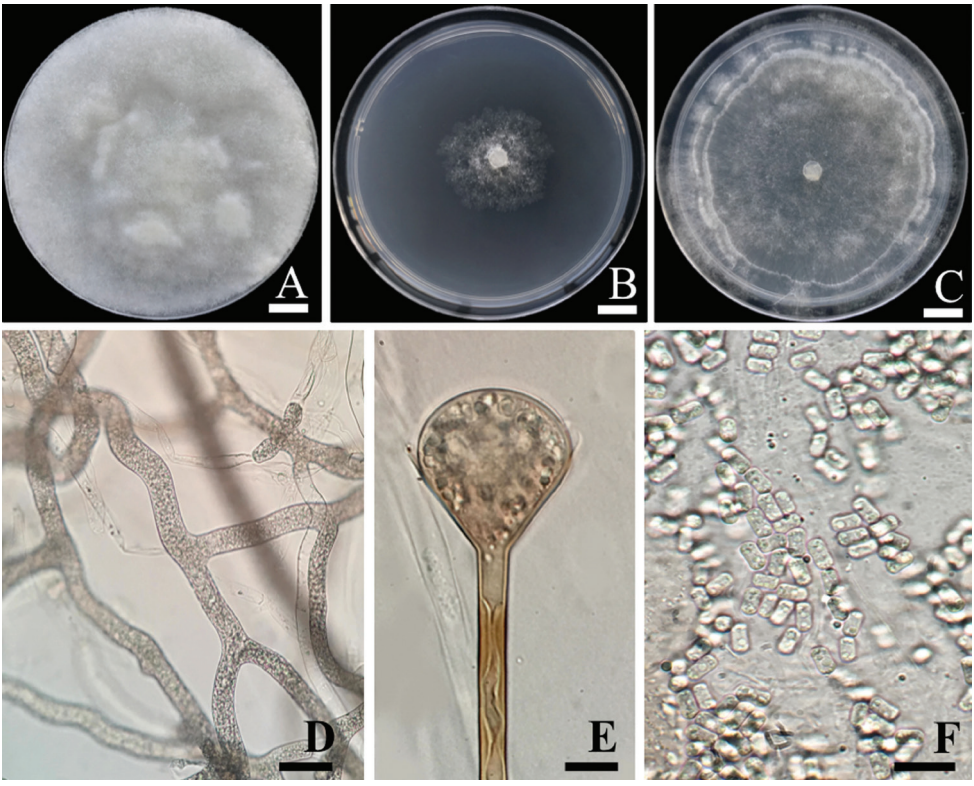

Figure 4. *Apophysomyces thailandensis* SDBR-CMUS26 (holotype). **A** colony on potato dextrose agar **B** Colony on malt extract agar **C** Colony on Czapek agar **D** Branched, aseptate hyphae **E** Funnel-shaped apophysis **F** Slightly trapezoidal sporangiospores. Scale bars: 10 mm (**A–C**), 10 µm (**D–E**), 20 µm (**F**).

Discussion

The present study identifies a new species of *Apophysomyces*, a soil fungus from Thailand based on morphological and physiological characteristics as well as on phylogenetic analyses. *Apophysomyces thailandensis* is characterized by its funnel- to bell-shaped apophyses and slightly trapezoidal sporangiospores. These morphological characteristics support its placement into the genus *Apophysomyces* (Misra et al. 1979; Alvarez et al. 2010; Bonifaz et al. 2014). Based on morphology, the slightly trapezoidal sporangiospores of *A. thailandensis* clearly distinguish it from *A. elegans* and *A. ossiformis*, with exceptions of *A. mexicanus*, *A. trapeziformis*, and *A. variabilis* (Table 6). However, the width of sporangiospores of *A. thailandensis* (2–3 µm wide) was found to be narrower than *A. elegans* (3–8 µm wide) (Misra et al. 1979; Alvarez et al. 2010), *A. ossiformis* (3–5.5 µm wide) (Alvarez et al. 2010), and *A. variabilis* (3–6 µm wide) (Alvarez et al. 2010).

Carbon assimilation profiles have been shown to be useful for differentiation of mucoralean genera (Schwarz et al. 2007). The current study found that *A. thailandensis* showed negative results for D-galactose, amygdalin, arbutin, salacin, and gentiobiose

Table 6. Origin, isolation source and microscopic observation of *Apophysomyces* species.

Apophysomyces species	Origin	Isolation source	Microscopic observation				
			Hyphae width (µm)	Sporangio-phores (µm)	Sporangia (µm)	Apophyses shape / size (µm)	Sporangiospore shape / size (µm)
A. elegans[a, b]	India	Soil	3.4–8	400–540 × 3.4–7.5	20–60	Funnel to bell / 10–46 × 11–46	Ovoid, broadly ellipsoidal to barrel-shaped / 5.4–12 × 3–8
A. mexicanus[c]	Mexico	Human necrotic lesion	3–5.5	100–700 × 3.5–7.0	25–30	Cub-funnel / 12–20 × 8–15	Slightly trapezoidal / 5–10 × 3–4
A. ossiformis[a]	USA	Cellulitis of human leg wound	3–5.5	100–400 × 2–3.5	15–50	Funnel / 15–20 × 15–20	Bone-like / 6–8 × 3–5.5
A. trapeziformis[a]	USA	Abdominal abscess of human	3–5.5	400 × 2–3.5	15–50	Funnel / 15–20 × 15–20	Trapezoid / 5–8.5 × 3–5
A. thailandensis[d]	Thailand	Soil	5–15	60–890 × 3.75–7.5	25–58	Funnel to bell / 21–52 × 19–46	Slightly trapezoidal / 5–9 × 2–3
A. variabilis[a]	Netherlands	Osteomyelitis of human	3–5.5	100–400 × 2–3.5	15–50	Funnel / 15–20 × 15–20	Trapezoid, ellipsoid, subtriangular or claviform / 5–14 × 3–6

[a]Alvarez et al. 2010, [b]Misra et al. (1979), [c]Bonifaz et al. (2014) and [d]This study.

assimilation. This agrees with a previous study, which reported that the genus *Apophysomyces* could not assimilate these five substances (Schwarz et al. 2007; Alvarez et al. 2010; Bonifaz et al. 2014) (Table 4). *Apophysomyces thailandensis* was positive in the assimilation of D-adonitol, D-arabitol, D-fructose, D-glucose, D-mannitol, D-mannose, D-maltose, D-ribose, D-sorbitol, D-trehalose, D-xylose, glycerol, glycogen, *N*-acetyl-glucosamine and xylitol, similar to other *Apophysomyces* species (Alvarez et al. 2010; Bonifaz et al. 2014). However, the assimilation of D-fucose, D-tagatose, D-turanose, and L-fucose and the non-assimilation of L-arabitol by *A. thailandensis* differs from the other *Apophysomyces* species (Alvarez et al. 2010; Bonifaz et al. 2014) (Table 4). The positive results in the nitrogen assimilation profiles and tolerance to various chemical agents for arginine, creatine, L-cysteine, L-leucine, L-lysine, L-ornithine, L-proline, L-tryptophan, nitrate, and 2% $MgCl_2$ of *A. thailandensis* are similar to other *Apophysomyces* species (Table 4) (Alvarez et al. 2010; Bonifaz et al. 2014). Nitrite assimilation and 2% NaCl intolerance of *A. thailandensis* separated it from the other *Apophysomyces* species (Alvarez et al. 2010; Bonifaz et al. 2014).

In the phylogenetic analysis based on multi-gene sequences of combined ITS, LSU, and the histone 3 gene, *A. thailandensis* formed a monophyletic clade, separate from the other *Apophysomyces* species. The ITS (ITS1+5.8S+ITS2) genetic distance between *A. thailandensis* and other *Apophysomyces* species ranged from 4.53% to 15.60% (Table 5). This genetic distance of ITS was greater than 3%, which is sufficient to indicate a new fungal species (Leavitt et al. 2013; Nilsson et al. 2008).

In the terrestrial environment, fungi play important roles in the biogeochemical cycling of elements (Gadd 2017; Frąc et al. 2018). Soil fungi can mobilize and solubi-

lize non-soluble minerals into forms available for cellular uptake and leaching from the system, e.g. complexation with organic acid, other metabolites and siderophores (Gadd 2010; Mapelli et al. 2012). In this study, pure cultures of *A. thailandensis* were able to solubilize different non-soluble minerals (Ca, Co, Cu, Fe, Mn, and Zn-containing minerals), and the solubilization demonstrated very different activities for the different minerals. This is similar to previous studies that reported other mucoralean genera (e.g. *Absidia*, *Cunninghamella*, *Mucor*, and *Rhizopus*) isolated from soils are able to solubilize non-soluble minerals (Ca, Fe, Mg and Zn-containing minerals) (Arrieta and Grez 1971; Kolo and Claeys 2005; Akintokun et al. 2007; Nenwani et al. 2010; Sharma et al. 2013; Patel et al. 2015; Alori et al. 2017; Ceci et al. 2018). This is the first report describing non-soluble mineral solubilization ability by the genus *Apophysomyces*.

In conclusion, the combination of morphological and physiological characteristics, and the molecular analysis strongly support our claim of a new fungus species. This discovery is considered important in terms of stimulating the investigations of soil fungi in Thailand and will help researchers to better understand the distribution and ecology of the genus *Apophysomyces*.

Acknowledgments

This work was supported by grants from Center of Excellence on Biodiversity (BDC), Office of Higher Education Commission (BDC-PG4-161008), Center of Excellence for Renewable Energy, and Center of Excellence in Microbial Diversity and Sustainable Utilization, Chiang Mai University, Chiang Mai, Thailand. We are grateful to Dr Eric McKenzie for proofreading the English.

References

Akintokun AK, Akande GA, Akintokun PO, Popoola TOS, Babalola AO (2007) Solubilization of insoluble phosphate by organic acid-producing fungi isolated from Nigerian soil. International Journal of Soil Science 2(4): 301–307. https://doi.org/10.3923/ijss.2007.301.307

Alfaro ME, Zoller S, Lutzoni F (2003) Bayes or bootstrap? A simulation study comparing the performance of Bayesian Markov Chain Monte Carlo sampling and bootstrapping in assessing phylogenetic confidence. Molecular Biology and Evolution 20(2): 255–266. https://doi.org/10.1093/molbev/msg028

Alori ET, Glick BR, Babalola OO (2017) Microbial phosphorus solubilization and its potential for use in sustainable agriculture. Frontiers in Microbiology 8: 971. https://doi.org/10.3389/fmicb.2017.00971

Alvarez E, Stchigel AM, Cano J, Sutton DA, Fothergill AW, Chander J, Salas V, Rinaldi MG, Guarro J (2010) Molecular phylogenetic diversity of the emerging mucoralean fungus *Apophysomyces*: proposal of three new species. Revista Iberoamericana de Micología 27(2): 80–89. https://doi.org/10.1016/j.riam.2010.01.006

Arrieta L, Grez R (1971) Solubilization of iron-containing minerals by soil microorganisms. Applied Microbiology 22(4): 487–490.

Bonifaz A, Stchigel AM, Guarro J, Guevara E, Pintos L, Sanchis M, Cano-Lira JF (2014) Primary cutaneous mucormycosis produced by the new species *Apophysomyces mexicanus*. Journal of Clinical Microbiology 52(12): 4428–4431. https://doi.org/10.1128/JCM.02138-14

Ceci A, Pinzari F, Russo F, Maggi O, Persiani AM (2018) Saprotrophic soil fungi to improve phosphorus solubilisation and release: in vitro abilities of several species. Ambio 47(1): 30–40. https://doi.org/10.1007/s13280-017-0972-0

Chakrabarti A, Ghosh A, Prasad GS, David JK, Gupta S, Das A, Sakhuja V, Panda NK, Singh SK, Das S, Chakrabarti T (2003) *Apophysomyces elegans*: an emerging zygomycete in India. Journal of Clinical Microbiology 41(2): 783–788. https://doi.org/10.1128/JCM.41.2.783-788.2003

Cooter RD, Lim IS, Ellis DH, Leitch IOW (1990) Burn wound zygomycosis caused by *Apophysomyces elegans*. Journal of Clinical Microbiology 28(9): 2151–2153.

Da Cunha KC, Sutton DA, Gené J, Capilla J, Cano J, Guarro J (2012) Molecular identification and *in vitro* response to antifungal drugs of clinical isolates of *Exserohilum*. Antimicrobial Agents and Chemotherapy 56(9): 4951–4954. https://doi.org/10.1128/AAC.00488-12

Darriba D, Taboada GL, Doallo R, Posada D (2012) jModelTest 2: more models, new heuristics and parallel computing. Nature Methods 9: 772. https://doi.org/10.1038/nmeth.2109

Edgar RC (2004) MUSCLE: multiple sequence alignment with high accuracy and high throughput. Nucleic Acids Research 32(5): 1792–1797. https://doi.org/10.1093/nar/gkh340

Fomina MA, Alexander IJ, Colpaert JV, Gadd GM (2005) Solubilization of toxic metal minerals and metal tolerance of mycorrhizal fungi. Soil Biology and Biochemistry 37(5): 851–866. https://doi.org/10.1016/j.soilbio.2004.10.013

Frąc M, Hannula SE, Bełka M, Jędryczka M (2018) Fungal biodiversity and their role in soil health. Frontiers in Microbiology 9: 707. https://doi.org/10.3389/fmicb.2018.00707

Gadd GM (2010) Metals, minerals and microbes: geomicrobiology and bioremediation. Microbiology 156: 609–643. https://doi.org/10.1099/mic.0.037143-0

Gadd GM (2017) The geomycology of elemental cycling and transformation in the environment. Microbiology Spectrum 5(1): 1–6. https://doi.org/10.1128/microbiolspec.funk-0010-2016

Glass NL, Donaldson GC (1995) Development of primer sets designed for use with the PCR to amplify conserved genes from filamentous ascomycetes. Applied and Environmental Microbiology 61(4): 1323–1330.

Guarro J, Chander J, Alvarez E, Stchigel AM, Robin K, Dalal U, Rani H, Punia RS, Cano JF (2011) *Apophysomyces variabilis* infections in humans. Emerging Infectious Diseases 17(1): 134–135. https://doi.org/10.3201/eid1701.101139

Hillis DM, Bull JJ (1993) An empirical test of bootstrapping as a method for assessing confidence in phylogenetic analysis. Systematic Biology 42(2): 182–192. https://doi.org/10.1093/sysbio/42.2.182

Hoffmann K, Pawłowska J, Walther G, Wrzosek M, de Hoog GS, Benny GL, Kirk PM, Voigt K (2013) The family structure of the *Mucorales*: a synoptic revision based on comprehensive multigene-genealogies. Persoonia 30: 57–76. https://doi.org/10.3767/003158513X666259

Kolo K, Claeys PH (2005) In vitro formation of Ca-oxalates and the mineral glushinskite by fungal interaction with carbonate substrates and seawater. Biogeosciences 2(3): 277–293. https://doi.org/10.5194/bg-2-277-2005

Kumla J, Suwannarach N, Bussaban B, Matsui K, Lumyong S (2014) Indole-3-acetic acid production, solubilization of insoluble metal minerals and metal tolerance of some scleroderma-toid fungi collected from northern Thailand. Annals of Microbiology 64(2): 707–720. https://doi.org/10.1007/s13213-013-0706-x

Kurtzman CP, Robnett CJ (1998) Identification and phylogeny of ascomycetous yeasts from analysis of nuclear large subunit (26S) ribosomal DNA partial sequences. Antonie van Leeuwenhoek 73(4): 331–371. https://doi.org/10.1023/A:1001761008817

Leavitt SD, Fernández-Mendoza F, Pérez-Ortega S, Sohrabi M, Divakar PK, Lumbsch HT, Clair St. LL (2013) DNA barcode identification of lichen-forming fungal species in the *Rhizoplaca melanophthalma* species-complex (Lecanorales, Lecanoraceae), including five new species. MycoKeys 7: 1–22. https://doi.org/10.3897/mycokeys.7.4508

Misra PC, Srivastava KJ, Lata K (1979) *Apophysomyces*, a new genus of the Mucorales. Mycotaxon 8(2): 377–382.

Mapelli F, Marasco R, Balloi A, Rolli E, Cappitelli F, Daffonchio D, Borin S (2012) Mineral-microbe interactions: biotechnological potential of bioweathering. Journal of Biotechnology 157(4): 473–481. https://doi.org/10.1016/j.jbiotec.2011.11.013

Nenwani V, Doshi P, Saha T, Rajkumar S (2010) Isolation and characterization of a fungal isolate for phosphate solubilization and plant growth promoting activity. Journal of Yeast and Fungal Research 1(1): 9–14.

Nilsson RH, Kristiansson E, Ryberg M, Hallenberg N, Larsson KH (2008) Intraspecific *ITS* variability in the kingdom Fungi as expressed in the international sequence databases and its implications for molecular species identification. Evolutionary Bioinformatics 4: 193–201. https://doi.org/10.4137/EBO.S653

Page RD (2001) TreeView. Glasgow University, Glasgow, Scotland.

Patel S, Panchal B, Karmakar N, Rajkumar, Jha S (2015) Solubilization of rock phosphate by two *Rhizopus* species isolated from coastal areas of South Gujarat and its effect on chickpea. Ecology, Environment and Conservation 21: 229–237.

Prakash H, Rudramurthy SM, Gandham PS, Ghosh AK, Kumar MM, Badapanda C, Chakrabarti A (2017) *Apophysomyces variabilis*: draft genome sequence and comparison of predictive virulence determinants with other medically important *Mucorales*. BMC Genomics 18(736): 1–13. https://doi.org/10.1186/s12864-017-4136-1

Ronquist F, Teslenko M, Van der Mark P, Ayres DL, Darling A, Höhna S, Larget B, Liu L, Suchard MA, Huelsenbeck JP (2012) MrBayes 3.2: efficient Bayesian phylogenetic inference and model choice across a large model space. Systematic Biology 61(3): 539–542. https://doi.org/10.1093/sysbio/sys029

Schwarz P, Lortholary O, Dromer F, Dannaoui E (2007) Carbon assimilation profiles as a tool for identification of zygomycetes. Journal of Clinical Microbiology 45(5): 1433–1439. https://doi.org/10.1128/jcm.02219-06

Sharma SB, Sayyed RZ, Trivedi MH, Gobi TA (2013) Phosphate solubilizing microbes: sustainable approach for managing phosphorus deficiency in agricultural soils. SpringerPlus 2: 587. https://doi.org/10.1186/2193-1801-2-587

Stamatakis A (2006) RAxML-VI-HPC: maximum likelihood-based phylogenetic analyses with thousands of taxa and mixed models. Bioinformatics 22(21): 2688–2690. https://doi.org/10.1093/bioinformatics/btl446

Tamura K, Stecher G, Peterson D, Filipski A, Kumar S (2013) MEGA6: Molecular Evolutionary Genetics Analysis version 6.0. Molecular Biology and Evolution 30(12): 2725–2729. https://doi.org/10.1093/molbev/mst197

Vitorino LC, Silva FG, Soares MA, Souchie EL, Costa AC, Lima WC (2012) Solubilization of calcium and iron phosphate and in vitro production of indoleacetic acid by endophytic isolates of *Hyptis marrubioides* Epling (Lamiaceae). International Research Journal of Biotechnology 3(4): 47–54.

White TJ, Bruns T, Lee S, Taylor J (1990) Amplification and direct sequencing of fungal ribosomal RNA genes for phylogenetics. In: Innis MA, Gelfand DH, Sninsky JJ, White TJ (Eds) PCR protocol, a guide to methods and applications. Academic Press, San Diego, 315–322. https://doi.org/10.1016/B978-0-12-372180-8.50042-1

MycoKeys 45: 93–109 (2018)
doi: 10.3897/mycokeys.45.29374
http://mycokeys.pensoft.net

RESEARCH ARTICLE

A peer-reviewed open-access journal
MycoKeys
Launched to accelerate biodiversity research

New species and records of *Pyxine* (Caliciaceae) in China

Mei-Xia Yang[1,2,3], Xin-Yu Wang[3], Dong Liu[3,4], Yan-Yun Zhang[3], Li-Juan Li[3], An-Cheng Yin[3], Christoph Scheidegger[1,2], Li-Song Wang[3]

1 *Swiss Federal Institute for Forest, Snow and Landscape Research (WSL), Zürcherstrasse 111, CH-8903 Birmensdorf, Zurich, Switzerland* **2** *University of Bern, Hochschulstrasse 6, 3012 Bern, Switzerland* **3** *Key Laboratory for Plant Diversity and Biogeography of East Asia, Kunming Institute of Botany, Chinese Academy of Sciences, Heilongtan, Kunming, Yunnan 650201, China* **4** *Korean Lichen Research Institute (KoLRI), Sunchon National University, 255 Jungang-Ro, Suncheon, Korea*

Corresponding author: *Li-Song Wang* (wanglisong@mail.kib.ac.cn)

Academic editor: *G. Rambold* | Received 20 September 2018 | Accepted 10 December 2018 | Published 29 January 2019

Citation: Yang M-X, Wang X-Y, Liu D, Zhang Y-Y, Li L-J, Yin A-C, Scheidegger C, Wang L-S (2019) New species and records of *Pyxine* (Caliciaceae) in China. MycoKeys 45: 93–109. https://doi.org/10.3897/mycokeys.45.29374

Abstract

In this study, the diversity of *Pyxine* Fr. in China was assessed based on morphological and chemical traits and molecular data are inferred from ITS and mtSSU sequences. Nineteen species were recognised, including three that are new to science (i.e. *P. flavicans* M. X. Yang & Li S. Wang, *P. hengduanensis* M. X. Yang & Li S. Wang and *P. yunnanensis* M. X. Yang & Li S. Wang) and three records new to China were found (i.e. *P. cognata* Stirt., *P. himalayensis* Awas. and *P. minuta* Vain.). *Pyxine yunnanensis* is diagnosed by the small size of the apothecia, a white medulla of the stipe and the presence of lichexanthone. *Pyxine flavicans* is characterised by broad lobes, a pale yellow medulla of the stipe and the presence of atranorin. *Pyxine hengduanensis* can be distinguished by its pale yellow medulla, marginal labriform soralia and the absence of atranorin. Detailed descriptions of each new species are presented, along with a key to the known species of *Pyxine* in China.

Keywords

China, lichenised fungi, new species, phylogeny

Introduction

The lichen genus *Pyxine* was first established by Fries (1825). Molecular data support the placement of *Pyxine* in a clade of taxa that were previously placed in Physciaceae and the circumscription of the family has thus changed to Caliciacese (Wedin and Grube 2002; Crespo et al. 2004; Gaya et al. 2012; Prieto and Wedin 2017). *Pyxine* is characterised by an adnate foliose thallus, an internal stipe colour of apothecia, dark brown hypothecium and generally two-celled brown ascospores (Awasthi 1982; Elix 2009; Kalb 1987; Kalb 2004). The genus *Pyxine* consists of approximately 70 species. Most species are pantropical to subtropical and a few species extend into temperate or oceanic regions (Elix 2009; Mongkolsuk et al. 2012; Kalb 1987; Moberg 1983; Wei and Hur 2007).

Regional studies on this genus have been carried out in Australia (Elix 2009), Brazil (Aptroot et al. 2014), India (Awasthi 1982; Nayaka et al. 2013), Thailand (Mongkolsuk et al. 2012) and North and Central America (Imshaug 1957; Jungbluth and Marcelli 2011). Prior to this study, 13 species have been reported in China, including *Pyxine berteriana*, *P. cocoes*, *P. consocians*, *P. copelandii*, *P. coralligera*, *P. endochrysina*, *P. limbulata*, *P. meissnerina*, *P. microspora*, *P. petricola*, *P. philippina*, *P. sorediata* and *P. subcinerea* (Hu and Chen 2003; Obermayer and Kalb 2010; Wei 1991).

Although many studies have been conducted, few molecular phylogenetic analyses have been completed (Gaya et al. 2012; Schmull et al. 2011; Prieto and Wedin 2017). In this study, morphological, chemical and molecular phylogenetic analyses were combined in order to re-evaluate the species composition and phylogenetic relationship of this genus in China. In our study, 31 sequences were newly generated from freshly collected specimens.

Methods

Morphological and chemical analyses

The specimens examined in this study were collected from the Hengduan Mountains region, Taiwan, Zhejiang, Hainan et al. from 1941 to 2016 and deposited in KUN-L (325 specimens) and in the Institute of Microbiology (HMAS-L, 5). Morphological characteristics were studied using a dissecting microscope (Nikon SMZ745T) and a light microscope (Nikon Eclipse Ci-S; Nikon Instruments, Tokyo Japan). Sections were made with a razor blade under a dissecting microscope and anatomical characteristics were examined and measured using a micrometer under light microscopy. Ten measurements each of the thallus, apothecia and ascospore dimensions were taken from a single apothecium per specimen and the ranges of these measurements, from smallest to largest, are presented in this study. The lichen secondary metabolites were analysed using spot reactions and thin-layer chromatography in a solvent C system, according to Orange et al. (2001).

DNA extraction and sequencing

Total genomic DNA was extracted from dried herbarium specimens using AxyPrep Multisource Genomic DNA Miniprep Kit 50-prep (Qiagen) according to the manufacturer's instructions. ITS (nrDNA ITS1-5.8S-ITS2) and mtSSU (mitochondrial small subunit rDNA) were amplified by polymerase chain reactions (PCR) using the primer pairs ITS1F (Gardes and Bruns 1993), ITS4 (White et al. 1990) and mtSSU1/mtSSU2R (Zoller et al. 1999).

Amplifications were performed in a 25 µl volume comprising 12.5 µl of 2× MasterMix (TapDNA Polymerase, 0.1 units/µl; technologies Co. Ltd), 1.0 µl of each primer, 8.5 µl ddH_2O and 2 µl DNA. Conditions for the PCR were: initial denaturation at 94 °C for 4 min, 34 cycles at 94 °C for 1 min, 54 °C for 1 min and 72 °C for 1.5 min, with a final extension at 72 °C for 10 min. PCR products were sequenced in an ABI3730X using amplification primers manufactured by Tsingke (Kunming, China).

ITS and mtSSU sequences were assembled with Seqman 7.0 (DNAStar) and manually edited using Mega6. DNA sequences were aligned with MAFFT version 7 with default parameters (Katoh et al. 2005) via the online resource (http://mafft.cbrc.jp/alignment/server/index.html).

Phylogenetic analyses

Maximum likelihood (ML) and Bayesian inference (BI) were conducted based on the two gene fragments combining ITS and mtSSU. The best-fitting substitution model was determined using MrModeltest 2.3 (Nylander 2005) and PAUP*4b10 (Swofford 2003), where the AIC values were calculated using JModelTest 3.7 (Posada 2008). ML analyses were performed using RAxML7.0.4 (Stamatakis 2006) with default settings (GTR) and support values were inferred from the 70% majority-rule tree based on 1000 non-parametric bootstrap pseudo-replicates. The Bayesian analyses were performed using MrBayes v3.1.2 (Huelsenbeck and Ronquist 2001) with 2,000,000 generations and four incrementally heated chains. MCMC (Markov Chain Monte Carlo) analysis started from a random tree that was sampled every 1000th generation, with the first 10% of trees discarded as burn-in. A majority-rule consensus tree was constructed from the remaining trees to estimate posterior probability (PP), with values greater than or equal to 0.95 considered indicative of strong support. Tracer v1.6 (Rambaut and Drummond 2003) was used to ensure that stationarity was achieved by checking whether the log-likelihood values of sample points reached a stable equilibrium. Phylogenetic trees were visualised using the programme FigTree 1.4.0 (Rambaut 2012). *Physcia dubia* and *Dirinaria applanata* were selected as outgroups.

Results

Nineteen species were recognised, including three that are new to science (i.e. *Pyxine flavicans* M. X. Yang & Li S. Wang, *P. hengduanensis* M. X. Yang & Li S. Wang and *P. yunnanensis* M. X. Yang & Li S. Wang) and three records new to China were found (i.e. *P. cognata* Stirt., *P. himalayensis* Awas. and *P. minuta* Vain.). Of the 39 sequences that were included in the phylogenetic analyses, 31 were newly generated (Table 1). A phylogenetic analysis using ITS and mtSSU sequences revealed 15 species. We were unable to obtain sequences from *P. copelandii*, *P. coralligera*, *P. microspora* and *P. philippina*, but the Chinese specimens agreed morphologically and chemically with the current circumscription of these species (Hu and Chen 2003; Obermayer and Kalb 2010; Wei 1991).

The ITS and mtSSU datasets were analysed separately and concatenated; both parsimony and Bayesian trees of ITS vs. mtSSU were congruent. A maximum likelihood phylogenetic tree was inferred from the combined dataset of ITS and mtSSU (Fig. 1). The monophyly of each species and the phylogenetic relationships between species were well supported (Fig. 1; MLBS > 90%, PP > 0.95). Specifically, the three new species were all monophyletic with a high support value: *Pyxine yunnanensis* (MLBS = 97%, PP = 1.00), *P. flavicans* (MLBS = 99%, PP = 0.99) and *P. hengduanensis* (MLBS = 98%, PP = 1.00).

Species of *Pyxine* were separated into two main clades, as inferred from the phylogenetic tree with strong support (Fig. 1). The ten species in Clade 1 are all characterised by the presence of soralia or isidia on the thallus, whereas the five species in Clade 2 contain lichexanthone and lack soralia and isidia. The two species *P. petricola* and *P. cocoes* are characterised by the presence of both lichexanthone and soralia.

Taxonomic treatment

Nineteen *Pyxine* species were confirmed in China, including three species new to science and three species hereby newly reported for the country, based on the following characteristics: presence of isidia and soredia, colour of the medulla, main compounds, reaction of K on the internal stipe of apothecia, nature of the substrate and colour of the thallus.

New species

***Pyxine flavicans* M. X. Yang & Li S. Wang, sp. nov.**
MycoBank No.: MB819956
Figure 2

Holotype. CHINA, YUNNAN PROVINCE, Nujiang Perf., Chide Vil., 1916 m elevation, 27°42'32"N, 98°43'19"E, on *Juglans*, 4 Aug 2015, *L. S. Wang* et al. KUN-L15-48196. GenBank accession No.: ITS = KY611884, mtSSU = KY751391.

Table 1. Specimen information and GenBank accession numbers for taxa used in this study. Newly obtained sequences are shown in bold.

Taxa	Locality	Voucher specimens	Accession Number	
			ITS	mtSSU
Pyxine sorediata 1	China: Yunnan	KUN 12-36993	**KY611891**	**KY751398**
P. sorediata 2	China: Yunnan	KUN 15-48546	**KY611892**	**KY751399**
P. sorediata 3	Sweden	Wetmore 91254 (UPS)	JX000111 –	– KX512973
P. hengduanensis 1	China: Yunnan	KUN 15-48082	**KY611889**	**KY751396**
P. hengduanensis 2	China: Yunnan	KUN14-43258	**KY611890**	**KY751397**
P. endochrysina 1	China: Xizang	KUN 14-46462	**KY611887**	**KY751394**
P. endochrysina 2	China: Xizang	KUN 14-46439	**KY611888**	**KY751395**
P. limbulata 1	China: Taiwan	KUN 15-49117	**KY611885**	**KY751392**
P. limbulata 2	China: Taiwan	KUN 15-49153	**KY611886**	**KY751393**
P. himalayensis 1	China: Yunnan	KUN 12-36055	**KY611881**	**KY751388**
P. himalayensis 2	China: Xizang	KUN 14-46410	**KY611882**	**KY751389**
P. flavicans 1	China: Yunnan	KUN 14-43995	**KY611883**	**KY751390**
P. flavicans 2	China: Yunnan	KUN 15-48196	**KY611884**	**KY751391**
P. meissnerina 1	China: Yunnan	KUN 12-34386	**KY611877**	**KY751384**
P. meissnerina 2	China: Yunnan	KUN 12-34377	**KY611878**	**KY751385**
P. consocians 1	China: Yunnan	KUN 15-49942	**KY611879**	**KY751386**
P. consocians 2	China: Yunnan	KUN 15-47417	**KY611880**	**KY751387**
P. petricola 1	China: Yunnan	KUN 13-40715	**KY611875**	**KY751382**
P. petricola 2	China: Sichuan	KUN 13-39419	**KY611876**	**KY751383**
P. cocoes 1	China: Taiwan	KUN 15-49457	**KY611874**	**KY751381**
P. minuta 1	China: Yunnan	KUN 13-40695	**KY611872**	**KY751379**
P. minuta 2	China: Yunnan	KUN 13-40630	**KY611873**	**KY751380**
P. yunnanensis 1	China: Yunnan	KUN 13-41372	**KY611870**	**KY751377**
P. yunnanensis 2	China: Yunnan	KUN 13-40596	**KY611871**	**KY751378**
P. berteriana 1	China: Yunnan	KUN 15-47921	**KY611868**	**KY751375**
P. berteriana 2	China: Yunnan	KUN 14-43730	**KY611869**	**KY751376**
P. subcinerea 1	China: Taiwan	KUN 15-48998	**KY611866**	**KY751373**
P. subcinerea 2	China: Taiwan	KUN 15-49012	**KY611867**	**KY751374**
P. subcinerea	USA Spain	NC 27708 MAF9852	HQ650705 –	– AY464080
P. cognata 1	China: Yunnan	KUN 14-43569	**KY611864**	**KY751371**
P. cognata 2	China: Yunnan	KUN 13-40767	**KY611865**	**KY751372**
P. berteriana var. *himalaica* 1	China: Yunnan	KUN 14-43571	**KY611862**	**KY751369**
P.berteriana var. *himalaica* 2	China: Yunnan	KUN 13-40706	**KY611863**	**KY751370**
Dirinaria applanata	India Spain	– MAF 9854	EU722342 –	– AY464079
Physcia dubia	Finland	T. Ahti 69359	JQ301695 –	– JQ301536

Description. Thallus 5–9 cm wide, attached to closely adnate. Lobes radiating, plane to convex, but often slightly concave towards the tips, (0.5) 1–3 (4) mm wide, subround at the apices. Upper surface white-grey to celadon, sparsely pruinose at the lobe tips or epruinose, isidia and soredia absent. Medulla pale yellow above, white below. Lower surface black in the centre, paler towards the margin; rhizines dense,

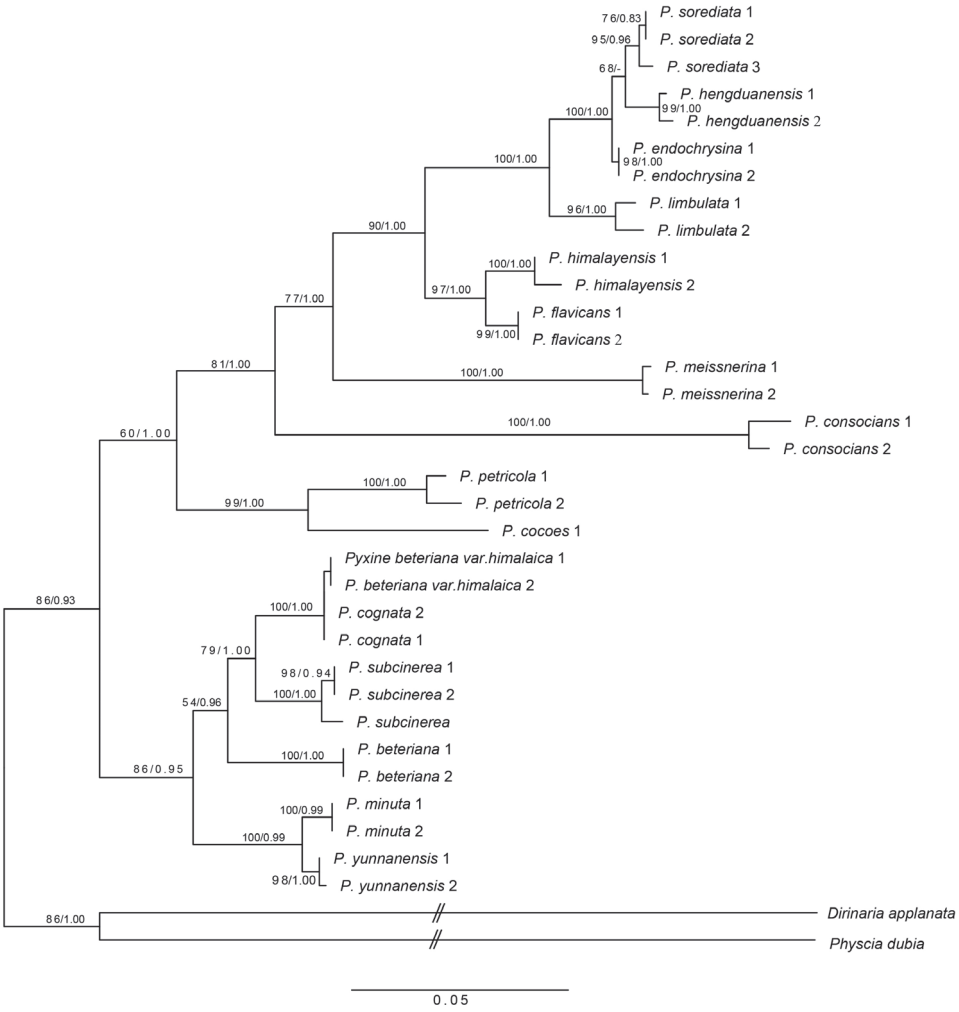

Figure 1. Phylogenetic relationship of *Pyxine* species occurring in China inferred from ITS and mtSSU sequences using maximum likelihood (values refer to ML bootstrap frequencies and Bayesian posterior probabilities).

furcate. Apothecia common, (0.5) 0.8–1.5 (2) mm wide, constricted at base, plane to possibly convex; margin black. Hymenium height 80–120 µm; hypothecium light brown to brown, internal stipe K– pale yellow to yellow; spores brown, two-celled, 18–20 × 6–8 µm. Upper cortex K+ yellowish, UV–; medulla K–, C–; containing atranorin, chloroatranorin (minor), zeorin and unknown terpenes.

Habitat and distribution. Growing on bark of *Quercus* and *Picea* spp. and on rocks around 1916–4000 m elevation in semi-arid environments; only known from south-western China.

Etymology. The epithet *flavicans* refers to the yellow medulla and internal stipe of the apothecia.

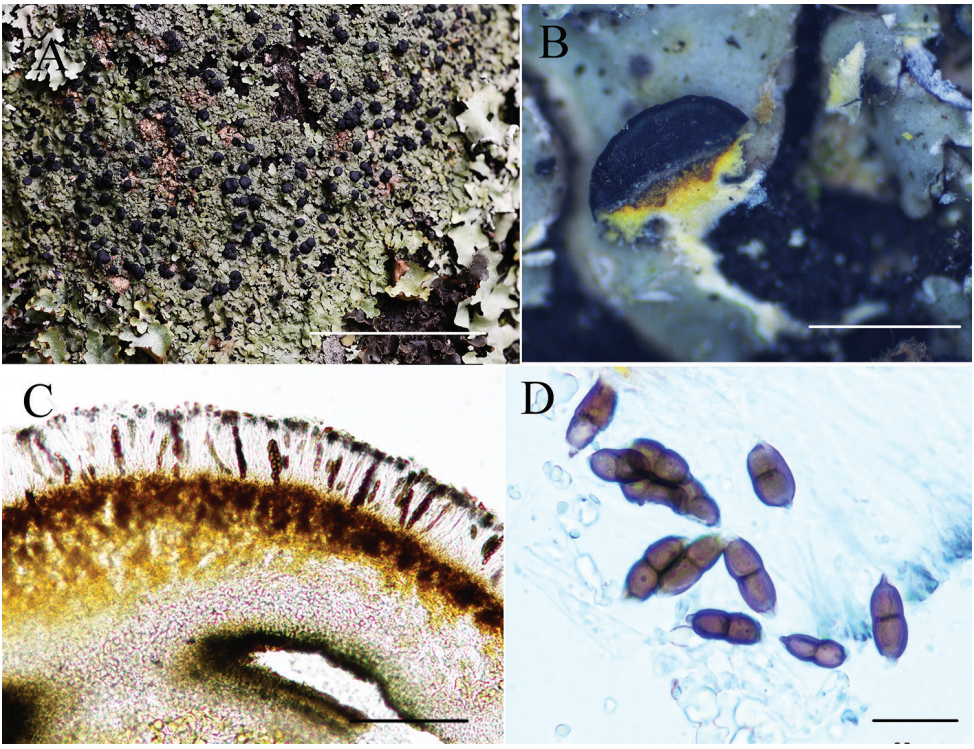

Figure 2. *Pyxine flavicans* (KUN-L 15-48196) photographed by Li-Song Wang and Meixia Yang. **A** habit **B** yellow internal stipe of apothecia **C** hymenium **D** ascospores from GAW (glycerine:alcohol:water=1:1:1). Scale bars: 5 cm (**A**); 0.5 cm (**B**); 100 µm (**C**); 20 µm (**D**).

Notes. *Pyxine flavicans* is characterised by flat corticated yellowish-grey to brownish-grey thalli, a constricted base, a pale yellow medulla and the presence of atranorin.

This species resembles *P. berteriana* in terms of lobe size, saxicolous habitat and internal stipe, but the latter has a yellow to yellowish-orange medulla and produces lichexanthone (Hu and Chen 2003). *Pyxine flavicans* is similar to *P. australiensis* Kalb regarding the absence of soredia and isidia and both species are frequently lignicolous but occasionally grow on rocks. However, *P. flavicans* differs from *P. australiensis* in having marginal and laminal pseudocyphellae, lichexanthone and a white medulla in the stipe (Elix 2009). *Pyxine flavicans* is similar to *P. himalayensis* in terms of the type of apothecia and lack of lichexanthone. However, *P. himalayensis* has a colourless internal stipe.

Selected specimens examined (KUN). CHINA: SICHUAN PROVINCE: Muli Co., 2850 m elev., on *Pinus yunnanensis*, 23 Aug 1983, *L. S. Wang* 83-1869(A); XIZANG PROVINCE: Chayu Co., along the road from Muruo Vil. to Bingzhongluo, 3833 m elev., 28°35.781'N, 98°06.404'E, on *Pinus armandii*, 26 Sep 2014, *L. S. Wang* et al. 14-46763; YUNNAN PROVINCE: Jianchuan Co., Shibao Mt., 2620 m elev., 26°22.920'N, 99°49.811'E, on bark, 24 Jun 2014, *L. S. Wang* et al. 14-43995; Nujiang Co., Chide Vil., 1916 m elev., 27°42'32.40"N, 98°43'18.59"E, on *Juglans*, 4 Aug 2015, *L. S. Wang* et al. 15-48196.

Pyxine hengduanensis **M. X. Yang & Li S. Wang, sp. nov.**
MycoBank No.: MB819957
Figure 3

Holotype. CHINA, YUNNAN PROVINCE, Nujiang Pref., Dizhengdang Vil., 1858 m elevation, 28°05'00.86"N, 98°19'39.97"E, on bark, 2 Aug 2015, *L. S. Wang* et al. KUN-L 15-48082. GenBank accession No.: ITS = KY611889, mtSSU = KY751396.

Description. Thallus corticolous, 4–9 cm wide, firmly to loosely adnate to substrate. Lobes linear, compact, imbricate to discrete, (0.5) 1–2.5 mm wide, upper cortex plane but often slightly concave towards the tips; pseudocyphellae linear, marginal; upper surface grey to greyish-green, lower-side black; rhizines dense, squarrosely branched. Soralia marginal, labriform; soredia grey to bluish-grey, powdery to granular. Medulla pale yellow. Dactyls and isidia absent. Apothecia absent. Upper cortex K+ yellowish, UV–; medulla K–, C–; containing chloroatranorin (minor) and unknown terpenes.

Habitat and distribution. Growing on bark of *Quercus* and *Alnus* spp. Range 1700 –3060 m elevation in semi-arid environments; known only from Yunnan, Sichuan and Xizang in China.

Etymology. The epithet *hengduanensis* refers to the type locality of the species, the Hengduan Mountains region.

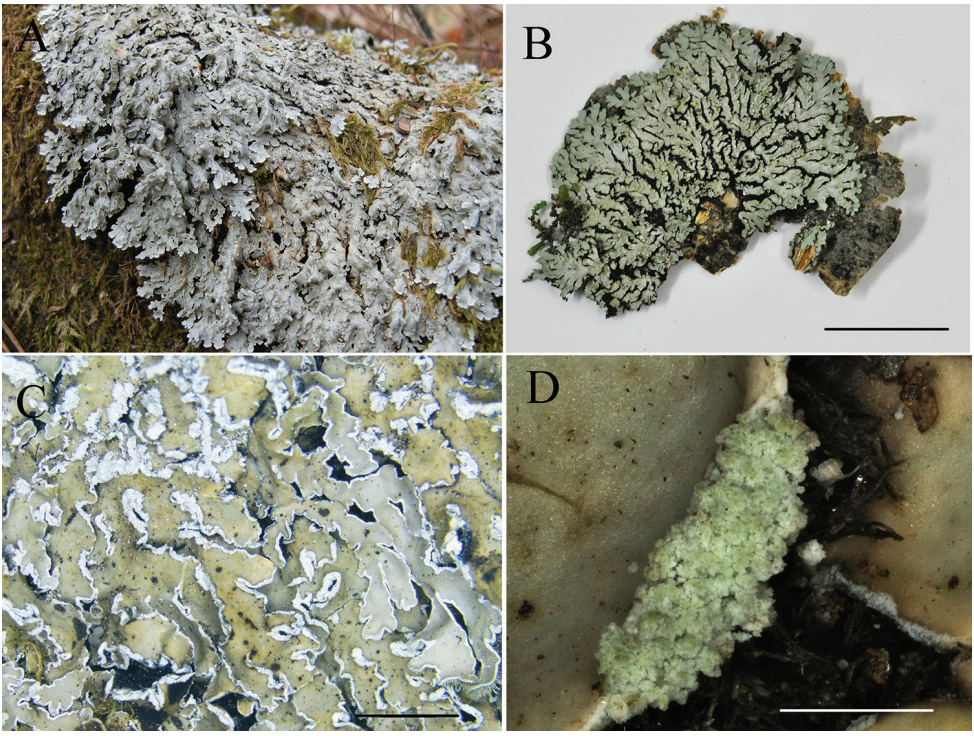

Figure 3. *Pyxine hengduanensis*: **A** (KUN-L 09-30247) photographed by Li-Song Wang, *in situ* at the type locality **B–D** (KUN-L 15-48082), photographed by Mei-xia Yang **B** Thallus **C** upper surface of thallus **D** marginal labriform soralia. Scale bars: 2 cm (**B**); 5 mm (**C**); 0.5 mm (**D**).

Notes. *Pyxine hengduanensis* is characterised by a corticolous habit, yellowish-grey to greyish-green thallus, marginal labriform soralia, pale yellow medulla and the absence of atranorin. *Pyxine hengduanensis* is most closely related to *P. sorediata*, as inferred from the phylogenetic tree (Fig. 1); *P. sorediata* is also corticolous but has a yellow or yellow-orange medulla and soralia that develop marginally from fissures and then become laminal and orbicular (Elix 2009), while *P. hengduanensis* has marginal labriform soralia developing from the centre of the pseudocyphellae, grey to bluish-grey soredia and a pale yellow medulla. *Pyxine hengduanensis* also resembles *P. retirugella* Nyl. (Elix 2009) in the marginal and laminal pseudocyphellae, but it differs in having white or creamy and K+ yellow turning red medulla and norstictic acid as the main compound (Mongkolsuk et al. 2012).

Selected specimens examined (KUN). CHINA: SICHUAN PROVINCE: Dukou Co., Yanbian Vil., Shibao Mt., 2900 m elev., 29 Jun 1983, *L. S. Wang* 83-635; Nanping Co., Jiuzhaigou, 2000 m elev., on *Pinus*, 23 Sep 1986, *L. S. Wang* 86-2591. XIZANG PROVINCE: Linzhi Co., 3060 m elev., 29°50'249"N, 94°44'728"E, on *Quercus* spp. 20 Aug 2007, *L. S. Wang* et al. 07-28389; YUNNAN PROVINCE: Luquan Co., 30 km from Sapanying Co. to Zehei Co., 2540 m elev., 26°04'24.53"N, 102°36'19.15"E, on moss, 19 Apr 2014, *L. S. Wang* et al. 14-43258; Lufeng Co., Heijin Vil., 1800 m elev., 25°20'146"N, 102°05'835"E, on bark, 1 May 2009, *L. S. Wang* 09-30247.

***Pyxine yunnanensis* M. X. Yang & Li S. Wang, sp. nov.**
MycoBank No.: MB819958
Figure 4

Holotype. CHINA, YUNNAN PROVINCE, Yongren Co., Lagu Vil., 1050 m elevation, 26°23.239'N, 101°25.120'E, on rock, 4 Dec 2013, *L. S. Wang* et al. KUN-L 13-41372. GenBank accession No.: ITS = KY611870, mtSSU = KY751377.

Description. Thallus saxicolous, up to 7 cm in diam., closely appressed to the substrate. Lobes radiating, irregularly branched, plane to slightly concave, 0.2–1.0 mm wide, subround to truncate at the apices. Upper surface pale grey to yellowish-grey, sparsely pruinose at the lobe tips or epruinose. Lower surface brownish-black, rarely pale brown, rhizines indistinct, sparse to moderately abundant, brownish-black to black. Isidia and soredia absent. Medulla pale yellow in the upper part, white in the lower part. Apothecia abundant, 0.2–0.8 mm wide, constricted at base, plane to possibly convex; margin black. Hymenium height 80–120 μm; hypothecium light brown to brown, internal stipe white; spore brown with two cells, 10–15 × 4–7 μm. Upper cortex K+ yellowish, UV+ yellow; medulla K–, C–; containing lichexanthone, chloroatranorin (minor), zeorin and unknown terpenes (detected by TLC).

Habitat and distribution. Growing on rocks around 1050–1650 m elevation in secondary forests in a dry to semi-arid environment; known only from Yunnan.

Etymology. The epithet *yunnanensis* refers to the province of the type locality of the species.

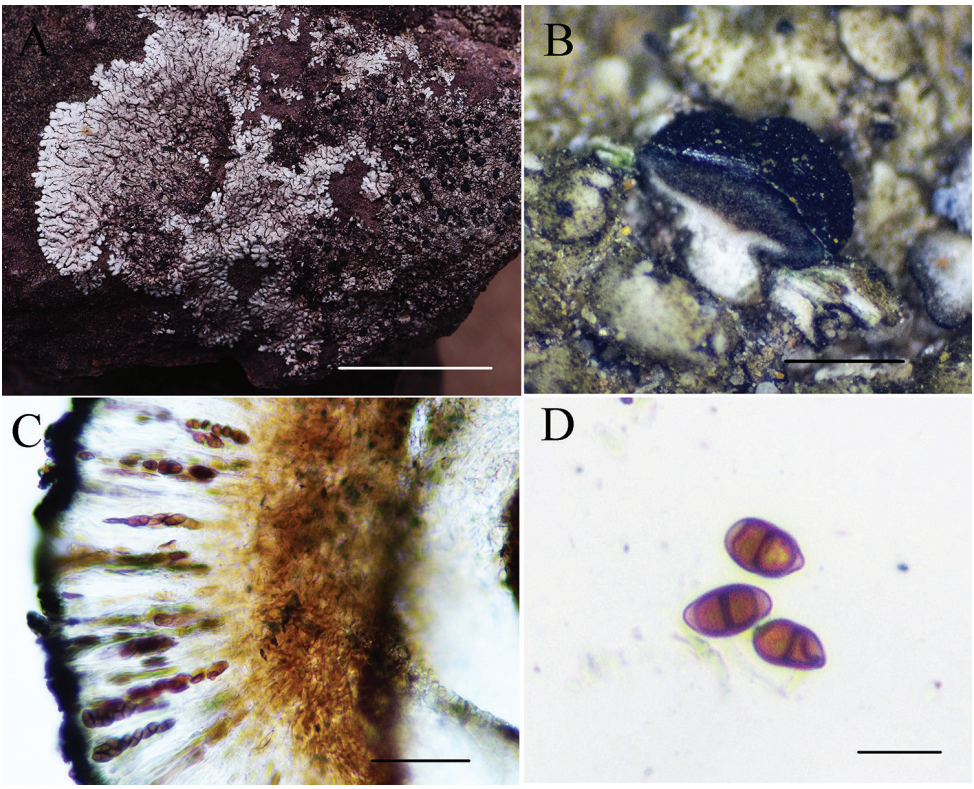

Figure 4. *Pyxine yunnanensis*: **A** (KUN-L 09-30247) photographed by Li-Song Wang, in situ at the type locality **B–D** (KUN-L 13-41372) photographed by Mei-xia Yang **B** white internal stipe of apothecia **C** hymenium **D** ascospores from GAW (glycerine:alcohol:water=1:1:1). Scale bars: 1 cm (**A**); 1 mm (**B**); 50 μm (**C**); 10 μm (**D**).

Notes. *Pyxine yunnanensis* is characterised by small and saxicolous thalli, rather small narrow apothecia (up to 0.8 mm in diam.), a white internal stipe and the presence of lichexanthone. *Pyxine minuta* Vain. (up to 3 cm in diam.) resembles *P. yunnanensis* (up to 7 cm in diam.) in its small thalli and the presence of lichexanthone, but differs in that its internal stipe is absent or indistinct and it has a white medulla (Awasthi 1982). *Pyxine pyxinoides* (Müll. Arg.) Kalb and *P. elixii* Kalb also grow on rocks, but *P. pyxinoides* differs from *P. yunnanensis* in that it has a white medulla, an indistinct internal stipe of the apothecia and smaller ascospores (10–15 × 4–7 μm) than those of *P. pyxinoides* (10–16 × 4.5–8.0 μm). *Pyxine elixii* can be distinguished by its orange medulla and lack of lichexanthone (Elix 2009).

Pyxine yunnanensis is closely related to *P. berteriana* in that they have a similar type and size of apothecia and lichexanthone is present, but *Pyxine berteriana* differs in that it occurs in incorticolous habitat and has a yellow medulla and a yellow medulla of the stipe.

Selected specimens examined (KUN). CHINA: YUNNAN PROVNCE: Yongsheng Co., Dongjiang of Renhe Town, 1130 m elev., 26°20.448'N, 101°06.908'E,

on rock, 7 Dec 2013, *L. S. Wang* et al. 13-41413; Shawan Village of Renhe Town, 1160 m elev., 26°19.449'N, 101°05.200'E, 7 Dec 2013, *L. S. Wang* et al. 13-40643, 13-40694, 13-40686, 13-40641, 13-40684; Lijiang City, east of Jinan Bridge, 1310 m elev., 26°47.725'N, 100°25.640'E, on rock, 8 Dec 2013, *L. S. Wang* et al. 13-40596.

New records

***Pyxine cognata* Stirt**

= *Pyxine berteriana* var. *himalaica* D.D. Awasthi

Description. Upper surface white to whitish-grey or grey-brown; isidia and soredia absent; medulla orange-yellow to orange; lower surface black in the centre, paler towards the margin; apothecia common, (0.3) 0.5–1.0 (1.5) mm wide; internal stipe upper part orange, K+ purple, P–; lower part yellow or much paler than upper part, K–, P–. Upper cortex K–, UV+ yellow, medulla K– or K+ pale red, C–, P– or P+ orange; containing lichexanthone (major), triterpenes, unknown pigment (minor) (detected by TLC).

Habitat and distribution. Growing on bark of *Quercus* and *Juglans* spp. Range 1090–2230 m elevation in semi-arid environments. Worldwide distribution: India (Awasthi 1982), Brazil (Aptroot 2014), Thailand (Mongkolsuk et al. 2012) and Australia (Elix 2009); newly recorded in China.

Notes. *Pyxine berteriana* var. *himalaica* was described by Awasthi (1982) as a variety based on the pale yellow to yellow medulla and a narrow distribution from the Himalayan region and central India. *Pyxine cognata* is very similar to *P. berteriana* var. *himalaica* in the presence of lichexanthone, the pigmented medulla and the lack of isidia and soredia. However, *Pyxine cognata* is distinguished by a faint pruina on the lobe tips, deep yellow to rust coloured medulla and slightly larger spores, as well as for being widely distributed in tropical regions. Therefore, the morphological and ecological differences between these two species are minor. In this study, we collected specimens of both species and found that they have a similar ecology and distribution pattern. Phylogenetic analysis inferred that *Pyxine berteriana* var. *himalaica* is clustered with *P. cognata* with a high support value (MLBS = 100%, PP = 1.00). Based on the combination of molecular, morphological and ecological information, we propose *P. berteriana* var. *himalaica* as a synonym for *P. cognata*.

Pyxine cognata is most similar to *P. berteriana* in that it contains lichexanthone, lacks isidia and soredia and has a pigmented medulla; however, *P. cognata* can be distinguished by the presence of lichexanthone in the cortex, an orange medulla and an orange-yellow internal stipe of apothecia with K+ purple. In comparison, *P. berteriana* has a pale yellow to yellow medulla and the internal stipe is pale yellow to yellow. (Kalb 1987). Despite the broad similarities, these species are not closely related; *P. cognata* seems to share a unique ancestor with *P. subcinerea*. *Pyxine subcinerea* differs in that it has marginal soralia and obscurascens-type apothecia (Elix 2009). (Fig. 1).

Selected specimens examined (KUN). CHINA: SICHUAN PROVINCE: Miyi Co., Malong north slope, 2100 m elev., on *Carya* spp., 5 Jul 1983, *L. S. Wang* 83-698; Dukou Co., Dabaoding, 1900 m elev., 21 Jun 1983, *L. S. Wang* 83-212. YUNNAN PROVINCE: Yuanmou Co. Langbapu Forest Soil, 1612 m elev., 25°41'01.76"N, 101°41'25.78"E, on branch, 21 Apr 2014, *c*14-43569, 14-43539; Yongren Co., from Menghu to Wanma, 1543 m elev., 26°13'45.15"N, 101°25'56.86"E, 3 Dec 2013, *L. S. Wang* et al. 13-40767.

Pyxine himalayensis Awas

Description. Thallus grey-white, soredia and isidia absent; medulla yellow to orange-yellow; apothecia common, laminal, constricted at base, up to 2 mm in diam.; internal stipe colourless, K–, hypothecium 50–80 µm thick, spores brown, 15–25 × 6–9 µm. Upper cortex K+ yellow, UV–, medulla K–, C–, P–; containing atranorin (major), +/– zeroin, triterpense.

Habitat and distribution. Growing on bark of *Rhododendron*, *Quercus*, *Alnus*, *Juglans*, *Sophora*, *Lonicera* and *Lyonia* spp. and rarely on rocks, at elevations of 1330–3600 m in semi-arid environments. Worldwide distribution: India (Awasthi 1982) and added here to the flora of China.

Notes. *Pyxine himalayensis* is distinctive for having lobes 1.5–3.0 mm wide, an orange medulla and a lack of isidia and soredia, lichexanthone and norstictic acid. *Pyxine himalayensis* was first described by Awasthi (1982) and it is characterised by an orange medulla and colourless internal stipe of apothecia. The closely related *Pyxine limbulata* is described as having a yellow medulla and a brown internal stipe (Hu and Chen 2003). There are 24 specimens of this species in the KUN-L. The phylogenetic analysis of ITS and mtSSU sequences confirm that these are independent species.

Selected specimens examined (KUN). CHINA: SICHUAN PROVINCE: Dukou City, Shibao Mt., 2800 m elev., 29 Jun 1983, *L. S. Wang* 83-628; Yuanyang Co., Bailing commune, 3100 m elev., on *Quercus*, 11 Aug 1983, *L. S. Wang* 83-1508; 3250 m elev., on stone, 10 Aug 1983, *L. S. Wang* 83-1483; Muli Co., Yazui forest farm, on *Quercus*, 3000 m elev., 20 Aug 1983, *L. S. Wang* 83-1589, 83-1596; Donglang, 3000 m elev., on bark, 10 Sep 1983, *L. S. Wang* 83-2220. XIZANG PROVINCE: Bomi Co., Gang vil., 2688 m elev., 29°52.983'N, 095°33.593'E, on branch of *Populus yunnanensis*, 20 Sep 2014, *L. S. Wang* et al. 14-46203, 14-46162. YUNNAN PROVINCE: Luquan Co., 30 km from Sapanying Co. to Zehei Co., 2540 m elev., 26°04'24.53"N, 102°36'19.15"E, on *Quercus*, 19 Apr 2014, *L. S. Wang* et al. 14-43218, 14-43204; Luquan Co., Zhongcun Vil., 2350 m elev., 25°20'146"N, 102°05'835"E, on bark of *Quercus*, 1 May 2009, *L. S. Wang* 09-30279.

Pyxine minuta Vain

Description. *Pyxine minuta* is characterised by narrow lobes, centrally subcrustaceous, saxicolous thalli, a whitish-grey or grey-brown upper surface; brownish-black lower

surface with black and simple rhizines, a lack of isidia and soredia and a white or whitish stramineous medulla. Apothecia common, 0.5–1.5 mm wide; internal stipe absent or not distinct. Upper cortex K+ yellowish, UV+ yellow, medulla K–, C–; containing lichexanthone (major) and terpenoids (detected by TLC).

Habitat and distribution. Growing on bark of *Quercus* spp. or rock around 1090–2230 m elevation in semi-arid environments. Worldwide distribution: India (Awasthi 1982), Australia (Rogers 1986) and newly recorded in China.

Notes. There is some confusion in the classification of *Pyxine minuta* and *P. pyxinoides*. *Pyxine minuta* is characterised by narrow lobes, an absent or indistinct internal stipe, small spores (11–16 (18) × 5–7 µm) and a white medulla. Based on the world key to *Pyxine* species with lichexanthone (Aptroot et al. 2014; Kalb 1987; Huneck et al. 1987), the characteristics of *Pyxine pyxinoides* are: Thallus without isidia, pustules or soredia, usually with apothecia; Medulla yellow, ochraceous or salmon; apothecium margin black, not thalline; apothecium without a clear stipe; one TLC run of a portion of the thallus without apothecia showed traces of a substance running like norstictic acid (Obermayer and Kalb 2010); neotropical. We did not find any specimens of *P. pyxinoides* in our collections.

Selected specimens examined (KUN). CHINA: SICHUAN PROVINCE: Dukou Co., Dabaoding, 1950 m elev., 21 Jun 1983, *L. S. Wang* 83-206. YUNNAN PROVINCE: Yongsheng Co., Shawan village of Renhe town, 1160 m elev., 26°19.449'N, 101°05.200'E, on rock, 7 Dec 2013, *L. S. Wang* et al. 13-40630, 13-40695; Yongren Co., Lagu village, 1050 m elev., 26°23.239'N, 101°25.120'E, on rock, 4 Dec 2013, *L. S. Wang* et al. 13-41380; Jinggu Co., on the way to Zhenyuan, 1800 m elev., 21 Aug 1994, *L. S. Wang* et al. 94-14247.

Key to the species of the genus *Pyxine* in China

1	Thallus UV+, lichexanthone present	**2**
–	Thallus UV–, lichexanthone absent	**12**
2	Thallus with vegetative propagules	**3**
–	Thallus lacking vegetative propagules	**7**
3	Thallus with soredia	**4**
–	Thallus with isidia	**5**
4	Medulla yellow	***P. subcinerea***
–	Medulla white	***P. cocoes***
5	Medulla yellow; isidia dactyliform	***P. endochrysina***
–	Medulla white; isidia cylindrical	**6**
6	Norstictic acid present	***P. consocians***
–	Norstictic acid absent	***P. coralligera***
7	Atranorin present	***P. cognata***
–	Atranorin absent	**8**
8	Medulla pale yellow to yellow	***P. berteriana***
–	Medulla white	**9**

9	Internal stipe of apothecia absent or indistinct	**10**
–	Internal stipe of apothecia well developed	**11**
10	Norstictic acid present, as well as other triterpenes	***P. microspora***
–	Norstictic acid absent	***P. minuta***
11	Internal stipe of apothecia brown, K+ red violet	***P. petricola***
–	Internal stipe of apothecia white, K–	***P. yunnanensis***
12	Thallus with soralia	**13**
–	Thallus lacking vegetative propagules	**16**
13	Medulla white, soralia laminal; norstictic acid present	***P. copelandii***
	Medulla yellow; soralia marginal; norstictic acid absent	**14**
14	Atranorin absent; soralia labriform	***P. hengduanensis***
–	Atranorin present; soralia granular, laminal or orbicular	**15**
15	Lobe margin without pseudocyphellae; soredia yellow	***P. meissnerina***
–	Lobe margin with intermittent pseudocyphellae; soredia grey to bluish-grey.	***P. sorediata***
16	Medulla yellow	**17**
–	Medulla white	***P. philippina***
17	Internal stipe of apothecia colourless	***P. himalayensis***
–	Internal stipe of apothecia brown or yellow	**18**
18	Internal stipe brown, K+ red violet	***P. limbulata***
–	Internal stipe of apothecia pale yellow; upper medulla yellow, lower medulla white	***P. flavicans***

Acknowledgements

The authors are grateful to Dr. Melissa Dawes for the scientific editing, as well as Prof. Bernard Goffinet from the University of Connecticut and Prof. James R. Shevock from the California Academy of Sciences for guidance and help with writing in English. Sincere thanks are extended to Institute of Microbiology, Chinese Academy of Sciences for the loan of specimens. This study was supported by grants from the National Natural Science Foundation of China (No. 31370069, 31400022, 31670028, 31750001), the Second Tibetan Plateau Scientific Expedition and the China Scholarship Council.

References

Amtoft A (2002) *Pyxine subcinerea* in the Eastern United States. Bryologist 105: 270–272. https://doi.org/10.1639/0007-2745(2002)105[0270:PSITEU]2.0.CO;2

Aptroot A, Jungbluth P, Cáceres M (2014) A world key to the species of *Pyxine* with lichexanthone, with a new species from Brazil. Lichenologist 46: 669–672. https://doi.org/10.1017/S0024282914000231

Awasthi DD (1982) *Pyxine* in India. Phytomorphology 30: 359–379.

Cáceres MES, Lücking R, Rambold G (2007) Phorophyte specificity and environmental parameters versus stochasticity as determinants for species composition of corticolous lichen communities in the Atlantic rain forest of northeastern Brazil. Mycological Progress 6: 117–136. https://doi.org/10.1007/s11557-007-0532-2

Cáceres MES, Lücking R, Rambold G (2008) Corticolous microlichens in northeastern Brazil: habitat differentiation between coastal Mata Atlântica, Caatinga and Brejos de Altitude. Bryologist 111: 98–117. https://doi.org/10.1639/0007-2745(2008)111[98:CMINBH]2.0.CO;2

Crespo A, Blanco O, Llimona X, Hawksworth DL (2004) Coscinocladium, an overlooked endemic and monotypic mediterranean lichen genus of Physciaceae, reinstated by molecular phylogenetic analysis. Taxon 53: 405–414. https://doi.org/10.2307/4135618

Elix JA (2009) Physciacae, 3. *Pyxine*. In: McCarthy PM (Ed.) Flora of Australia Volume 57. Lchens 5, ABRS & CSIRO Publishing, Canberra & Melbourne, 517–533.

Gaya E, Högnabba F, Holguin A, Molnar K, Fernández-Brime S, Stenroos S, Arup U, Søchting U, den Boom PV, Lücking R, Sipman HJM, Lutzoni F (2012) Implementing a cumulative supermatrix approach for a comprehensive phylogenetic study of the Teloschistales (Pezizomycotina, Ascomycota). Molecular Phylogenetics and Evolution 63: 374–387. https://doi.org/10.1016/j.ympev.2012.01.012

Gardes M, Bruns TD (1993) ITS primers with enhanced specificity for basidiomycetes application to the identification of mycorrhizae and rusts. Molecular Ecology 2: 113–118. https://doi.org/10.1111/j.1365-294X.1993.tb00005.x

Hu GR, Chen JB (2003) The lichen family Physciaceae (Ascomycota) in China VI. The genus *Pyxine*. Mycotaxon 86: 445–454.

Huelsenbeck JP, Ronquist F (2001) MRBAYES: Bayesian inference of phylogenetic trees. Bioinformatics 17: 754–755. https://doi.org/10.1093/bioinformatics/17.8.754

Huneck S, Morales MA, Kalb K (1987) The chemistry of *Dirinaria* and *Pyxine* species (Pyxinaceae) from South America. Journal of the Hattori Botanical Laboratory 62: 331–338.

Imshaug HA (1957) The lichen genus *Pyxine* in North and Middle America. Transactions of the American Microscopical Society 56: 246–269.

Jungbluth P, Marcelli MP (2011) The *Pyxine pungens* complex in Sao Paulo state, Brazil. Bryologist 114: 166–177. https://doi.org/10.1639/0007-2745-114.1.166

Kalb K (1987) Brasilianische Flechten, 1. Die Gattung *Pyxine*. Berlin-Stuttgart, J. CRAMER, 5–82.

Kalb K (2004) New or otherwise interesting lichens II. Bibliotheca Lichenologica 88: 301–329.

Kashiwadani H (1977a) On the Japanese species of the genus *Pyxine* (Lichens) (1). Journal of Japanese Botany 52(5): 137–144.

Kashiwadani H (1977b) On the Japanese species of the genus *Pyxine* (Lichens) (2). Journal of Japanese Botany 52(6): 161–168.

Kashiwadani H (1977) The genus *Pyxine* (Lichen) in Papua New Guinea. Bull. Natl. Sci. Mus. ser. B (Botany) 3: 63–70.

Katoh K, Kuma K, Toh H, Miyata T (2005) MAFFT version 5: improvement in accuracy of multiple sequence alignment. Nucleic Acids Research 33: 511–518. https://doi.org/10.1093/nar/gki198

McCarthy PM, Kantvilas G, Louwhoff SHJJ (2001) Lichenological Contributions in Honour of Jack Elix. Bibliotheca Lichenologica 78: 141–167.

Moberg R (1983) Studies on Physciaceae (Lichen) II. The genus *Pyxine* in Europe. Lichenologist 15(2): 161–167. https://doi.org/10.1017/S0024282983000250

Mongkolsuk P, Meesim S, Poengsungnoen V, Kalb K (2012) The lichen family Physciaceae in Thailand – I. The genus *Pyxine*. Phytotaxa 59: 32–54. https://doi.org/10.11646/phytotaxa.59.1.2

Nayaka S, Upreti DK, Ponmurugan P, Ayyappadasan G (2013) Two new species of saxicolous *Pyxine* with yellow medulla from southern India. Lichenologist 45: 3–8. https://doi.org/10.1017/S0024282912000618

Nylander JAA (2005) Mrmodeltest v. 2.3. Uppsala: Computer program distributed by the author.

Obermayer W, Kalb K (2010). Notes on three species of *Pyxine* (Lichenized Ascomycetes) from Tibet and adjacent regions. Bibliotheca Licheologica 104: 247–267.

Orange A, James PW, White FJ (2001) Microchemical Methods for the Identification of Lichen. 2nd ed. British Lichen Society, London, 1–101.

Posada D (2008) jModelTest: phylogenetic model averaging. Molecular Biology and Evolution 25: 1253–1256. https://doi.org/10.1093/molbev/msn083

Prieto M, Wedin M (2017) Phylogeny, taxonomy and diversification events in the Caliciaceae. Fungal Diversity 82: 221–238. https://doi.org/10.1007/s13225-016-0372-y

Rambaut A, Drummond AJ (2003) Tracer v1.6. Available from website http://tree.bio.ed.ac.uk/software/tracer/

Rambaut A (2012) FigTree: Tree figure drawing tool, v.1.4.0. Institute of Evolutionary Biology, University of Edinburgh. http://tree.bio.ed.ac.uk/software/figtree/

Rogers RW (1986) The genus *Pyxine* (Physciaceae, lichenized ascomycetes) in Australia. Australia Journal of Boany 34: 131–154. https://doi.org/10.1071/BT9860131

Schmull M, Miadlikowska J, Pelzer M, Stocker-Wörgötter E, Hofstetter V, Fraker E, et al. (2011) Phylogenetic affiliations of members of the heterogeneous lichen-forming fungi of the genus *Lecidea* Sensu Zahlbruckner (lecanoromycetes, ascomycota). Mycologia 103(5): 983–1003. https://doi.org/10.3852/10-234

Stamatakis A (2006) RAxML-VI-HPC: maximum likelihood-based phylogenetic analyses with thousands of taxa and mixed models. Bioinformatics 22: 2688–2690. https://doi.org/10.1093/bioinformatics/btl446

Shukla V, Upreti DK (2008) Effect of metallic pollutants on the physiology of lichen, *Pyxine subcinerea* stirton in Garhwal Himalayas. Environmental Monitoring & Assessment 141: 237–243. https://doi.org/10.1007/s10661-007-9891-z

Swofford DL (2003) PAUP*. Phylogenetic Analysis Using Parsimony (*and Other Methods). Sunderland, Massachusetts: Sinauer Associates.

Swinscow TDV , Krog H (1975) The genus *Pyxine* in the East Africa. Norwegian Journal of Botany 22: 43–68.

Wedin M, Tibell L (1997) Phylogeny and evolution of Caliciaceae, Mycocaliciaceae and Sphinctrinaceae (Ascomycota), with notes on the evolution of the prototunicate ascus. Canadian Journal of Botany 75: 1236–1242. https://doi.org/10.1139/b97-837

Wedin M, Grube M (2002) Parsimony analyses of mtSSU and nIT rDNA sequences reveal the natural relationships of the lichen families Physciaceae and Caliciaceae. Taxon 51: 655–660. https://doi.org/10.2307/1555020

Wei JC (1991) An enumeration of lichens in China. International Academic publishers, Beijing, 216–218.

Wei XL, Hur JS (2007) Foliose genera of Physciaceae (lichenized Ascomycota) of South Korea. Mycotaxon 102: 127–137.

White TJ, Bruns TD, Lee S, Taylor JW (1990) Amplification and direct sequencing of fungal ribosomal genes for phylogenetics. In: Innis MA, Gelfand DH, Sninsky JJ, White TJ (Eds) PCR Protocols. Academic Press, San Diego, 315–322.

Zoller S, Scheidegger C, Sperisen C (1999) PCR primers for the amplification of mitochondrial small submit ribosomal DNA of lichen-forming ascomycetes. Lichenologist 31(5): 511–516. https://doi.org/10.1006/lich.1999.0220